ISAS - INTERNATIONAL SCHOOL
FOR ADVANCED STUDIES

Numerical Study of Strongly Correlated Electron Systems

Thesis submitted to the
International School for Advanced Studies
– Condensed Matter Sector–
for the degree of

Doctor Philosophiæ

CANDIDATE
Qingfeng ZHONG

SUPERVISOR
Dr. Sandro SORELLA

September 1994

SISSA - SCUOLA INTERNAZIONALE SUPERIORE STUDI AVANZATI
TRIESTE
Strada Costiera 11

TRIESTE

Contents

List of Figures

List of Tables

Acknowledgements

My acknowledgements are due, in the first place, to all of my tutors in SISSA, whose teaching has made direct and indirect contribution to the present dissertation.

I am particularly grateful to Professor E. Tosatti, the director of the SISSA Condensed Matter sector, for his acceptance of me as a SISSA student, erecting an important signpost in my life that directs me into a new route of my academic career. I wish to express my sincere gratitude to Dr. S. Sorella for having brought me to the amusing computational physics and strongly correlated electron systems and for having offered me constant and enlightening guidance and encouragement. With his help, I succeeded in switching my center of research to computational physics without too much effort. I am also greatly indebted to Dr. A. Parola particularly during the work of the anisotropic Heisenberg model and the single hole problem, which becomes part of the thesis.

I owe a separate debt of thanks to Dr D.F. Wang for his collaboration with me in tackling the exact solution of long range Hubbard model in one dimension, which is not included in this thesis[1], and Dr G. Santoro for helping me to develop the code of the density matrix renormalization group.

Again, I would like to thank Dr. S. Sorella for the insightful discussions in the course of writing the present dissertation and for having supplied valuable criticisms and detailed suggestions for improving the work. I am extremely grateful to Dr. R. Valente and Dr. P. Focher for their helping with the LaTeXto edit the manuscript.

Finally, to the INFM and the SISSA secretaries, particularly to S. Gustin, A.Porettii, C. Parma, R. Iancer, A. Parma and F. Sparagna for having devoted their time and patience to the solution of my various problems, I offer my sincere thanks.

I assume full responsibility for possible errors of any sort in the dissertation.

Abstract

In this thesis, we present some systematic studies on low dimensional strongly correlated systems: the Heisenberg spin magnets and the t-J_z model for the two dimensional lattices. We have studied these systems through numerical and analytical research. Various physical properties of the systems are obtained in our approach. The results obtained are believed to provide useful insights about the correlated behaviors of the model systems, which are closely related and motivated by the discoveries of the high temperature superconductors.

First, we have proposed a new method concerning the spin wave theory on finite lattices. In this thesis we have developed a systematic spin wave expansion for the quantum fluctuations of a generic spin Hamiltonian on a finite lattice, where $1/zS$ is the small parameter. The idea was applied to the J_1-J_2 Heisenberg model in the square lattice and the Heisenberg model in the triangular lattice (AHT) in two dimensions. By comparing with the exact diagonalization results, we have shown that for large enough J_2, the ground state with long range antiferromagnetic order is instable. The non-Néel ordered state sets in at a smaller value of J_2 than the previous estimates. For the triangular lattice, contrary to the previous results of finite size extrapolation, we also show that the ground state on the triangular lattice indeed has long range Néel order. The new method has also been applied to the J_x-J_y model.

Second, we have studied an anisotropic spin magnet in two dimensions, through long wavelength field theory, numerical research, combined with the finite size spin wave theory. A possible spin liquid is suggested to exist in this two dimensional system, and a phase transition from the gapless spin liquid phase to a ordered phase occurs at the critical anisotropy $\alpha_c = 0.1$. In particular, we have found that the gapless spin liquid phase may be thought of as a set of decoupled spin chains, exhibiting the one dimensional feature.

Third, we have introduced a new method, which we called Lanczos Spectra Decoding (LSD), to extract information about dynamical correlation functions of many-body Hamiltonians with a few Lanczos iterations and without the limitation of finite size. We apply this technique to understand the low energy properties and the dynamical spectral weight of a simple model describing the motion of a single hole in a quantum antiferromagnet: the t-J_z model in two spatial dimensions and for a double chain lattice. The simplicity of the model allows us a well controlled numerical solution, especially for the two chain case. We have found that the single hole ground state in the infinite system is continuously connected with the Nagaoka fully polarized state. Analogously we have obtained an accurate determination of the dynamical spectral weight relevant for the photoemission experiments. The spectral weight is in qualitative agreement with the old approximate techniques: the retraceable path approximation for $J_z = 0$ and the string theory for $J_z > 0$. However, contrary to the previous approximations, the band tails for $J_z = 0$ or the asymptotic $J_z \to 0$ one hole ground state again approach the Nagaoka energy. We have given a simple ana-

lytical argument, supported by our numerical data, showing that the vanishing of the spectral weight close to the Nagaoka energy is faster than any power law. We have also been able to show that spin charge decoupling is an exact property in the Bethe lattice but it is not fulfilled in more realistic lattices where the hole can describe closed loop paths during its motion. Our detailed numerical results on this simple model represent a benchmark for possible developments to the more interesting t-J model in the physical small J limit.

Finally, we have discussed possible physical applications of the results, in particular, related to the high temperature superconducting materials.

Chapter 1

Introduction

In this thesis, we have studied several two dimensional models of strongly correlated electron systems. This is a highly challenging issue at the current time, because of its importance for the anomalous properties observed in the high temperature cuprate superconductors. Much of the work presented in the forthcoming chapters is inevitably technical. In this introduction, we would like to introduce readers to broader issues and questions related to this work and attempt to place the work of this thesis in its proper context. Following that, a short historical review of the models which we will study will be presented. The technique review will be retained until it is used.

1.1 General Review

In the last two decades, there have been exciting breakthrough in condensed matter physics, mainly due to the discovery of the high temperature superconducting materials, as well as due to the discovery of the quantum Hall effects. The experimental breakthrough has shed new light on the excitement of the strongly correlated systems. In the mean time, various attempts to explain these correlated behaviors have introduced some new concepts of importance, such as the spin charge decoupling, fractional statistics, etc.

In 1986, Bednorz and Muller[2] found that the cuprate materials have phase transitions to superconducting state at a critical temperature which is much higher than the conventional transition temperature. Shortly after that, Anderson [3] realized that the superconductivity could not be understood before the thorough investigation of the normal state of the new materials. There is a lot of experiments showing that the reference compounds of the high temperature superconductors have a broken symmetry ground state. For example, the ground state of La_2CuO_4 is a Mott insulator, *i.e.* insulating because of the large value of the onsite Coulomb repulsion, U. The appearance of long range

antiferromagnetic order, the paramagnetic susceptibility and the apparent absence of an energy gap in the optical spectrum at energies below $3eV$ all lead to this conclusion. Upon doping, the hole is introduced in the CuO_2 planes, which are the common feature of the high temperature superconductors and the antiferromagnetic long range order fades away. The carriers of the superconductor, *i.e.* the holes, are mainly confined on the CuO_2 planes. The low dimensionality and the strongly correlations between the holes are widely believed responsible for the novel behaviours.

The discovery of high temperature superconductors had a sobering effect for theoreticians. In particular, it soon becomes clear that high temperature conductivity had to be the result of an interplay between various different phenomena which were not yet sufficiently understood even by themselves. These phenomena include:

- The generation of magnetic correlations as a consequence of strong interactions between electrons and the influence of mobile vacancies on such magnetic states;
- The particular behavior of electrons in the vicinity of a Mott-Hubbard metal-insulator transition;
- The effect of static disorder on the correlated behavior of electrons;
- The peculiarities of two-dimensional fermi system;
- The preconditions for superconductivity in a strongly correlated system.

Anderson[3] first proposed that a doped Mott insulator described by the one band Hubbard model should contain the basic physics of the high-T_c superconductors. The model was proposed independently in 1963 by Gutzwiller, Hubbard and Kanamori[4, 5, 6], to describe the competition between delocalization and correlations in narrow-band transition metal.

$$H = -t \sum_{<nn>,\sigma} c^{\dagger}_{i\sigma} c_{j\sigma} + U \sum_{i} c^{\dagger}_{i\uparrow} c_{i\uparrow} c^{\dagger}_{i\downarrow} c_{i\downarrow} \tag{1.1}$$

where $c_{i\sigma}$ ($c^{\dagger}_{i\sigma}$) are the electron annihilation (creation) operators of spin $\sigma = (\uparrow, \downarrow)$ at site i, $< nn >$ indicates summation over nearest neighbours, the indices i, j run over N lattice sites, the two-body interaction is on-site and repulsive($U > 0$).

For $U = 0$, H reduces to a system of non-interacting electrons, while for $t = 0$ (atomic limit) the electrons are fully localized, and at half-filling the ground state contains exactly one electron per site, *i.e.* the system is insulating. The latter feature still holds for finite t and $U = \infty$, and the corresponding system has been shown to be an antiferromagnetic insulator.

In the large U limit, it is more convenient to use a canonical transformation to project out the doubly occupied sites, costing energy U. This leads to the

so-called t-J model:

$$H = -t \sum_{<i,j>,\sigma} (c^{\dagger}_{i\sigma} c_{j\sigma} + h.c.) + J \sum_{<i,j>} (\mathrm{S}_i \cdot \mathrm{S}_j - \frac{1}{4} n_i n_j). \qquad (1.2)$$

where the constraint of no double occupancy is understood. n_i is the density operator at site i with $n_{i\sigma} = c^{\dagger}_{i\sigma} c_{i\sigma}$. $J = 4t^2/U$ under this convention. The spin density operator S_i is defined as $\mathrm{S}_i = c^{\dagger}_i \frac{\vec{\sigma}}{2} c_i$.

Zhang and Rice[7] also showed that the low-energy physics of cuprate superconductors is determined by the singlet state formed by the additional hole on oxygen with the existing hole copper. The hopping of this singlet is described by an effective t-J model which makes this model even more pertinent to high-T_c superconductors.

At exact half-filling case $n_i = 1$ for all i, the t-J model is reduced to the so-called Heisenberg model.

$$H = J \sum_{<i,j>} \mathrm{S}_i \cdot \mathrm{S}_j \qquad (1.3)$$

This model was introduced by Dirac early in 1929. van Vleck has used it to study the magnetic solid. Although this model is rather old and longstanding, a number of questions arose following the discovery of the copper-oxide superconductors.

Before going on with the specific models, we would like to stress the important role of the dimensionality in understanding the strongly correlated electron systems.

The fields of low-dimensional systems have been expanding during the last decade, particularly due to the discoveries of the quasi-one-dimensional organic conductors, the Quantum Hall Effect and high temperature superconductivity. In addition to these three fields, there are also other systems, such as mesoscopic systems, quantum dots, where low dimensionality is a key feature. In parallel with these experimental developments, there have been many exciting theoretical developments of conceptual importance, such as the notions of soliton-like excitations and the spin-charge decoupling, fractional statistics and fractional charges.

The low dimensionality takes a much more important role in strongly correlated systems rather than in the conventional solid state physics, which is characterized by the free and independent particle approximation. For example, in the electron system, as well known, in three or higher dimensions, the interaction can be renormalized. This lead to the famous Landau fermi liquid theory. But in lower dimensions the conventional perturbation theory has infrared singularity which is not renormalizable. In one dimension, this gives the so-called Luttinger liquid. It has been a challenging question whether the conventional perturbation theory may be also applied to two dimensional systems. We will see another example of a spin systems, where low dimensionality is of importance, in the next section.

1.2 Heisenberg Hamiltonian

The study of the Heisenberg Hamiltonian goes back to the early days of quantum mechanics. However, the antiferromagnet was not as well understood as the ferromagnet.

In one dimension, the quantum spin chain with $s = \frac{1}{2}$ is exactly solvable by Bethe-ansatz. The ground state does not have long-range antiferromagnetic order and the correlation function decays as a power law. The low energy excitations are gapless. For arbitrary spin ($S \neq \frac{1}{2}$), there is not exact solution. However, Haldane[8] argued that The half-integer spin chains have gapless ground states with algebraic correlation function, and the integer spin chains have finite energy gap above the ground state in which the correlation function decays exponentially.

Beyond one dimension, the exact solution for the ground-state energy or wave function of the Hamiltonian on an infinite lattice is unknown. There are some rigorous proofs regarding the nature of the ground state, however. It has been shown that the ground state of the three-dimensional antiferromagnetic Heisenberg model for spin $S \geq 1$[9] and quite recently for $S = \frac{1}{2}$ is characterized by antiferromagnetic long-range order. The long-range order disappears at some finite critical temperature in 3D. In two dimensions, the Heisenberg model cannot exhibit long-range order for any spin at finite temperature[10]. The situation may be quite different for the ground state (T=0) of these models. It has been shown that antiferromagnetic long-range order exists in the ground state of the isotropic antiferromagnetic Heisenberg model on a square lattice[11] and on a hexagonal lattice[12] for any $S \geq 1$. So far, no rigorous proof is available for the existence or noexistence of antiferromagnetic long-range order in the ground state of the isotropic spin-$\frac{1}{2}$ antiferromagnetic Heisenberg model on a square lattice. The extensive numerical and experimental results have lead to the conclusion that the 2D Heisenberg model displays long range antiferromagnetic order and that there is no evidence of any exotic behavior in the unfrustrated model.

Again, the behavior of the systems shows strong dependence on the dimensionality, in which it is embedded.

1.3 Spin Liquid State

The search for disordered (spin liquid) ground states in two dimensional electronic models has been pursued since the seminal work of Fazekas and Anderson [13] on quantum antiferromagnet in frustrated lattices. This problem has been revived in the last few years due to the resonating valence bond conjecture of high temperature superconductors.

On the other hand, although many studies indicate that there exists a finite zero-temperature staggered magnetization in the 2D square lattice, it has also

been shown that the energy difference of ordered and disordered states is very small; therefore it is of great interest to test the stability of the long range order under various frustrations.

1.3.1 Heisenberg Model on the Triangular Lattice

One way of destroying antiferromagnetic long range order is by introducing the lattice frustration. The simplest one in this catalog is the triangular lattice. It was indeed the first system to be proposed by Fazekas and Anderson[13] as a candidate for a spin-liquid.

The situation is puzzling as regards the triangular lattice case. On this lattice the "frustration" implies that the classical system is not very stable ($E_{cl} =< 2\mathrm{s}_i.\mathrm{s}_j >= -1/4$), and the spin-wave calculations predict an important reduction (by about one half) of the sublattice magnetization by quantum fluctuations[14, 15, 16]. Perturbation theory[17], series expansions[18] and high temperature calculations[19] have been developed, which suggest that the spin-wave calculations possibly underestimate this renormalization. Many variational calculations have been done exhibiting either ordered [20, 21] or disordered solutions[22, 23, 24].

In the square lattice case, numerical methods (Q.M.C., Ulam's or Trotter-Suzuki methods) have brought very interesting indications on Néel order[25, 26, 27, 28, 29]. Unfortunately these methods which allow to handle large samples cannot be applied to the triangular case: they lay on a property of positivity of offdiagonal matrix elements which is violated in the triangular case; it is the well known sign problem which plagues many studies of strongly correlated fermions. Exact diagonalization of the Hamiltonian are thus the last resort to gather new information on these models. This approach has been developed by other authors[30, 31, 32, 33, 34, 35, 36, 37]. Most of them conclude to the absence of Néel order for the triangular Heisenberg antiferromagnet (AHT) at $T = 0$. However, the results is shown strongly dependent on the extrapolation. Unlike the square lattice, there is no established systematic extrapolation formulae for the triangular lattice.

We have developed a scheme for applying a systematic SWT on a finite lattice. It has the advantage that one can directly check the accuracy of the results on the small size system, while yielding reliable prediction on the infinite system. By using the finite size spin wave theory, we will show that the ground state of the Heisenberg model on a triangular lattice is, contrary to the finite size scaling, an ordered state. The finite size scaling has to take into account the deviation from the simple $N^{-\frac{1}{2}}$ behavior. This, in turn, strongly supports that the spin wave theory is an extremely good quantitative approximation for the antiferromagnets.

1.3.2 J_1-J_2 Model

The antiferromagnetic long-range order might be destroyed by introducing frustrating interaction. The simplest one of these is to take into account the next-nearest neighbor antiferromagnetic interaction. This leads to the so-called J_1-J_2 model.

$$H = J_1 \sum_{<nn>} \mathbf{S}_i \cdot \mathbf{S}_j + J_2 \sum_{<nnn>} \mathbf{S}_i \cdot \mathbf{S}_j \tag{1.4}$$

This model has a classical phase transition at $\frac{J_2}{J_1} = 0.5$. In the classical limit, for $\alpha < \frac{1}{2}$ the ground state has conventional Néel order with two sublattices. When $\alpha > \frac{1}{2}$, the same classical limit yields a ground state where the previous sublattices are decoupled and each one has antiferromagnetic order. At $\alpha = \frac{1}{2}$ any state with total spin equal zero for an elementary square is a possible ground state. This includes the two configurations discussed above as well as many others with no long range order. In the quantum case, it has been argued that there is a spin liquid state between the two ordered states.

Many questions remain still open especially in 2D and $S = \frac{1}{2}$ for this simple model. For example there is now a considerable amount of numerical work [38][39] in order to detect a first realization of a spin liquid state for large enough J_2. Linear spin-wave theory [40] and series expansion [18] have indeed predicted a possible transition for $J_2 > 0.38$. However on a rigorous ground very little is known.

We have applied the finite size spin wave theory to the frustrated 2D Heisenberg model. In the $J_1 - J_2$ Heisenberg model we have found that SWT works very well for small frustration ($J_2 < 0.2$) and an accurate estimate of spin-rotation invariant quantities can be obtained with only few terms of the expansion in $\frac{1}{S}$. We finally confirm the existence of a non classical spin-liquid state for large J_2.

1.3.3 J_x-J_y Model

Despite considerable efforts, the evidence in favor of a spin liquid in two dimensional frustrated quantum antiferromagnets is weak at best, with the single exception of the kagomé lattice where a disordered ground state is plausible, even if the presence of nonconventional magnetic order is still possible.

As well known the one dimensional Heisenberg chain has a spin liquid ground state, it is persuasible that in two dimensions when the anisotropy is sufficiently strong the one dimensional behaviour may be extended to two dimensions. This leads us to the so-called J_x-J_y model. This model does *not* introduce frustration and therefore presents several advantages with respect to the previously investigated systems, the most important being the absence of any plausible order parameter competing with the Néel staggered magnetization $\mathbf{m} = \sum_{\mathbf{R}} \mathbf{S}_{\mathbf{R}} \exp(\mathbf{Q} \cdot \mathbf{R})$ [$\mathbf{Q} = (\pi, \pi)$]. The model is defined by the Hamilto-

nian

$$H = \sum_{\mathbf{R}} \left[J_x \mathbf{S}_{\mathbf{R}} \cdot \mathbf{S}_{\mathbf{R}+\mathbf{x}} + J_y \mathbf{S}_{\mathbf{R}} \cdot \mathbf{S}_{\mathbf{R}+\mathbf{y}} \right] \tag{1.5}$$

where $\mathbf{S}_{\mathbf{R}}$ are spin 1/2 operators living on a square lattice, $\mathbf{x}$ and $\mathbf{y}$ are unit vectors and $0 \leq J_y \leq J_x$.

The first term in the Hamiltonian represents a stack of one dimensional Heisenberg chains, and the second term represents the coupling between the chains. In the limit of extreme anisotropy $\alpha = \frac{J_y}{J_x} = 0$, the two dimensional system is a stack of decoupled spin $\frac{1}{2}$ chains, each of which is disordered in its ground state due to strong quantum fluctuation. At finite anisotropy, each chain begins to couple to the others and finally, in the limit of perfect isotropy $\alpha = 1$, the system becomes the ordinary two dimensional Heisenberg spin system with ordered ground state. A phase transition have to happen for $\alpha \in [0, 1]$.

The isotropic limit ($J_y = J_x$) has been extensively studied by exact diagonalization [41] and quantum Monte Carlo[27, 42] with the resulting evidence of a finite staggered magnetization in the thermodynamic limit[42] $m \sim 0.3075$ quite close to the spin-wave theory (SWT) estimate $m = 0.3034$[43]. Physically, the strongly anisotropic model (1.5) describes a system of weakly coupled AF chains whose study has attracted considerable interest among theoreticians and experimentalists in view of the possibility to observe the peculiar features of one dimensional physics[44].

The presence of an order-disorder transition in model (1.5) has been conjectured by several authors[45, 46] and can be motivated by the standard mapping of the 2D quantum model (1.5) into the (2+1) dimensional $O(3)$ non linear sigma model (NLσM) defined by the action

$$S = \frac{1}{2} \int dx dy dt \left[\Upsilon_x (\partial_x \mathbf{n})^2 + \Upsilon_y (\partial_y \mathbf{n})^2 + \chi_0 (\partial_t \mathbf{n})^2 \right] \tag{1.6}$$

where $\mathbf{n}$ is a unit vector. The lowest order estimates of the parameters give $\Upsilon_x = J_x/4$, $\Upsilon_y = J_y/4$, $\chi_0^{-1} = 4a^2(J_x + J_y)$ where a is the lattice spacing. Two limits of the action (1.6) can be easily analyzed: The isotropic model is known to be ordered for the physically relevant parameters[47] while the $J_y \to 0$ limit of the action (1.6) correctly describes a stack of uncoupled (1+1) dimensional models which are disordered at any finite "temperature" $g = (\Upsilon_x \chi_0 a^2)^{-1/2}$ owing to the Mermin Wagner theorem[10]. Most interestingly, the order–disorder transition occurs at a *finite* value of the spatial anisotropy and belongs to the universality class of the classical three dimensional Heisenberg model.

The finite size spin wave theory predicts a phase transition at $\alpha \sim 0.1$, which is consistent with the numerical exact diagonalization results. We will also show that the ground state of the spin liquid state has gapless excitations and it may be thought of as decoupled one dimensional chains. Finally, a phase diagram will be calculated by the spin wave theory.

1.4 Single Hole Motion in a Antiferromagnetic Background

During the last few years, a huge amount of analytical and numerical work has been devoted to the study of the t-J model. [48] However the physics contained in the t-J model is far from clear because of the interplay between antiferromagnetic long range order and charge degrees of freedom. Exact numerical methods are usually limited to a very small linear size in more than 1D and practically nothing about the low energy physics has been understood numerically.

In this thesis we will make a detailed numerical study of an oversimplified version of the t-J model, *i.e.* neglecting the spin fluctuations in the exchange term ($\mathbf{S}_i \cdot \mathbf{S}_j - S_i^z S_j^z$ in Eq. (1.2)) and considering only the properties of a single hole. Due to the simplification of the model, we are able to work directly in the infinite size system and have a satisfactory description for the low energy dynamics of a single hole in such a simple model of an antiferromagnet:

$$H = -t \sum_{<i,j>,\sigma} (c_{i\sigma}^{\dagger} c_{j\sigma} + h.c.) + J_z \sum_{<i,j>} S_i^z S_j^z . \tag{1.7}$$

A basic motivation of this work is also to obtain reliable numerical results on this simple t-J_z model since it maybe useful for further developments on the more interesting t-J model. For instance already Trugman[49] and Kane, Lee and Read[50] used the t-J_z model in order to test the prediction of a given approximation on the t-J model. Most recently, Prelovšek and Sega[51] also carried out a calculation of this model at low doping. In fact most of the physical properties of the t-J model remain probably valid even for the t-J_z model. In this respect it is worth mentioning that the t-J model and the t-J_z model have the same limit for J or J_z — 0 and for infinite spatial dimensions the two model coincide, since the spin fluctuations are irrelevant. [52]

The single hole problem represents certainly a further simplification but is still physically relevant, since the single particle excitations in magnetic insulators can actually be studied by the photoemission and the inverse photoemission spectroscopy.

For a single hole a rigorous theorem proven by Nagaoka[53] is known for $J_z = 0$. The so called Nagaoka theorem states that for a bipartite finite lattice in more than one dimension $d > 1$ the ferromagnetic state with maximum spin is the unique ground state in any subspace with given total spin projection, say on the z axis.

A complete description of the one hole spectrum in the $J_z = 0$ limit, not limited to the ground state, was first given in [54], where the so-called "retraceable path approximation" (RPA) was introduced. In the Ising limit as a hole hops in a Néel state, it scrambles the spin along its path. In order to return the spin configuration to its original state, it was argued[54] that, to a good approximation, one can consider only paths in which the hole retraces its path

back to the origin, thereby returning all of the spins to their original position. In this approximation one can write down an explicit analytic solution for the Green's function:

$$G_k(\omega) = \frac{z\sqrt{\omega^2 - 4(z-1)} - (z-2)\omega}{2(\omega^2 - z^2)} \tag{1.8}$$

and the spectral weight $A(k,\omega) = -\frac{\text{sgn }\omega}{\pi} ImG_k(\omega)$ reads

$$A(\omega) = \frac{z\sqrt{4(z-1)t^2 - \omega^2}}{4\pi(z^2t^2 - \omega^2)} \tag{1.9}$$

where $z = 2d$ is the number of nearest neighbors. The spectral weight is completely incoherent and dispersionless with a one particle band, which is 75% narrower (in 3D) than the noninteracting band. The RPA is exact in 1D and for the Bethe lattice (where Nagaoka theorem does not apply), and recently it has been shown to be exact in the limit of infinite spatial dimensionality. [52]

For finite J_z/t, the competition between the kinetic energy t favoring the ferromagnetic configuration and the exchange energy J_z favoring the antiferromagnetic alignment of the neighboring spins makes the problem of particular interest. By neglecting closed loops, *i.e.* in the Bethe lattice case, a closed solution is possible [55, 56] which we will refer in the following as the "string picture". In the string picture, the hole moves in an antiferromagnetic background, leaving behind a string of overturned spins, which costs an energy proportional to the length of the path. The overturned spins behave like an effective linear potential for the hole. In the continuum limit, valid for $J_z \to 0$, the problem is reduced to a one dimensional Schrödinger equation with a linear potential $V \sim xJ_z$ where x is the length of the string.

$$H = -\sqrt{z-1}t\frac{\partial^2}{\partial x^2} + \frac{J_z(z-2)}{2}x - 2\sqrt{z-1}t. \tag{1.10}$$

The solution of this equation leads to a series of bound states, with energies

$$E_n = a_n\sqrt{z-1}t(\frac{J_z(z-2)}{2\sqrt{z-1}t})^{2/3} - 2\sqrt{z-1}t \tag{1.11}$$

where a_n are the zeros of the Airy function $Ai(z)$. Recently, Vollhardt *et al* [52] have shown that the string picture is exact up to order $\frac{1}{d^2}$, where d is the spatial dimensionality.

Contrary to the $J_z = 0$ case for finite J_z the spectral weight has δ-function peaks at energies E_n. The weight of the δ-function at the lowest energy is called the quasiparticle weight Z and is found to vanish linearly in J_z, using the continuous limit (1.10).[50]

Later Kane, Lee and Read[50] introduced a self-consistent Born approximation that can be considered as an extension of the retraceable path approximation to the more physical t-J model. Their approach is widely accepted

since they were able to reproduce the asymptotic behavior of the t-J_z model in the string picture and a big amount of numerical work on small lattices seems to be in qualitative agreement with the theoretical predictions of this theory.[57, 58, 59]

In the retraceable path approximation or in the string picture and similarly within the self-consistent Born approximation, it is important to neglect closed loop paths in order to simplify the analytic structure of the one hole Green's function. However this is certainly an approximation even in the simple t-J_z model. In fact the most important effect due to the inclusion of closed loop paths in this model was first noted by Trugman.[49] In 2D a hole can hop around a square plaquette one and half times without disturbing the spin background with a net translation to the next-nearest-neighbor along the diagonal. This means that the hole can "unwind" the string and self-generate a next-nearest-neighbor hopping. The hole does not have an infinite effective mass in this case but has a finite mobility. Therefore the full localization of charge carriers in RPA and the string picture is an artifact of the approximation.

In this work, we will apply the Lanczos method to the infinite two chains and two dimensional lattice. A variational result is obtained for the ground state energy and wave function. Then we will introduce a novel method, which we called the Lanczos Spectra Decoding, to analyse the data and extract information for the dynamical correlation functions in the thermodynamical limit. We will also discuss the problem of spin charge decoupling, phase separation and the spin configuration in the ground state.

Another interesting issue is whether the spin and charge degrees of freedom are decoupled or not.[60, 61] Spin charge decoupling is well known to occur in one dimension where a one electron excitation can be decomposed into a spinon excitation which carries spin and no charge and a holon excitation which carries charge and no spin. We will show in the present thesis that spin charge decoupling is *exact* in the Bethe lattice with arbitrary coordination number z and present some numerical work, ruling out the possibility of spin charge decoupling in physically relevant lattices where closed loops are allowed.

1.5 Structure of the Thesis

In Chapter 2, we will introduce the finite size spin wave theory in order to get a reasonable comparison between theory predictions and numerical calculations. We will give in detail the treatment of the singular spin wave modes, which exist in any finite system. The validity of the finite size spin wave theory will be shown in Chapter 3. We will study three magnetic models there, namely, the J_1-J_2 model, the J_x-J_y model and the Heisenberg model on the triangular lattice(AHT). The finite size spin wave theory successfully predicts the spin liquid state in the first two models. However, the AHT exhibits an ordered ground state.

Chapter 4 will be dedicated to the study of the J_x-J_y model. We will investigate this system numerically there. We will try to show that the disordered phase is gapless and its long wavelength properties can be interpreted in terms of decoupled one dimensional chains. A phase diagram will be presented at the end of this Chapter.

In the following chapters, we will concentrate mainly on the single hole problem in the t-J_z model and we will make use of the Lanczos method to calculate the single hole spectral function in the infinite system. In Chapter 5, we will first introduce a transformation to eliminate the charge degree of freedom to get an effective spin Hamiltonian in a given momentum subspace. Then we will consider the consequence of the spin charge decoupling on the single hole spectral function. We will use the Lanczos method in order to diagonalize the effective spin Hamiltonian in the infinite lattice (Chapter 6). We will concentrate on two chains (2C) and two-dimensional (2D) square lattices. The 2C case is much more easy for numerical study compared to the 2D lattice. However the 2C lattice is already important for the t-J_z model, because it already satisfies the basic properties of an higher dimensional lattice, such as the existence of closed loop paths and the validity of the Nagaoka theorem.

Most of the above results were obtained by use of the Lanczos Spectra Decoding method, which allows us to analyze the Lanczos data in the infinite system, where only a relative small number of Lanczos iterations is possible (Chapter 6). The validity of the Lanczos Spectra Decoding is proved analytically and numerically in the Bethe lattice case (Chapter 7). In Chapter 7, we will also present our numerical results for both the $J_z = 0$ and the finite J_z case in 2C and 2D lattice. Finally we will discuss about the formation of a ferromagnetic polaron around the hole for small J_z, and about the analytic form of the spectral weight close to the Nagaoka energy.

Chapter 2

Finite Size Spin Wave Theory

In this chapter, we will develop a systematic $\frac{1}{S}$ spin wave expansion for a generic spin model on finite size lattice[62]. In the next chapter we will present the finite size spin wave calculation for the J_1-J_2 model, the J_x-J_y model on the two dimensional square lattice and the Heisenberg model on the triangular lattice. Comparison between the theoretical predictions and the numerical calculations on the finite size system show that the finite size spin wave theory is efficient for studying the ground state properties of the spin system.

Anderson[63] extended the spin-wave theory introduced by Holstein and Primakoff[64] for ferromagnets to the study of the ground state of antiferromagnets with large spin S. Following Anderson, during the same year, Kubo[65] using the Holstein-Primakoff transformation and an expansion in powers of $\frac{1}{S}$, derived Anderson's results. The foundation of spin-wave theory is the assumption that antiferromagnetic long-range order exists in the ground state and that the amplitude of zero-point motion of quantum fluctuations about the classical Néel state is small. Initially, this approach was thought to be an expansion in powers of $\frac{1}{S}$. Later, however, it became clear that the result of spin-wave theory is the leading order in a perturbation-theory expansion in the number of loops, which is also an expansion in powers of $\frac{1}{z}$, z being the coordination number. Still this expansion is strictly valid for higher dimensional lattices, where z is large and the fluctuations are suppressed. Since the role of quantum fluctuations becomes more important for small S and lower dimensionality, it is natural to question the speed of convergence of this approach for the smallest possible spin case, the spin-$\frac{1}{2}$ antiferromagnet.

For clarity, we will consider the Heisenberg model in this chapter. First we will present a short introduction for the conventional spin wave theory. The following section will be devoted to the finite size problem, where the delicate

of the singular modes is given in detail.

2.1 Spin-Wave Theory

We consider an $L \times L$ square lattice of lattice spacing a and $N = L^2$ sites. The degrees of freedom are vector spin operators $\mathbf{S}_r$ attached to the site at r and obey the usual commutation relations

$$[S_r^\alpha, S_{r'}^\beta] = iS_r^\gamma \delta_{r,r'} \tag{2.1}$$

where the superscripts α, β, and γ stand for the x, y, and z components or any cyclic permutation of them. We consider periodic boundary conditions. (Notice that in our units $\hbar = 1$ and the lattice spacing $a = 1$.)

We wish to find the eigenstates and eigenvalues of Heisenberg Hamiltonian. Let $|S_r^z\rangle$ denote the eigenstates of the operator S_r^z with eigenvalue S_r^z. (We will use the same symbol both for the operator and the eigenvalues of the operator.) The Hilbert space in which the Hamiltonian operates is spanned by the basis

$$|\{S_r^z\}\rangle \equiv \prod_r |S_r^z\rangle \tag{2.2}$$

Since the Hamiltonian commutes with the operators of the total spin and the z component of the total spin, namely,

$$\begin{aligned} S_{tot}^2 &\equiv |\sum_r S_r|^2 \\ S_{tot}^z &\equiv \sum_r S_r^z \end{aligned} \tag{2.3}$$

we may choose to work in a subspace with well-defined eigenvalues of S_{tot} and S_{tot}^z. Specially, Marshall[66] proved that the ground state of the antiferromagnetic Heisenberg model on a bipartite lattice is characterized by $S_{tot} = 0$.

In order to define the ground-state staggered magnetization, we add a field h to the Hamiltonian, which couples to the spins of the two sublattices differently,

$$H' = H + h\sum_r (-1)^{|r|} S_r^z \tag{2.4}$$

where $|r| \equiv x + y$ and x, y are the two components of the vector r. Then, we define

$$\begin{aligned} m_z^\dagger &\equiv \tfrac{1}{N}\sum_r (-1)^{|r|} S_r^z \\ m^\dagger &\equiv \lim_{h\to 0}\lim_{N\to\infty} \langle 0|m_z^\dagger|0\rangle \end{aligned} \tag{2.5}$$

Provided that we take the thermodynamic limit before we set the external sublattice field h to zero, if the ground-state expectation value $m^\dagger$ remains finite we

shall say that the ground state is characterized by antiferromagnetic long-range order.

First, we introduce the Holstein-Primakoff transformation as implemented for antiferromagnets. An equivalent representation to the spin basis is obtained by labeling the basis states by the eigenvalues of the "spin-deviation" operator

$$n_r \equiv S - S_r^z \tag{2.6}$$

When the site r is on one sublattice, say A, and

$$n_r \equiv S + S_r^z \tag{2.7}$$

for a site r on the other sublattice B. In this representation the Hilbert space is spanned by

$$|\{n_r\}\rangle \equiv \prod_r |n_r\rangle \tag{2.8}$$

and eigenvalues of n_r are 0, 1, ..., 2S. A general state can be expressed as

$$|\psi\rangle = \sum_{\{n_r\}} C(\{n_r\})|\{n_r\}\rangle \tag{2.9}$$

The operator S^z is diagonal in this representation, while $S_r^\dagger$ and S_r^- when r is on the A sublattice have the following properties:

$$\begin{aligned} S_r^\dagger|n_r\rangle &= \sqrt{2S\left[1-\tfrac{n_r-1}{2S}\right]n_r}|n_r-1\rangle \\ S_r^-|n_r\rangle &= \sqrt{2S(n_r+1)\left[1-\tfrac{n_r}{2S}\right]}|n_r+1\rangle \end{aligned} \tag{2.10}$$

When the site r is on the B sublattice, the action of the above two operators is intercharged. It is a convenient bookkeeping device to introduce the operators

$$\begin{aligned} a_r^\dagger|n_r\rangle &\equiv \sqrt{n_r+1}|n_r+1\rangle \\ a_r|n_r\rangle &\equiv \sqrt{n_r}|n_r-1\rangle \end{aligned} \tag{2.11}$$

and similarly when r is on the B sublattice. The operators $a_r^\dagger$ and a_r obey the usual commutation relations for two-component system of bosons,

$$\begin{aligned} [a_r, a_{r'}^\dagger] &= \delta_{r,r'} \\ [a_r, a_{r'}] &= [a_r^\dagger, a_{r'}^\dagger] = 0 \end{aligned} \tag{2.12}$$

These equations can be obtained by applying the operators to a general state and using the definitions. We find

$$\begin{aligned} S_r^\dagger &= \sqrt{2S}f_s(n_r)a_r \\ S_r^- &= \sqrt{2S}a_r^\dagger f_s(n_r) \\ S_r^z &= S - n_r \\ n_r &= a_r^\dagger a_r \\ f_s(n_r) &= \sqrt{1-\tfrac{n_r}{2S}} \end{aligned} \tag{2.13}$$

for r on the A sublattice and

$$\begin{aligned} S_r^{\dagger} &= \sqrt{2S}a_r^{\dagger}f_s(n_r) \\ S_r^{-} &= \sqrt{2S}f_s(n_r)a_r \\ S_r^{z} &= -S + n_r \\ n_r &= a_r^{\dagger}a_r \end{aligned} \tag{2.14}$$

when r is on the B sublattice.

In the Eq. (2.11) the eigenvalue n_r is free to take any value from 0 to ∞ rather than from 0 to 2S. There is no discrepancy, since the sector of states with $0 \leq n_r \leq 2S$ will not be connected to states with $n_r \geq 2S$ because $|n_r = 2S\rangle$ is annihilated by $S_r^{-}(S_r^{\dagger})$ when r is on $A(B)$ sublattice:

$$S_r^{-}|n_r = 2S\rangle = 0 \tag{2.15}$$

The Hamiltonian can be expressed in terms of a and $a^{\dagger}$, operators using the expressions for S^z, $S^{\dagger}$, and S^{-}, and therefore the spin problem is transformed to an equivalent problem of interacting bosons:

$$\begin{aligned} H &= -NdJS^2 + 2dJS\sum_r n_r \\ &+ JS\sum_{\langle r,r'\rangle}[f_S(n_r)a_r f_S(n_{r'})a_{r'} + a_r^{\dagger}f_S(n_r)a_{r'}^{\dagger}f_S(n_{r'})] \\ &- J\sum_{\langle r,r'\rangle} n_r n_{r'} \end{aligned} \tag{2.16}$$

The operator $f_S(n_r)$, if we allow n_r to take values from 0 to ∞, can be expanded as

$$f_S(n_r) = 1 - \frac{n_r}{4S} - \frac{n_r^2}{32S^2} - \cdots \tag{2.17}$$

We emphasize that if we truncate this expansion at any order, condition(2.15), which decouples the physical from the unphysical states, is no longer satisfied. If, on the other hand, we restrict ourselves in the physical subspace of 2S+1 dimensions, then this operator can be written as

$$f_S(n_r) = \sum_{m=0}^{2S} d_m(S)n_r^m \tag{2.18}$$

In the linear spin-wave approximation introduced by Anderson[63] for antiferromagnets, one retains in Eq. (2.16) terms up to quadratic in the boson operators. This means that $f_S(n_r)$ is approximated by 1 and the last term of Eq. (2.16) is neglected, *i.e.*,

$$H_{lsw} = -NdJS^2 + 2dJS\sum_r n_r + JS\sum_{\langle r,r'\rangle}(a_r a_{r'} + a_r^{\dagger}a_{r'}^{\dagger}) \tag{2.19}$$

This Hamiltonian connects the physical states with $0 \leq n_r \leq 2S$ with states having $n_r \geq 2S$. If the ground state expectation value of n_r is small compared to $2S$, this approximation makes sense. This condition can be checked once the spectrum of H_{lsw} is found.

A quadratic Hamiltonian such as H_{lsw} can always be diagonalized. We introduce the Fourier transforms of these operators as

$$a_k = \sqrt{\frac{1}{N}} \sum_r e^{ik\cdot r} a_r \tag{2.20}$$

where the vectors k correspond to the reciprocal space of the lattice. We perform a canonical transformation to new operators α_k and $\alpha_k^\dagger$, which also obey boson commutation relations,

$$a_k = u_k \alpha_k + v_k \alpha_{-k}^\dagger \tag{2.21}$$

where α_k and $\alpha_k^\dagger$ satisfy the same commutation relation as a_k, $a_k^\dagger$. Substituting Eq. (2.21) in H_{lsw}, the functions u_k, v_k are determined so that the coefficient of $\alpha_k^\dagger \alpha_k^\dagger$ is zero. We obtain

$$\begin{aligned} u_k &= \sqrt{\tfrac{1+\epsilon_0(k)}{2\epsilon_0(k)}} \\ v_k &= -sgn(\gamma_k)\sqrt{\tfrac{1-\epsilon_0(k)}{2\epsilon_0(k)}} \end{aligned} \tag{2.22}$$

where

$$\begin{aligned} \gamma_k &\equiv \tfrac{1}{d} \sum_\mu cos(k \cdot e_\mu) \\ \epsilon_0(k) &= \sqrt{1-\gamma_k} \end{aligned} \tag{2.23}$$

where e_μ is the unit vector in the μ direction, and

$$H_{lsw} = E_0^0 + \sum_k 2\omega_0(k) n_k^\alpha \tag{2.24}$$

where

$$\begin{aligned} n_k^\alpha &= \alpha_k^\dagger \alpha_k \\ E_0^0 &= -dJSN(S+\xi) \\ \xi &\equiv \tfrac{2}{N} \sum_k [1 - \sqrt{1-\gamma_k^2}] \\ \omega_0(k) &= 2dJS\sqrt{1-\gamma_k^2} \end{aligned} \tag{2.25}$$

The ground state $|\psi_0\rangle$ is defined by the conditions $\alpha_k|\psi_0\rangle = 0$ for all k in the Brillouin zone. For square lattice, $\xi = 0.158$ and the ground state energy per site in the linear spin-wave approximation is -0.658.

Keeping terms up to $\frac{1}{S}$ in the expansion[43], we find that the diagonal terms of the Hamiltonian have the form

$$H = E_0 + \sum_k \omega(k)[2(n_k^\alpha + n_{k_1}^\alpha n_{k_2}^\alpha) - 2(1+C_{12}) n_{k_1}^\alpha n_{k_2}^\alpha] + \cdots \tag{2.26}$$

where

$$\begin{aligned} E_0 &= -dJS^2N\left[1+\tfrac{\xi}{2S}\right]^2 \\ \omega(k) &= \omega_0(k)\left[1+\tfrac{\xi}{2S}\right] \\ C_{12} &\equiv \sqrt{1-\gamma_{k_1}^2}\sqrt{1-\gamma_{k_2}^2} \end{aligned} \tag{2.27}$$

The ground state energy per site in this approximation for the spin- $\frac{1}{2}$ model on a square lattice is $\frac{E_0}{JN} = -0.6705$. Since the energy of the Néel state is -0.5 and in the linear spin-wave approximation is -0.658, and the next correction in the $\frac{1}{S}$ expansion is small, one might conclude that there is an apparent convergence in the case of the ground state energy. It is very different, however, to justify an expansion in powers of $\frac{n_r}{2S}$ and therefore the expansion parameter for $S = \frac{1}{2}$ is really the expectation value of n_r. That is to say, the ground state is in a linear superposition of state with very small amplitude for those with large n_r. Therefore the convergence of the expansion could be explained if

$$\epsilon \equiv \frac{1}{N}\sum_k \langle n_k \rangle \ll 1 \tag{2.28}$$

We obtain

$$\epsilon = \frac{1}{2N}\sum_k \left[\frac{1}{\sqrt{1-\gamma_k^2}} - 1\right] \tag{2.29}$$

and, for a square lattice, $\epsilon = 0.197$, which is a rather small number.

The energy of the elementary excitations is given by $\omega(k)$ and, in the long-wavelength limit $\omega(k \to 0) = ck$. We define

$$Z_c \equiv \frac{c}{c_0} \tag{2.30}$$

where c_0 is the "bare" spin-wave velocity obtained in the linear spin-wave approximation, namely, $c_0 \equiv \sqrt{2}Ja$. For the antiferromagnet on a square lattice in the above approximation the ratio $Z_c = 1 + \xi = 1.158$.

The ground state expectation value of the staggered magnetization operator for $S = \frac{1}{2}$ is obtained as

$$m^\dagger = \frac{1}{2} - \epsilon \tag{2.31}$$

and for a square lattice $m^\dagger = 0.3034$. Hence spin-wave theory predicts an ordered ground state with finite staggered magnetization approximately 61% of its classical value. In one dimension the integral (in the thermodynamical limit) diverges logarithmically due to the long-wavelength modes. This instability can be attributed to the fact that the ground state fails to develop long-range order in one dimension. The fact that the integral diverges also means that there is no small expansion parameter, and that the perturbative expansion around an ordered state is incorrect for spin chains. Note that even in higher dimensions,

the singular modes exist. However, they do not contribute to the integral in the thermodynamical limit. This is a concrete example of how low dimensionality is important to determine the physics of systems. The singular modes will take an extremely important role in our finite size system study, where the Brillouin zone is only composed of finite points.

We wish to add to the Hamiltonian a term of the form $H_\perp \sum_r S_r^x$. The perpendicular susceptibility is defined as $\chi_\perp \equiv \frac{\partial M_\perp}{\partial H_\perp}$, where $\langle M_\perp \rangle$ is the ground state expectation value of $\frac{1}{N}\sum_r S_r^x$. $\chi_\perp$ describes the response to an external magnetic field in a direction perpendicular to the staggered magnetization. We define

$$Z_\chi \equiv \frac{\chi_\perp}{\chi_{\perp,0}} \tag{2.32}$$

where $\chi_{\perp,0} \equiv \frac{1}{4dJ}$. Including the next correction in the $\frac{1}{S}$ expansion, we obtain the value $Z_\chi = 1 - \xi - 2\epsilon = 0.448$ for an isotropic spin-$\frac{1}{2}$ square lattice antiferromagnet.

2.2 Spin-Wave Theory in Finite Lattice

Numerical methods on spin Hamiltonians are generally limited to calculation of ground state correlation functions on a given *finite* lattice. Indeed in any finite size simulation the antiferromagnetic order parameter m is extracted by a systematic finite size study on a square lattice $N = L \times L$ of the spin-spin correlation function $C(R - R') = < \mathbf{S}_R \cdot \mathbf{S}'_R >$, *i.e.* :

$$m = \lim_{L\to\infty} \sqrt{\frac{1}{N}\sum_R (-1)^R C(R)}$$

Despite the accuracy between the extrapolated order parameter m and the spin-wave prediction, the validity of SWT is still questionable in principle since the agreement is based on a single (or few) extrapolated quantities. In some other cases, the systematic formulae for extrapolation is very hard to get. For the above reasons it is important to apply spin-wave theory directly on finite size and compare exact data obtained by Lanczos or Monte Carlo with the SWT approximation.

Several attempts to generalize SWT on finite size have recently been published [67][68]. However, as it will became clear in the following, all these approaches are based on unnecessary approximations to avoid spurious finite size divergencies for the $k = 0 = (0,0)$ and $k = Q = (\pi,\pi)$ spin-wave modes. In these approaches these divergencies are removed by imposing an *ad hoc* holonomic constraint on the sublattice magnetization: it is set to zero (as it should) on any finite size.

In the present section we derive a systematic spin wave expansion on a finite lattice. We show here that the mentioned spin-wave divergencies ("Goldstone

modes") do not affect spin rotation invariant quantities and a straightforward calculation of the spin-spin correlation function $C(R-R')$ is possible up to second order in $1/S$, fully consistent with the spin-wave theory expansion.

In order to simplify the derivation, we consider only the leading term in S. The high order contribution is straight forward. The classical state is the antiferromagnetic (Néel) state and we can use the following Holstein-Primakoff transformation:

$$\begin{array}{rclcrcl} S_i^\dagger &=& \sqrt{2S}(1-\frac{n_i}{4S})a_i & & S_j^\dagger &=& \sqrt{2S}a_j^\dagger(1-\frac{n_j}{4S}) \\ S_i^z &=& S-n_i & & S_j^z &=& n_j-S \end{array} \tag{2.33}$$

where a and $a^\dagger$ are canonical creation and destruction boson operators, and $n_i = a_i^\dagger a_i$ is the number of bosons at the site i. The indices i,j label lattice points R_i and R_j belonging to the two magnetic sublattices. After substituting these expressions in the Hamiltonian, we can use translation invariance and write the leading term of the Hamiltonian in terms of

$$a_k^\dagger = \frac{1}{\sqrt{N}}\sum_r e^{-ikr}a_r^\dagger$$

$$H = S^2 E_C + SH_{SW} + O(1)$$

$$E_C = -\frac{JZ}{2}N$$

is the classical energy and H_{SW} reads:

$$H_{SW} = JZ\sum_k [D_k a_k^\dagger a_k + \frac{1}{2}\eta_k(a_k^\dagger a_{-k}^\dagger + a_k a_{-k})] \tag{2.34}$$

Here $Z = 2d$ is the number of nearest neighbours, $\eta_k = \frac{\cos k_x + \cos k_y}{2}$, and the diagonal part in this particular case is constant $D_k = 1$. The leading part of the Hamiltonian is free and can be generally diagonalized by the known Bogoliubov transformation which acts independently on any k wavevector:

$$a_k = u_k\alpha_k + v_k\alpha_{-k}^\dagger$$

with

$$u_k = \sqrt{\frac{D_k+\epsilon_k}{2\epsilon_k}}$$

$$v_k = -sgn(\eta_k)\sqrt{\frac{D_k-\epsilon_k}{2\epsilon_k}}$$

$$\epsilon_k = \sqrt{D_k^2-\eta_k^2}$$

being the spin wave energy in unit of JZS. However the $k=0$ and $k=Q$ modes, important at finite size, cannot be diagonalized by this transformation

since u_k and v_k are not defined in this case. We can in fact define two hermitian operators that commute with the Hamiltonian

$$Q_x = a_0^\dagger + a_0$$

$$Q_y = i(a_Q^\dagger - a_Q)$$

and write the singular $k = 0, Q$ contributions in (2.34) in the form:

$$H_S = \frac{J_1 SZ}{2}(D_0 Q_x^2 + D_Q Q_y^2 - D_0 - D_Q).$$

The physical meaning of these two operators becomes clear if we use the Holstein-Primakoff transformation for the total spin along the x (y) axis $S^{Tot}_{x(y)} = \sum_R S_R^{x(y)}$. Then at leading order $Q_x = S_x^{Tot}/\sqrt{\frac{S}{2N}}$ and $Q_y = S_y^{Tot}/\sqrt{\frac{S}{2N}}$ and the singular part of the Hamiltonian

$$H_S \propto (S_x^{Tot})^2 + (S_y^{Tot})^2$$

represents a term which clearly favours the singlet ground state, in agreement with the Lieb-Mattis theorem[69].

Since Q_x and Q_y commute with the Hamiltonian, and $[Q_x, Q_y] = 0$, we can formally diagonalize the Hamiltonian *in a finite size* in a basis where Q_x and Q_y have definite quantum numbers. In the chosen basis Q_x and Q_y become classical numbers ranging continuously from $-\infty$ to ∞ and the Hamiltonian H_S becomes a simple classical contribution. The ground state has then $Q_x = Q_y = 0$, *i.e.* it is a singlet (as it should on any finite size and for any S)[69] and can be formally written as the normalizable Fock state $|0>_\alpha$ of the operators α_k, a_0 and a_Q projected onto the subspace of $Q_x = Q_y = 0$:

$$|\psi_{SW}> = \int_{-\infty}^{\infty} d\alpha \int_{-\infty}^{\infty} d\beta e^{i\alpha Q_x + i\beta Q_y} |0>_\alpha \tag{2.35}$$

This state is the formal ground state $|\psi_G>$ of H for $S \to \infty$ and includes usual spin-wave fluctuations on the Néel state $|N>$, i.e.

$$|0>_\alpha = \left(\prod_{k \neq 0,Q} \frac{e^{\frac{1}{2}\frac{v_k}{u_k} a_k^\dagger a_{-k}^\dagger}}{u_k} \right) |N>$$

Unfortunately ψ_{SW} after projection on $Q_x = Q_y = 0$ is eigenstate of operators with continuous spectrum and, as it is easily seen from (2.35), it cannot be normalized. This singular behaviour is a consequence of the large S expansion, since at any finite S the Hilbert space is finite and any operator on a finite

Hilbert space has a discrete spectrum. As a consequence for infinite S a Bose condensation of the $k = 0, Q$ modes occurs since the expectation value for the average number of modes

$$\frac{< \psi_{SW} | a_k^+ a_k | \psi_{SW} >}{< \psi_{SW} | \psi_{SW} >}$$

diverges for $k = 0$ or Q.

Nevertheless a systematic finite size study of *spin-rotation invariant quantities* as for example the ground state energy and the spin-spin correlation function $C(R - R')$ is indeed possible. For example the ground state energy derived in the previous example for Heisenberg Hamiltonian is perfectly finite and well defined on any finite lattice. In fact, having in mind that $Q_x = Q_y = 0$, we get for the contribution to the energy linear in S – the spin wave term –:

$$< H_{SW} >= E_{SW} = \sum{}' \frac{JZ}{2}(\epsilon_k - D_k) \; - \frac{JZ}{2}(D_0 + D_Q)$$

where $\sum{}'$ means summation over all k but $k = 0, Q$ in the Brillouin zone. Note also the non vanishing negative term coming from the careful analysis of the singular contribution H_S. This term is negligible at infinite size but is important for any accurate estimate of the energy at finite size.

2.3 Regularization

In order to calculate the next order correction in $\frac{1}{S}$ to the energy it is important – as well known by standard perturbation theory – to compute the expectation value of the perturbation V on the unperturbed state $|\psi_{SW} >$

$$< V >= \frac{< \psi_{SW} | V | \psi_{SW} >}{< \psi_{SW} | \psi_{SW} >} \tag{2.36}$$

Unfortunately as we have seen $< \psi_{SW} | \psi_{SW} >$ is infinite due to the presence of the singular modes at $k = (0, 0)$ and $k = (\pi, \pi)$ and Eq. (2.36) takes the indeterminate form $\frac{\infty}{\infty}$. The gaussian integral in Eq. (2.35) can be formally evaluated, yielding

$$|\psi_{SW} >= \exp[\frac{1}{2}(a_Q^{\dagger 2} - a_0^{\dagger 2})]|0 >_\alpha \tag{2.37}$$

Then it is easily verified that $Q_x|\psi_{SW} >= Q_y|\psi_{SW} >= 0$.

In order to regularize expression (2.37) without changing its gaussian form it is enough to introduce a parameter δ

$${}_R < \psi_{SW}| =_\alpha < 0|exp[\frac{\delta}{2}(a_Q^{\dagger 2} - a_0^{\dagger 2})] \tag{2.38}$$

In this way $\lim_{\delta \to 1} {}_R < \psi_{sw}| = < \psi_{sw}|$.

We define a regularization of the expression (2.36) by

$$\frac{< \psi_{SW}|V|\psi_{SW} >}{< \psi_{SW}|\psi_{SW} >} = \lim_{\delta \to 1} \frac{{}_R < \psi_{SW}|V|\psi_{SW} >}{{}_R < \psi_{SW}|\psi_{SW} >} \tag{2.39}$$

The previous form has the following advantages

- Both numerator and denominator are finite for $\delta \neq 1$
- The Wick's theorem can be applied because both ${}_R < \psi_{SW}|$ and $|\psi_{SW} >$ are gaussian "quasi-free" wavefunctions.
- If the perturbation contains the singular operators Q_x and Q_y, they do not contribute: $Q_x = 0$ and $Q_y = 0$ exactly for any δ.

The results obtained with such regularization should represent the correct $S \to \infty$ limits for spin rotational invariant correlation functions. In fact, at the end of the analytical calculation we have verified that $< S^2 >= 0$ up to the next leading order in $\frac{1}{S}$. Instead using a different regularization, say

$$< V >= \lim_{\delta \to 1} \frac{{}_R < \psi|V|\psi >_R}{{}_R < \psi|\psi >_R} \tag{2.40}$$

$< S^2 > \neq 0$, probably because the item (3) is not satisfied for the latter regularization (2.40).

It is clear however that a more rigorous mathematical analysis is necessary to prove that the $S \to \infty$ limits does not depend on the regularization, at least among all the possible ones that do not invalidate the singlet nature of the ground state.

Chapter 3

J_1-J_2 Model, J_x-J_y Model and Heisenberg Model on the Triangular Lattice

In this chapter, we will use the finite size spin wave theory to study several spin models in two dimensions. These includes the frustrated Heisenberg model (J_1-J_2 model)[62], the anisotropic Heisenberg model (J_x-J_y model)[70] and the Heisenberg model on a triangular lattice (AHT).[71]

3.1 J_1-J_2 Model

In order to get the spin-spin correlation function $C(r)$, we add the following spin-rotation and translation invariant term to the Heisenberg Hamiltonian

$$H' = \frac{1}{2} J_1 h_r \sum_{R\tau_\mu} \mathbf{S}_R \cdot \mathbf{S}_{R+\tau_\mu}$$

where the vectors τ_μ are equivalent lattice vectors in any of the possible orthogonal directions with $|\tau_\mu| = |r|$. By use of the Helmann-Feynman theorem the spin-spin correlation function is obtained by differentiating the ground state energy of the Hamiltonian in presence of the external perturbation with respect to h_r,

$$C(r) = \frac{2}{ZNJ_1} \frac{d}{dh_r} E_G(h_r).$$

In the following we describe in detail the calculation of the spin-spin correlation function on opposite sublattice. For $J_2 \ll 0.5$ th classical Néel state is still stable. Then the Hamiltonian can be expanded as:

$$H = S^2 E_C + S H_{SW} + H_{int} \tag{3.1}$$

where

$$E_C = -\frac{1}{2}(1-\alpha-h_r))J_1 N Z$$

where $\alpha = \frac{J_2}{J_1}$. H_{SW} is the leading free boson term in the expansion with

$$D_k = 1-\alpha(1-\delta_k)+h_r$$

$$\eta_k \rightarrow \eta_k + h_r\tau_k$$

$$\delta_k = \cos k_x \cos k_y$$

$$\tau_k = \frac{1}{Z}\sum_{\tau_\mu} e^{ik\tau_\mu}$$

and

$$\begin{aligned} H_{int} = & -\tfrac{1}{2N}J_1 Z \sum_{k_1k_2k_3k_4} \delta(k_1-k_2+k_3-k_4) \\ & (\eta_{k_1-k_2}-\alpha\delta_{k_1-k_2}+\beta\tau_{k_1-k_2})a^\dagger_{k_1}a_{k_2}a^\dagger_{k_3}a_{k_4} \\ & -\tfrac{1}{4N}J_1 Z \sum_{k_1k_2k_3k_4} [\delta(k_1-k_2-k_3-k_4)(\eta_{k_4}+\beta\tau_{k_4})a^\dagger_{k_1}a_{k_2}a_{k_3}a_{k_4} \\ & +\delta(k_1+k_2-k_3-k_4)\alpha\delta_{k_4}a^\dagger_{k_1}a^\dagger_{k_2}a_{k_3}a_{k_4}] + h.c \end{aligned} \tag{3.2}$$

The next leading contribution to the energy is obtained by the evaluation of

$$E_{int} = \frac{<\psi_{SW}|H_{int}|\psi_{SW}>}{<\psi_{SW}|\psi_{SW}>}$$

with the chosen regularization (2.39).

$$E_{int} = -\frac{1}{2}J_1 Z\frac{N}{4}(C_\eta^2 + h_r C_\tau^2 - \alpha C_\delta'^2) + H_{fs} \tag{3.3}$$

where

$$C_\eta = \frac{2}{N}\sum_k{}'(V_k^2+\eta_k U_k V_k)$$

$$C'_\delta = \frac{2}{N}\sum_k{}'(1-\delta_k)V_k^2$$

and C_τ is obtained substituting the function η_k with τ_k in the expression for C_η, while H_{fs} comes out after a careful treatment of the singular modes , yielding a finite size correction to the ground state energy:

$$H_{fs} = \frac{1}{2}J_1 Z(C_\eta + h_r C_\tau)$$

Differentiating

$$E_G = S^2 E_C + S E_{SW} + E_{int}$$

with respect to h_r and letting $h_r = 0$, we can get the spin-spin correlation function between two sites on different sublattices

$$\langle \mathrm{S}_0 \cdot \mathrm{S}_r \rangle = -(S - \frac{1}{2}C_\tau + \frac{1}{N})^2 + \frac{1}{N^2} - \frac{1}{2}\bar{C}_\eta \frac{\partial C_\eta}{\partial h_r} \tag{3.4}$$

where

$$C_\tau(r) = \frac{1}{N}\sum_k{}' \left\{ \frac{(1-\alpha+\alpha\delta_k) - \eta_k e^{ikr}}{[(1-\alpha+\alpha\delta_k)^2 - \eta_k^2]^{\frac{1}{2}}} - 1 \right\}$$

$$\bar{C}_\eta = C_\eta - C'_\delta$$

and

$$\frac{\partial C_\eta}{\partial h_r} = \alpha \frac{1}{N}\sum_k{}' \frac{[e^{ikr}(1-\alpha+\alpha\delta_k) - \eta_k]\eta_k(1-\delta_k)}{[(1-\alpha+\alpha\delta_k)^2 - \eta_k^2]^{\frac{3}{2}}}.$$

Similarly, we have the spin-spin correlation function between two sites on the same sublattice for $r \neq 0$

$$\langle \mathrm{S}_0 \mathrm{S}_r \rangle = (S - \frac{1}{2}C'_\tau)^2 - \frac{1}{2}\bar{C}_\eta \frac{\partial C'_\eta}{\partial h_r} \tag{3.5}$$

where

$$C'_\tau(r) = \frac{1}{N}\sum_k{}'(1-e^{ikr}) \left\{ \frac{(1-\alpha+\alpha\delta_k)}{[(1-\alpha+\alpha\delta_k)^2 - \eta_k^2]^{\frac{1}{2}}} - 1 \right\}$$

and

$$\frac{\partial C'_\eta}{\partial h_r} = \alpha \frac{1}{N}\sum_k{}'(1-e^{ikr}) \frac{(1-\delta_k)\eta_k^2}{[(1-\alpha+\alpha\delta_k)^2 - \eta_k^2]^{\frac{3}{2}}}.$$

In the previous quantities the singular contributions of the $k = 0, k = Q$ modes cancel out at the end of the calculation after many non trivial simplifications and E_{int} is perfectly defined and finite quantity, as well as its derivatives with respect to the field h_r.

The above equations fulfil the sum rule $N\sum C(R) = 0$ order by order in $\frac{1}{S}$, consistent with a singlet ground state[69].

Thus we have finally obtained an ordered expansion of the spin spin correlation function:

$$C(R) = (-1)^R S^2 + \alpha(R)S + \beta(R).$$

The order parameter m can then be expanded in the following way:

$$m(L) = S + \hat{\alpha} + \hat{\beta}/S$$

with $\hat{\alpha}$ and $\hat{\beta}$ simply related to the functions $\alpha(R)$ and $\beta(R)$ on finite size:

$$2\hat{\alpha} = \frac{1}{N}\sum(-1)^R \alpha(R)$$

$$2\hat{\beta} = \left(\frac{\sum(-1)^R\beta(R)}{N} - \hat{\alpha}^2\right)$$

The ground state energy per site for $h_r = 0$ is given by:

$$E = \frac{J_1}{2}\sum_{\mu}[C(\eta_\mu) + \alpha C(\delta_\mu)]$$

The low energy and long wave length physics of the Heisenberg magnets is determined by the two physical quantities: spin wave velocity and spin wave stiffness, as predicated by non linear σ model. Fisher and Ziman[72, 73] have shown that the spin wave velocity and spin wave stiffness is related to the finite size correction to the ground state energy and the square magnetization as:

$$\begin{aligned} \Delta E &= \frac{c_0}{\sqrt{N}}c \\ \Delta M^2 &= \frac{z}{4\rho_s\sqrt{N}}c' \end{aligned} \tag{3.6}$$

where c_0 is the spin-wave velocity and ρ_s is the spin stiffness. c and c' are two pure numbers which depend only on the lattice structure. For the square lattice,

$$c = \frac{1}{2\pi}\sum_{m\neq 0}\frac{1}{|m|^3} = 1.438.$$

$$c' = -\frac{1}{\sqrt{N}}\sum_{m\neq 0}\frac{1}{|m|} = -0.6208.$$

Within the finite size frame, both the correction to the ground state energy and the square magnetization can be calculated easily, hence the spin wave velocity and the spin wave stiffness.

$$\Delta E = -\frac{J_1 SZ}{4\pi N^{\frac{1}{2}}}c\left[\sqrt{2(1-2\alpha)} - \frac{1-\alpha}{S\sqrt{2(1-2\alpha)}}C_\eta(\infty) + \frac{\sqrt{2}\alpha}{S\sqrt{(1-2\alpha)}}C'_\delta(\infty)\right] \tag{3.7}$$

$$\Delta M^2 = \left(\frac{1}{2}M(\infty) - S\right)\sqrt{\frac{2}{(1-2\alpha)}}\frac{c'}{\sqrt{N}} - \frac{1}{2}\bar{C}_\eta(\infty)\alpha\left[\frac{1}{2(1-2\alpha)}\right]^{\frac{3}{2}}\frac{c'}{\sqrt{N}} \tag{3.8}$$

where $C_\eta(\infty)$, $C'_\delta(\infty)$, $\bar{C}_\eta(\infty)$ and $M(\infty)$ is the corresponding quantities calculated on the infinite lattice.

We show in Tab. 3.1 a comparison of spin-wave results and exact data on finite systems obtained mainly with Quantum Monte Carlo. The accuracy of the spin wave theory is confirmed even for any finite and large size. The finite size order parameter is always slightly smaller than the spin-wave prediction (with exception of the 12×12 lattice where error bars are too large). Our results give therefore a strong support to the existence of long range order in the $S = \frac{1}{2}$ Heisenberg antiferromagnet, and that the ground state can be

L	m_1	m_2	m_{exact}	E_1	E_2	E_{exact}
4	0.5238	0.5251	0.5259	-0.6920	-0.7026	-0.7017
6	0.4501	0.4545	0.4581	-0.6676	-0.6801	-0.6789
8	0.4133	0.4173	0.420	-0.6620	-0.6746	-0.6734
10	0.3913	0.3945	0.397	-0.6600	-0.6726	-0.6715
12	0.3766	0.3793	0.378	-0.6591	-0.6717	-0.6706
∞	0.3034	0.3034	0.3075	-0.6579	-0.6704	-0.6692

Table 3.1: First and second order contribution in $\frac{1}{S}$ for the staggered magnetization (m_1 and m_2) and ground state energy per site (E_1 and E_2) for the square lattice Heisenberg antiferromagnet as a function of the lattice size $N = L \times L$ for $J_2 = 0$. The exact values are obtained by diagonalization [38] or by quantum Monte Carlo[42].

$\frac{J_2}{J_1}$	m_1	m_2	m_{exact}	E_1	E_2	E_{exact}	L
0.05	0.5184	0.5122	0.5223	-0.6711	-0.6815	-0.6806	4
0.10	0.5118	0.5193	0.5180	-0.6508	-0.6607	-0.6598	=
0.15	0.5034	0.5166	0.5129	-0.6313	-0.6402	-0.6395	=
0.20	0.4922	0.5150	0.5066	-0.6128	-0.6200	-0.6199	=
0.30	0.4553	0.5283	0.4885	-0.5801	-0.5791	-0.5830	=
0.40	0.3602	0.7357	0.4573	-0.5592	-0.5233	-0.5511	=
0.10	0.4318	0.4439	0.445	-0.6281	-0.6397		6
0.20	0.4038	0.4344	0.431	-0.5914	-0.6004		=
0.30	0.3548	0.4414	0.405	-0.5595	-0.5613		=
0.40	0.2407	0.6309	0.370	-0.5377	-0.5121		=
0.05	0.2876	0.2922		-0.6383	-0.6504		∞
0.10	0.2687	0.2804		-0.6193	-0.6308		=
0.15	0.2458	0.2685		-0.6010	-0.6114		=
0.20	0.2171	0.2576		-0.5836	-0.5924		=
0.30	0.1301	0.2580		-0.5527	-0.5541		=
0.40	-0.0606	0.5086		-0.5312	-0.5078		=

Table 3.2: Same as in Tab. 3.1, for different values of J_2, and increasing sizes 4×4 (top), 6×6 (middle, data for m_{exact} taken from Ref. [39]) and $\infty \times \infty$ (bottom).

naturally represented by the Néel state dressed by small quantum fluctuations. The order parameter is very much close to the spin-wave predictions and in close agreement with the Monte Carlo estimate.

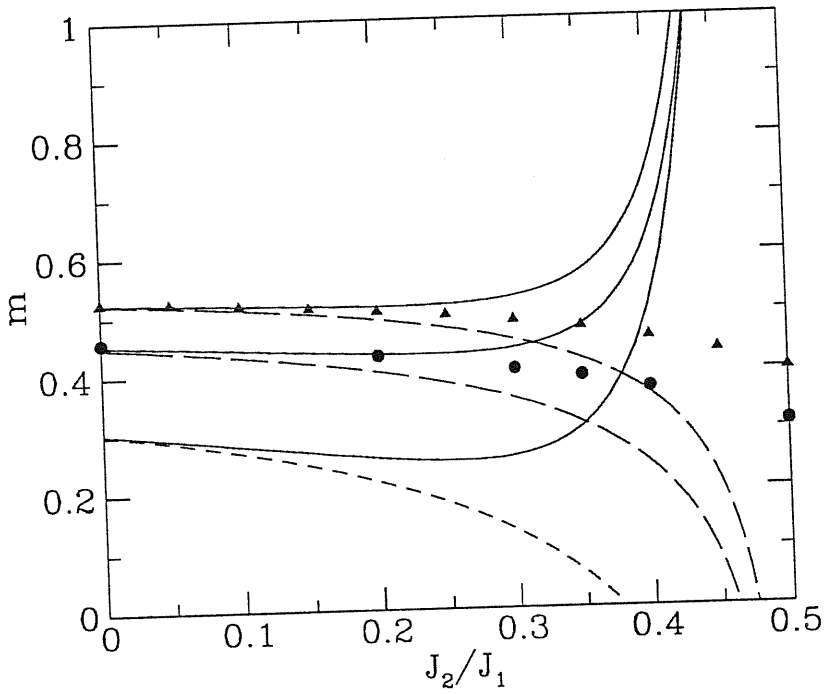

Figure 3.1: First order $S+\hat{\alpha}$ (dashed lines) and second order (continuous lines) correction $S+\hat{\alpha}+\frac{1}{S}\hat{\beta}$ for the order parameter m plotted for $S=1/2$ for a 4×4 (upper curves) and 6×6 lattice (lower curves). The full squares and triangles are the exact diagonalization data for the 4×4 and 6×6 respectively. The arrows indicate the value of J_2 where the second order contribution is worse than the first order estimate, suggesting a breakdown of the expansion.

As we turn on J_2 (See Tab. 3.1) the spin model is strongly frustrated and we expect the spin-wave expansion to be convergent or at least accurate in the

region where the order parameter is the same as in the classical case ($S \to \infty$). With this technique we can therefore detect a possible spin liquid state by looking for a breakdown of the spin-wave expansion for large J_2. We show in Fig.3.1 the order parameter as predicted by spin-wave theory compared with the available exact results on a 4×4 and 6×6 lattice as a function of $\frac{J_2}{J_1}$. The agreement is very good for $\frac{J_2}{J_1} < 0.2$ and in fact the second order contribution seems already enough to give an accurate answer. The infinite size prediction plotted in the same picture should therefore be quite reliable in this region.

For J_2 large enough the second order term does not improve the first order estimate and we can define a crossover value of $J_2 = J_C$ where the second order contribution becomes a worse estimate of the order parameter compared to first order one. As shown in Fig.3.1 we get $J_C = 0.30$ for the 4×4 lattice and $J_C = .35$ for the 6×6 one. These results indicate that a possible breakdown of the spin-wave expansion occurs already at $J_2 \sim 0.30$. This estimate is slightly different from the linear spin-wave result (see Fig.3.1) where a critical value of $\frac{J_2}{J_1} = 0.38$ for $S = \frac{1}{2}$ was found when the first order contribution of the order parameter $m_1 = S + \hat{\alpha}$ vanishes. However the next leading contribution to linear spin-wave $m_2 = S + \hat{\alpha} + \frac{\hat{\beta}}{S}$, that we have explicitly calculated in this work, indicates that the previous estimate is quite approximate because the higher order corrections have opposite sign and become more and more relevant close to the transition point.

3.2 J_x-J_y Model

Although it has been shown that the renormalization group flow drives the isotropic model towards weak coupling, making the spin wave theory asymptotically exact at long wavelengths, the validity of the spin wave theory in the anisotropic system is not obvious. In order to check the validity of the spin wave theory in the anisotropic system and to determine the critical point of the phase transition to the spin liquid state, we have perform the finite size spin wave analysis for the J_x-J_y model. Comparison between the results of the exact diagonalization and those of the finite size spin wave theory gives a estimate of $\frac{J_y}{J_x} \sim 0.1$ as the critical point.

From similar calculation as in the last section, the ground state energy is given by

$$E = C + H_{sw} + H_{int} \tag{3.9}$$

where

$$\begin{aligned}
C &= -\tfrac{1}{2}(J_x + J_y)S(S+1)Nz' \\
H_{sw} &= JSz' \sum_k{}' \sqrt{(1+\alpha)^2 + (\eta_x + \alpha\eta_y)^2} \\
H_{int} &= -\tfrac{1}{2}Jz'\tfrac{N}{4}(C_{\eta_x}^2 + \alpha C_{\eta_y}^2) + \tfrac{1}{2}Jz'(C_{\eta_x} + \alpha C_{\eta_y}) \\
\eta_x &= cosk_x \\
\eta_y &= cosk_y \\
C_{\eta_x} &= \tfrac{2}{N}\sum_k{}' (V_k^2 + \eta_x U_k V_k) \\
C_{\eta_y} &= \tfrac{2}{N}\sum_k{}' (V_k^2 + \eta_y U_k V_k) \\
\alpha &= \tfrac{J_y}{J_x}
\end{aligned} \tag{3.10}$$

In order to calculate the spin-spin correlation function, a magnetic field is introduced as in the last section. By using Helmann-Feynman theorem, We have the spin-spin correlation function

$$\langle \mathbf{S}_0 \cdot \mathbf{S}_\tau \rangle = -(S - \frac{1}{2}C_\tau)^2 + \frac{1}{N^2} - \frac{1}{4}\alpha C \frac{\partial C_{\eta_y}}{\partial \beta} \tag{3.11}$$

for the opposite sublattice.

$$\langle \mathbf{S}_0 \cdot \mathbf{S}_\tau \rangle = (S - \frac{1}{2}C'_\tau)^2 - \frac{1}{4}\alpha C \frac{\partial C'_{\eta_y}}{\partial \beta} \tag{3.12}$$

for the same sublattice but $r \neq 0$, where

$$\begin{aligned}
C_\tau &= \tfrac{1}{N}\sum_k{}' \left\{ \frac{(1+\alpha) - (\eta_x + \alpha\eta_y)e^{ikr}}{\sqrt{(1+\alpha)^2 - (\eta_x + \alpha\eta_y)^2}} \right\} \\
C'_\tau &= \tfrac{1}{N}\sum_k{}' (1 - e^{ikr}) \left\{ \frac{(1+\alpha)}{\sqrt{(1+\alpha)^2 - (\eta_x + \alpha\eta_y)^2}} - 1 \right\} \\
\tfrac{\partial C_{\eta_y}}{\partial \beta} &= 2\tfrac{1}{N}\sum_k{}' \frac{(\eta_x - \eta_y)[(1+\alpha)e^{ikr} - (\eta_x + \alpha\eta_y)]}{[(1+\alpha)^2 - (\eta_x + \alpha\eta_y)^2]^{\frac{3}{2}}} \\
\tfrac{\partial C'_{\eta_y}}{\partial \beta} &= 2\tfrac{1}{N}\sum_k{}' \frac{(\eta_x - \eta_y)[(1+\alpha)(1 - e^{ikr})(\eta_x + \alpha\eta_y)}{[(1+\alpha)^2 - (\eta_x + \alpha\eta_y)^2]^{\frac{3}{2}}} \\
C &= \tfrac{1}{N}\sum_k{}' \frac{(\eta_x - \eta_y)(\eta_x + \alpha\eta_y)}{\sqrt{(1+\alpha)^2 - (\eta_x + \alpha\eta_y)^2}}
\end{aligned} \tag{3.13}$$

In above expression, it is easy to show that when $J_y = 0$, *i.e.* $\alpha = 0$, the last term vanishes, when $J_y = J_x$, *i.e.* $\alpha = 1$, the last term also vanishes due to the fact that $C = 0$. In both cases, the previous results are recovered. Here the two different behaviors in one and two dimensions are coined in a single formulae.

From the calculated spin-spin correlation functions, the order parameter is calculated as we have done in the last section.

In order to check the validity of the spin wave theory, we have performed Lanczos diagonalization on several lattices up to 32 sites. The finite size spin wave theory compares quite favorably to numerical results in bipartite lattices for sufficient large J_y. As a consequence, SWT is able to describe the leading size corrections in finite lattices and therefore represents a powerful method for analyzing small size data.

The breaking down of the spin wave theory occurs at $\frac{J_y}{J_x} \sim 0.1$, as shown in Fig.3.2 where a finite size estimate of the order parameter is plotted as a function of the anisotropy α. The breakdown of SWT at $\alpha < 0.1$ again suggests that a qualitative change in the ground state properties is occurring in this regime.

It is important to note that the critical point increases, when higher order expansions are included. The *increase* of the critical anisotropy parameter α_c in going from first to second order gives confidence about the actual occurrence of the transition, which is in fact enhanced by quantum fluctuations. Therefore, on the basis of the field theory mapping and SWT, we expect that by lowering the anisotropy parameter $\alpha = J_y/J_x$ a disordered phase sets in within a finite interval $\alpha_c > \alpha > 0$. This prediction should be qualitatively correct because field theory methods are known to reproduce the physics of QAF both in the isotropic two dimensional limit[47] and in the one dimensional ($\alpha = 0$) case, provided the topological term is included in (1.6)[8].

More detailed study of the spin liquid state in this model will be presents in the next chapter.

3.3 Heisenberg Model on the Triangular Lattice

The triangular lattice consists of three sublattices, A, B and C, with spins on each sublattice at an angle of $\frac{2\pi}{3}$ to those on the other two sublattices. Nearest-neighbor pairs of spins are on different sublattices, while each spin is on the same sublattice as all of its second neighbors at distance $\sqrt{3}$, nearest-neighbor spacings. We choose a particular classical ground state with spins on the A sublattice oriented along the z axis, and those on the B and C sublattice oriented $\frac{2\pi}{3}$ away from the z axis in the x-z plane (the sites are lying in the x-z plane and the rotation between A and B is around the y axis perpendicular to the plane). We then introduce the three kinds of Holstein-Primakoff bosons a, b and c, on the sublattice A, B and C, respectively to parameterized the spin operators. The species a describes the quantum fluctuations of the spin away from its classical direction z: $S_z = S - a^\dagger a$, $S^\dagger = a\sqrt{2S}$ and $S^- = a^\dagger\sqrt{2S}$ (at leading order). On the other sublattices we have to take into account the $\frac{2\pi}{3}$

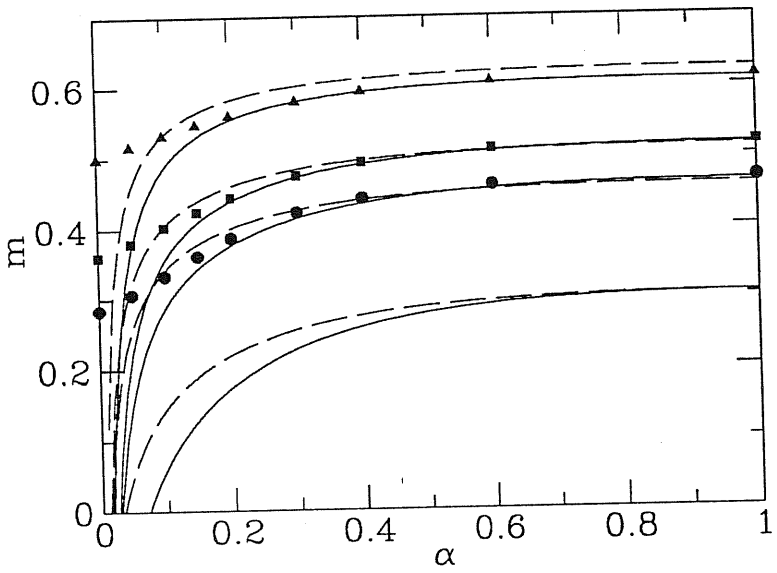

Figure 3.2: Order parameter $m = \sqrt{S(\pi,\pi)/V}$ for different lattice sites compared with the first (dashed lines) and second order (continuous line) SWT results. The Lanczos data are obtained on tilted lattices $L\sqrt{2} \times L\sqrt{2}$ with $L = 2$ (triangles), $L = 3$ (squares) and $L = 4$ (circles). The lowest curves refers to the infinite size SWT results.

rotation so that on the C sublattice:

$$\begin{aligned} S_x &= \tfrac{\sqrt{3}}{2}(S - c^\dagger c) + \sqrt{2S}\left[-\tfrac{1}{2}\tfrac{c+c^\dagger}{2}\right] \\ S_z &= -\tfrac{1}{2}(S - c^\dagger c) + \sqrt{2S}\left[-\tfrac{\sqrt{3}}{2}\tfrac{c+c^\dagger}{2}\right] \\ S_y &= \sqrt{2S}\tfrac{c-c^\dagger}{2i} \end{aligned} \tag{3.14}$$

at the order we need in the $\frac{1}{S}$ expansion. On the B sublattice, we just rotate by $-\frac{2\pi}{3}$. We then substitute in the Hamiltonian and expand, keeping only the quadratic part in the H-P oscillators.

It is then necessary to introduce the Fourier transforms of the bosonic operator a, b and c. Each sublattice is itself triangular so that all k vectors are living in a hexagonal Brillouin zone. This leads to the following formula:

$$H = \frac{1}{6} JSz \sum_k \left[(\alpha_k^\dagger, \beta_k) H_0(k) \begin{pmatrix} \alpha_k \\ \beta_k^\dagger \end{pmatrix} - 3 \right] \tag{3.15}$$

where

$$\alpha_k = \begin{pmatrix} a_k \\ b_k \\ c_k \end{pmatrix} \tag{3.16}$$

and $\alpha_k = \beta_{-k}$. The new Hamiltonian to be diagonalized is $H_0(k)$, a 6×6 matrix of the form

$$H_0(k) = \begin{pmatrix} 1+M & -3M \\ -3M & 1+M \end{pmatrix} \tag{3.17}$$

where

$$M = \begin{pmatrix} 0 & z & z^* \\ z^* & 0 & z \\ z & z^* & 0 \end{pmatrix} \tag{3.18}$$

In this formula, the complex number z is given by

$$z = \frac{1}{12} \sum_L e^{ik\delta_L} \tag{3.19}$$

where $L = 1, 2, 3$ and the two-dimensional vectors δ_L are pointing towards half of the neighbors of a site. We made use of the set

$$\delta_1 = (1, 0), \qquad \delta_2 = (-\frac{1}{2}, \frac{\sqrt{3}}{2}), \qquad \delta_3 = (-\frac{1}{2}, -\frac{\sqrt{3}}{2}) \tag{3.20}$$

The key observation is that all the 3×3 blocks building $H_0(k)$ are permutation matrices and thus can be diagonalized simultaneously in the basis.

$$\begin{aligned} u_1 &= (1, 1, 1) \\ u_2 &= (1, j, j^2) \\ u_3 &= (1, j^2, j) \end{aligned} \tag{3.21}$$

with $j = exp(2i\pi/3)$. The appearance of the cubic roots of the unity is the manifestation of the ternary symmetry of the problem.

Choosing that

$$U = \begin{pmatrix} 1 & 1 & 1 \\ 1 & j & j^2 \\ 1 & j^2 & j \end{pmatrix} \tag{3.22}$$

we can diagonalize the Hamiltonian $H_0(k)$ to a block form

$$H_0'(k) = \begin{pmatrix} U^{-1} & 0 \\ 0 & U \end{pmatrix} \begin{pmatrix} 1+M & -3M \\ -3M & 1+M \end{pmatrix} \begin{pmatrix} U & 0 \\ 0 & U^{-1} \end{pmatrix} \tag{3.23}$$

Then the Hamiltonian is decoupled to three modes:

$$H_0^i(k) = \begin{pmatrix} 1+\rho_i & -3\rho_i \\ -3\rho_i & 1+\rho_i \end{pmatrix} \tag{3.24}$$

where $i = 1, 2, 3$ and $\rho_1 = z + z^*$, $\rho_2 = zj^2 + z^*j$ and $\rho_3 = zj + z^*j^2$.

The three 2×2 Hamiltonian have the usual form as that in the square lattice. However, only the first mode can be diagonalized by the usual Bogoliubov transformation. This is because that for the other two modes $\rho_i(k) \neq \rho_i(-k)$. For example,

$$\rho_2(k) = \rho_3(-k) \neq \rho_2(-k) \tag{3.25}$$

We have to carefully symmetrize the other two mode, which leads to the mixture of the 2^{nd} and 3^{rd} modes. Finally, to the leading order,

$$H_0 = JSz \sum_k [\omega_1(\alpha_1^\dagger \alpha_1 + \frac{1}{2}) + 2\omega_2(\alpha_2^\dagger \alpha_2 + \frac{1}{2})] - \frac{3}{2} JNSz \tag{3.26}$$

where

$$\begin{aligned} \omega_1(k) &= \sqrt{(1-2\rho_1)(1+4\rho_1)} \\ \omega_2(k) &= \sqrt{(1-2\rho_2)(1+4\rho_2)} \end{aligned} \tag{3.27}$$

To the leading order of $\frac{1}{S}$, there are three Goldstone modes due to the structure of the lattice. It is important to note that two of them are degenerate.

The remind part of the calculation is the same as in the last two section. We will not repeat them here. It turns out that in the first order perturbation theory the singular modes (now the singular mode is located at $k = (0, 0)$) cancel. Both of the ground state energy and the staggered magnetization have the same form as in the infinite lattice with summation over all possible points of the Brillouin zone except the singular modes.

Comparison with the results of the exact diagonalization shows that the ground state has Néel long range order, contrary to the previous results of the finite size extrapolation. (See Fig.3.3) Bernu *et al* carried out the same analysis with the symmetry study of the numerical spectra and got the same results. [74] (Fig.3.3 is taken from their unpublished paper).

Finite-size scaling analysis indicates that the leading correction to these parameters should go as $N^{-1/2}$; analysis of the results (see fig.3.3) shows that for these small values of N the subleading correction is important: the $N \to \infty$ extrapolation is thus rather difficult, but an extrapolation to a zero value seems highly improbable.

The careful comparison between the exact results and the first-order spin-wave results leads us to conclude that the spin-wave approximation seems an

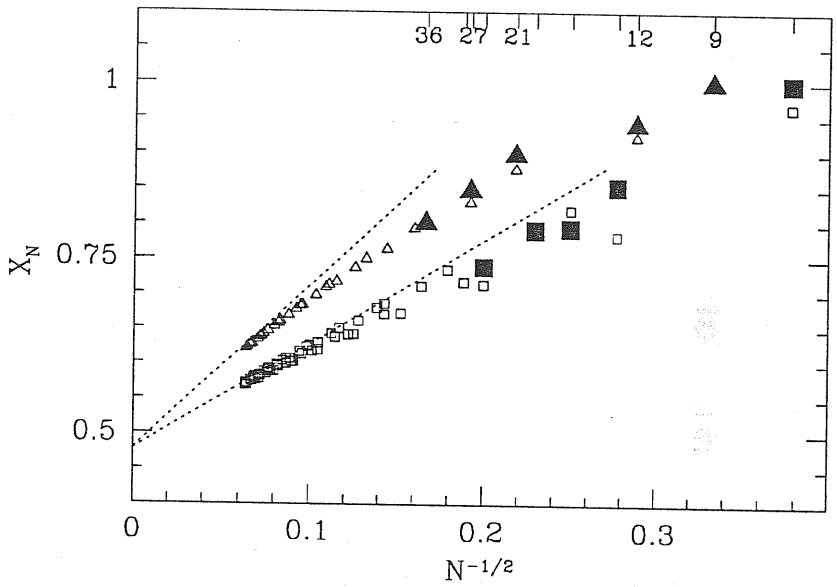

Figure 3.3: Néel order parameter as a function of the sample size. The order parameter is normalized by its maximum value. Triangles (resp. squares) stand for $N = 3p$ (resp. $N = 3p+1$) samples; black symbols stand for diagonalization results; open symbols stand for first order spin-wave results; dotted lines : large N fits ($N > 5000$) of first-order spin-wave results ($X_N = X_\infty + aN^{-1/2}$).

extremely good quantitative approximation for the considered sizes; on the basis of the present data, it seems highly hazardous to adopt other estimate of the thermodynamic limit than the spin-wave results[15]

Chapter 4

Spin Liquid State in the J_x-J_y Model

As we have shown in the previous chapter, there exists a finite regime in anisotropy parameter space, where spin wave theory breaks down and a spin liquid state sets in. In this chapter, we will present a detailed study of the spin liquid state.[70] We will also discuss the difference behaviors between the even and odd numbers of chains. The two dimensional square lattice is shown following the behaviors of the odd numbers of chains. A phase diagram for a generic spin model will be presented in the end of this chapter.

4.1 Energy Spectrum and Gapless State

Further numerical evidence of the phase transition can be obtained by the structure of the energy spectrum as a function of the total uniform magnetization. According to a recent analysis[75] the presence of Néel long range order in the thermodynamic limit reflects in the structure of the energy spectrum in finite size systems. In fact, if long range antiferromagnetic order is present in the system, the dependence of the energy $E(S)$ on the total spin S must follow the approximate relation:

$$E(S) \sim E(0) + S(S+1)/(2I_N) \tag{4.1}$$

up to a maximum value S_{max} of the order of the square root of the number of sites N. Eq. (4.1) approximately reproduces the energy spectrum of a spin-S rigid rotator with a momentum of inertia per site I_N/N corresponding to the uniform susceptibility χ of the model. Notice that this criterion correctly reproduces the absence of antiferromagnetic long range order in one dimension where the energy spectrum scales as[8] $E(S) \sim E(0) + S^2/(2\chi N)$. The relation (4.1)

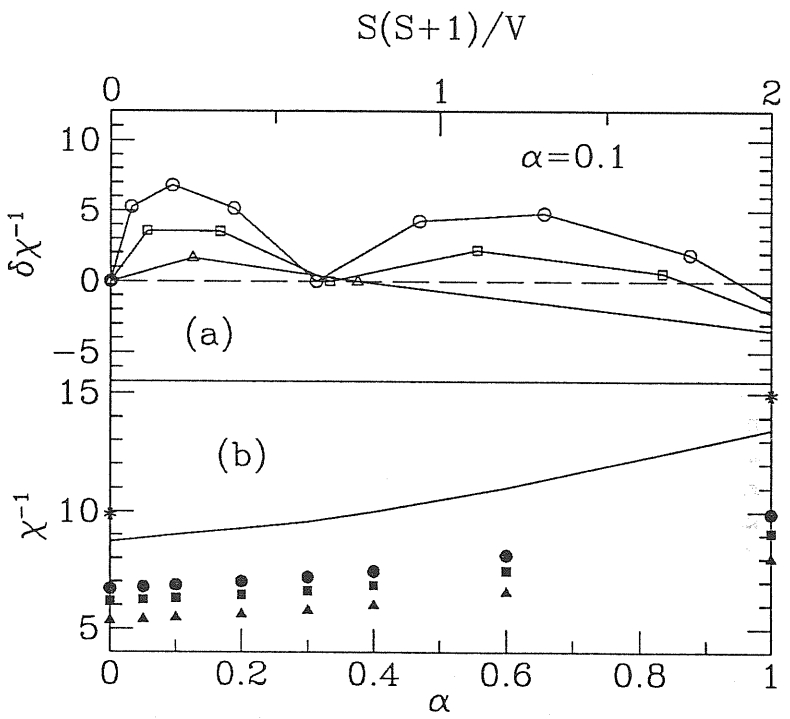

Figure 4.1: *a*): rigid rotator anomaly $\delta\chi^{-1} = V(E(S) - E(0)) - 1/(2\chi_L)$, where χ_L is estimated on finite sizes for 8 (triangles), 18 (squares) and 32 (circles) lattice sites. The continuous lines are guides to the eye, the dashed line represents the ideal behaviour in a quantum antiferromagnet. *b*): Finite size scaling of the inverse susceptibility. The finite size data (notation as in Fig.3.2) extrapolated (see text) to infinite size (continuous line). The stars are the exact values in the isotropic and one dimensional case.

is in fact quite well verified both for the isotropic system and for the anisotropic

ones up to $\alpha \sim 0.1$ where significant discrepancies appear (see Fig.4.1a). The strong deviations from Eq. (4.1) which develop in the numerical data can be directly related to the asymptotic decoupling of the chains in the square lattice, leading to an approximate *linear* dependence $E(S) \sim E(0) + \Delta S$. This anomaly does not seem to scale to zero in the thermodynamic limit but instead persists in all the lattices we have analyzed. From our finite size data an accurate estimate of the uniform susceptibility can be extracted by a quadratic fit of the energy spectrum $E(S)$ at small but finite (uniform) magnetization S/N. The results can then be extrapolated to infinite volume by use of a finite size scaling of the form[42] $\chi^{-1} = \chi_\infty^{-1} + A N^{-1/2} + B/N$ which is known to work both in the isotropic limit and in one dimension (extreme anisotropy). The extrapolation, shown in Fig.4.1b for several values of the anisotropy parameter, is in fact in good agreement with the known values at $\alpha = 0$ and $\alpha = 1$ (also shown in the figure) and predicts a smooth, featureless susceptibility in the whole anisotropy range. This result indicates that the system remains gapless across the phase transition and suggests that the nature of the disordered phase of this model might be more exotic than the expected nondegenerate singlet, in agreement with a conjecture put forward by Haldane[8].

4.2 Even *v.s.* Odd Number of Chains

However, the possibility of a gapless phase contrasts with the commonly accepted phase diagram of the model (1.5) defined on two chains[76, 77] where a gap $\Delta(\alpha)$ is believed to open at every finite value of the anisotropy parameter α. The disordered phase in the two chain model is in fact continuously connected with the $\alpha \to \infty$ limit where the gap is interpreted as the effect of the finite size of the lattice along the y direction. The same result actually holds for every *even* number of chains while an *odd* chain model remains gapless all the way to the $\alpha \to \infty$ limit. Therefore it is not too surprising that the Hamiltonian (1.5) on square clusters preserves the peculiarities of the odd chain sequence and does not open a gap at any α. In finite clusters, however, a gap is always present and we must investigate whether it disappears in the thermodynamic limit. We have analyzed the finite size scaling of the gap in the case of two chains ($L \times 2$), three chains ($L \times 3$) with antiperiodic boundary conditions along the y direction, and for square clusters. For any α the lowest excited state is always a triplet but its size dependence is quite different in the three cases. In order to see whether a gap is present in the strong anisotropic region we assumed that, for $\alpha \to 0$ and $L \to \infty$, the gap $\Delta(L, \alpha)$ can be expressed in a scaling form, as usual near a critical point:

$$\Delta(L, \alpha) = \Delta(L, 0)\, F\left[\alpha L \,(\log\, L)^{1/2}\right] \tag{4.2}$$

where the one dimensional gap $\Delta(L, 0)$ is known to scale as $1/L$. The specific form (4.2) has been chosen in order to match with first order perturbation theory

in α and does not depend on the number of chains of our lattice. However, the scaling function $F(x)$ behaves quite differently in the three geometries, as can be seen in Fig.4.2. The correctness of our scaling form (4.2) can be inferred by the collapse of the finite size numerical data on a smooth curve in all cases, provided α is sufficiently small. The region where the universal curve $F(x)$ is defined increases with growing size and the thermodynamic limit at fixed (small) α corresponds to the large x region of the scaling curve which should be extrapolated from the finite size data. In the two chain model $F(x)$ clearly goes through a minimum and then grows, suggesting a linear asymptotic behavior at large x which implies a finite gap of order J_y at small α in agreement with field theoretical analysis[76]. Instead, the scaling function is always monotonic both in the three chain case and, even more convincingly, in the square clusters, supporting the absence of a gap in these systems.

4.3 Decoupling and Phase Diagram

In order to understand how a disordered gapless phase may appear in 2D it is useful to consider other physical quantities like the spin-wave velocity and the momentum dependence of the magnetic structure factor. Again, SWT provides a valuable help in the interpretation of the numerical results. The spin velocity is almost constant at all anisotropies ranging between the one dimensional value $c_x = \pi/2$ and the isotropic limit[42] $c_x \sim 1.56$ which are both reproduced within 10% by second order SWT generalized to anisotropic models. A surprising result of SWT is the enhancement of the anisotropy in the spin velocity ratio induced by quantum fluctuations:

$$\left(\frac{c_y}{c_x}\right)^2 = \alpha Z(\alpha) \quad Z(\alpha) = 1 - \frac{1}{2S} C(\alpha) \tag{4.3}$$

$$C(\alpha) = \frac{1}{N} {\sum_k}' \frac{(\cos k_x - \cos k_y)(\cos k_x + \alpha \cos k_y)}{\sqrt{(1+\alpha)^2 - (\cos k_x + \alpha \cos k_y)^2}}$$

In fact, while at lowest order the spin velocity ratio coincides with the anisotropy parameter, the one loop calculation always reduces the $Z(\alpha)$ factor. Obviously, the correction $C(\alpha)$ vanishes at the isotropic point $\alpha = 1$ but diverges logarithmically in the $\alpha \to 0$ limit. Therefore, SWT suggests the occurrence of a decoupling transition at a finite value of α signaled by $Z(\alpha_c) = 0$. The same anisotropy renormalization factor $Z(\alpha)$ governs the long wavelengths behavior of the physical correlation functions. In particular, the magnetic structure factor behaves as

$$S(k_x, k_y) \propto \sqrt{k_x^2 + \alpha Z(\alpha) k_y^2} \tag{4.4}$$

In order to verify these predictions we tested Eq.(4.4) against Lanczos diagonalization in the 32 sites lattice. The results are shown in Fig.4.3 together with the

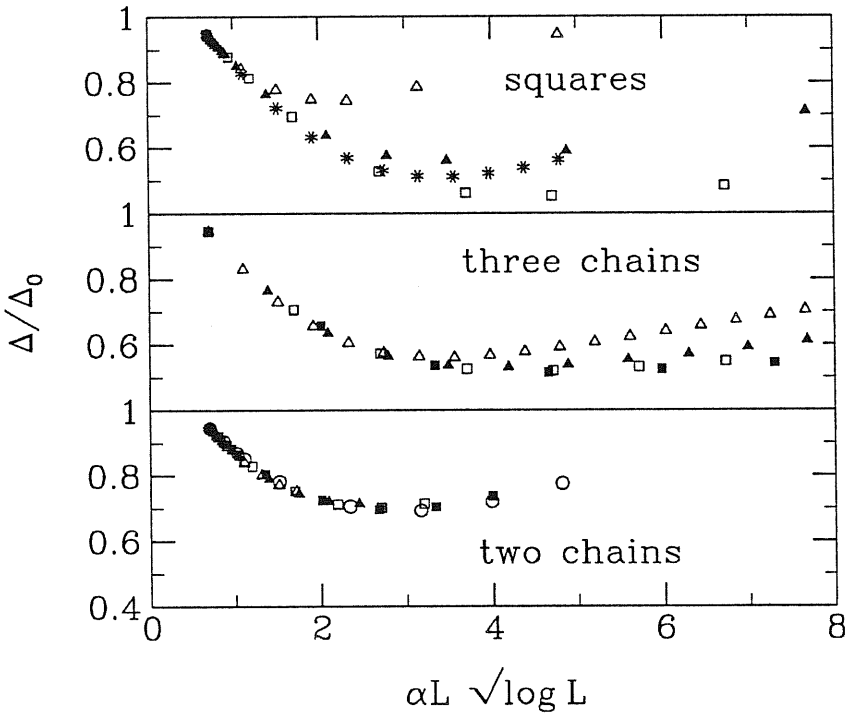

Figure 4.2: Diagonalization data of the gap scaling function (see Eq. 4.2) for the two chain model, three chains and square clusters. For the two and three chains, open triangles refer to $L = 4$, full triangles $L = 6$, open squares $L = 8$, full squares $L = 10$, open circles $L = 12$. For the square clusters open triangles correspond to 8 sites, full triangles to 18 sites, open squares to 32 sites and stars to the 4×4 cluster.

zero and one loop SWT results for the spin velocity ratio in the thermodynamic limit. The numerical data are in good agreement with the spin-wave results

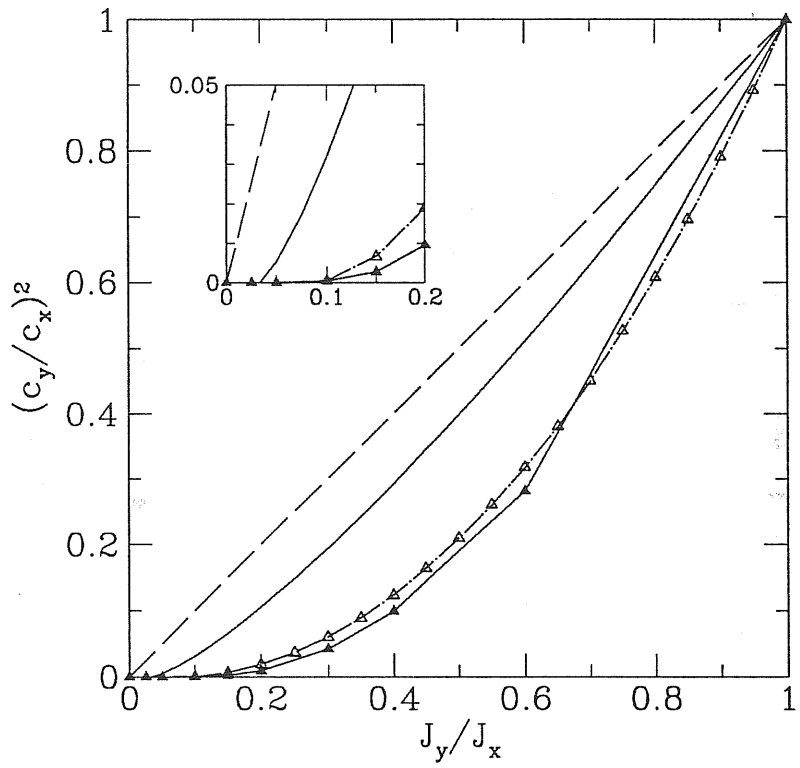

Figure 4.3: Square of the spin velocity ratio vs. anisotropy. The dashed line is the leading SWT result, the continuous line includes the one loop correction in the thermodynamic limit. Finite size estimates on a 32-site lattice for $\alpha Z(\alpha)$ are obtained by exact diagonalization (full triangles) and second order finite size SWT [62] (open triangles).

in the 32 site lattice, and show an even larger effect. Therefore we are led to conclude that at long wavelengths a decoupling transition may actually occur in strongly anisotropic spin models. The phase diagram of the anisotropic model

(1.5) suggested by SWT is depicted in Fig.4.4 for generic spin S systems. The transition line where the staggered magnetization vanishes has been calculated at the lowest order spin-wave level together with the locus $Z(\alpha) = 0$ where we expect a "decoupling transition". At the same order in $1/S$ we have found that these two lines approximately coincide up to a critical value of α beyond which the system disorders without decoupling. In the strong anisotropy limit the transition is characterized by the vanishing of both the staggered magnetization and the spin velocity ratio leading to a picture of basically uncoupled chains with interesting experimental consequences about the possibility to observe 1D behavior in real systems. We believe that this phase diagram is qualitatively correct although higher order terms in the SWT expansion (available only for the magnetization) may quantitatively change the phase transition line. In order to fully characterize the disordered phase, topological defects must be taken into account leading to a possible difference between integer and half integer spin systems[8].

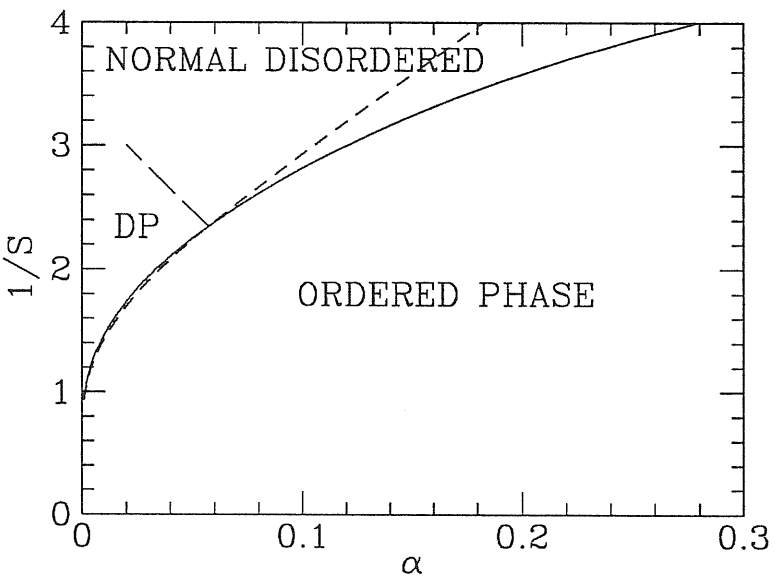

Figure 4.4: Phase diagram of the spatially anisotropic Heisenberg model obtained via one loop SWT. The order parameter vanishes along the continuous line and the spin-wave velocity ratio along the dashed line. The long dashed line indicates a crossover transition between a decoupled phase (DP) and a normal disordered phase with a finite spin velocity ratio.

Chapter 5

t-J_z Model

In the following chapter, we will study another different but related topic, *i.e.* the doped spin systems. This is highly challenge problem in understanding the strongly correlated electron systems.[78, 79] In order to minic the problem, we will concentrate on the single hole in the Néel background. With the new Lanczos Spectra Decoding (LSD), we successfully solve the problem in the infinite two chains and the square lattice. Despite the neglecting of the spin fluctuations, our results is believed to provide useful insights in the strongly correlated electron systems.

In this chapter, we will first introduce a transformation to eliminate the charge degree of freedom to get an effective spin Hamiltonian in a given momentum subspace. With this effective Hamiltonian, we can formally express the single hole Green's function as an expansion of the skeleton paths. Then we will discuss the effect of spin charge decouling on the single hole Green's function. We will show that spin charge decoupling is an exact property in the Bethe lattice but it is not fulfilled for more realistic lattices where the hole can describe closed loop paths during its motion.

5.1 Effective Spin Hamiltonian

The t-J_z Hamiltonian (1.7) is translation invariant and the most general one-hole state with total spin $S_z^T = M_z - \frac{1}{2}$ and total momentum $-p$ (hole momentum p) can be written as

$$|\psi_p> = \frac{1}{\sqrt{N}} \sum_{R,\sigma} e^{ipR} c_{R,\sigma} T_R |S_O> \tag{5.1}$$

where $|S_O>$ is a pure spin state that satisfies: i) $n_R|S_O> = |S_O>$ for all sites R, ii) $n_{1O}|S_O> = |S_O>$ *i.e.* the spin at the origin is fixed to $\sigma_0 = -\frac{1}{2}$, iii) the total spin along the z-axis is a well defined quantum number on the state

$|S_O>$, *i.e.* $S_z^T|S_O>= M_z|S_O>$. The operator T_R in (5.1) is the translation operator that brings the origin O to the lattice point R. It is formally defined by:

$$T_R c_{R',\sigma} T_{-R} = c_{R+R',\sigma} \tag{5.2}$$

States with definite momentum $|\psi_p>$ are eigenstates of T_R such that $T_R|\psi_p> = e^{-ipR}|\psi_p>$, as it is easy to check using relation (5.2) in the definition (5.1). Note also that the sum over σ in the definition of $|\psi_p>$ in (5.1) is used only for later convenience since $c_{R,\sigma}T_R|S_O>= T_R c_{O,\sigma}|S_O>$, which is non vanishing only for $\sigma = -\frac{1}{2}$.

The state $|\psi_p>$ in (5.1) represents the most general one-hole state with given hole momentum p and definite total spin projection along the z-axis S_z^T. In fact, the Hilbert space spanned by $|S_O>$ contains $D_{S_O} = \binom{N-1}{N_\uparrow}$ vectors, while the Hilbert space of one hole contains $D_H = \binom{N}{N_\uparrow}\binom{N-N_\uparrow}{N-N_\uparrow-1}$ vectors, where $N_\uparrow = \frac{S_z^T+N}{2}$ is the number of spin up electrons. Since all of the one hole states with definite momentum have the same dimension, such dimension is equal to $\frac{D_H}{N}$, *i.e.* it is exactly equal to the dimension D_{S_O} of a spin system defined on $N-1$ sites.

After the identification of the one hole Hilbert space with the Hilbert space of a spin model it is then possible to derive a pure spin-Hamiltonian. We evaluate the expectation value of the t-J_z Hamiltonian on the one-hole state $|\psi_p>$, $E_p =<\psi_p|H|\psi_p>$, and consider first the case $J_z = 0$:

$$E_p = \frac{t}{N} \sum_{R_1,R_2,R,\tau_\mu,\sigma,\sigma_1,\sigma_2} e^{-ip(R_1-R_2)} < S_O|T_{-R_1} c^\dagger_{R_1,\sigma_1} \hat{P}\ c_{R+\tau_\mu,\sigma} c^\dagger_{R,\sigma} c_{R_2,\sigma_2} T_{R_2}|S_O> \tag{5.3}$$

Now i) $\sigma_1 = \sigma_2$ since the total S_z^T has to be conserved in order to give a non-vanishing contribution in E_p. ii) $R = R_2$ and $R+\tau_\mu = R_1$, otherwise we create a doubly occupied site which is projected out either by $\hat{P}$ or by overlapping with $<S_O|$. Finally we obtain that $E_p =<S_O|H_p^{eff}|S_O>$ with:

$$H_p^{eff} = t \sum_{\sigma,\sigma',\tau_\mu} e^{-ip\tau_\mu} T_{-\tau_\mu}(c^\dagger_{\tau_\mu,\sigma'} c_{\tau_\mu,\sigma} c^\dagger_{O,\sigma} c_{O,\sigma'}). \tag{5.4}$$

H_p^{eff} acts only on spin states and in fact for $S = \frac{1}{2}$ it is possible to express the term between parenthesis in terms of spin operators only:

$$\chi_{R_i,R_j} = \sum_{\sigma,\sigma'} c^\dagger_{R_i,\sigma'} c_{R_i,\sigma} c^\dagger_{R_j,\sigma} c_{R_j,\sigma'} = \frac{1}{2} n_{R_i} n_{R_j} + 2\mathbf{S}_{R_i}\cdot\mathbf{S}_{R_j} \tag{5.5}$$

Finally H_p^{eff} reads:

$$H_p^{eff} = t\sum_{\tau_\mu} e^{-ip\tau_\mu} T_{-\tau_\mu}\chi_{O,\tau_\mu} = t\sum_{\tau_\mu} e^{ip\tau_\mu}\chi_{O,\tau_\mu} T_{\tau_\mu}. \tag{5.6}$$

Notice that the product of the operators $T_{-\tau_\mu}$ and χ_{O,τ_μ} appearing in H_p^{eff} is still a permutation of spins which leaves the origin O unchanged. Moreover the operator χ just interchanges the spins at sites R_i and R_j we have that $\chi_{R_i,R_j} = \chi_{R_j,R_i}$ and that $\chi^2_{R_i,R_j} = 1$.

Analogously for $J_z \neq 0$, by following the same steps, we have to add to H_p^{eff} the conventional spin contribution without all the bonds connecting the hole at the origin O:

$$H_p^{eff} = t \sum_{\tau_\mu} e^{ip\tau_\mu} \chi_{O,\tau_\mu} T_{\tau_\mu} + J_z \sum_{(i,j)\neq O} S^z_{R_i} S^z_{R_j} \tag{5.7}$$

The full Hamiltonian commutes with $\mathbf{S}_O$ (since it actually does not depend on the spin at the origin) and thus it can be defined on $N-1$ sites.

In conclusion for any eigenstate $|S_O>$ of H_p^{eff} with definite $S^z_O|S_O>= -\frac{1}{2}|S_O>$ we have an eigenstate of the t-J_z Hamiltonian written in the form (5.1). In fact, by use of the variational principle any eigenstate of (1.7) or (5.6) is obtained by $\frac{\delta}{\delta\psi_p} < \psi_p|H|\psi_p >= 0$, $\frac{\delta}{\delta S_O} < S_O|H|S_O >= 0$ with the condition $< \psi_p|\psi_p >= 1$, $< S_O|S_O >= 1$ respectively. Since $E_p =< \psi_p|H|\psi_p >=< S_O|H_p^{eff}|S_O >$ and $< \psi_p|\psi_p >=< S_O|S_O >$, it clearly follows that all the eigenstates of H_p^{eff} with definite spin at the origin define a true eigenstate of H by use of (5.1). The one hole problem can be therefore formulated in terms of a diagonalization of a pure spin Hamiltonian H_p^{eff} for the given momentum p. [80] A similar effective Hamiltonian can be obtained for the t-J model, by substituting S^z with S in (5.7).

It is interesting to note that H_p^{eff} is not translational invariant and that the momentum of the hole appears as a simple parameter. It is just this property that will allow us to diagonalize the t-J_z model in certain momentum subspace in the infinite lattice.

As it is shown in the Appendix many useful dynamical quantities such as the Green's function and current operators can be easily translated in terms of spin operators acting on this spin Hilbert space where the hole is fixed at the origin.

5.2 Green's Function for $J_z = 0$

Following Brinkman and Rice[54], we can expand the Green's function G in terms of the momenta $< H|(H_p^{eff})^k|H >$ of the Hamiltonian on the translation invariant ground state of the undoped system $|H>$. For $J_z = 0$ at vanishing doping the Hamiltonian is classical and $|H>$ is given by:

$$|H>= \frac{1}{\sqrt{2}}(|N> + |N'>) \tag{5.8}$$

where $|N>$ and $|N'>$ are the two possible determination of the Néel state.

The one hole Green's function can be generally written as a summation of all possible path described by the hole during its motion through the lattice. A path is then defined by a set of coordinates $\{R_l\}^n$ with $l = 1, ..., k$, which are connected by nearest neighbor vectors τ_μ

$$R_l - R_{l-1} = \tau_{\mu_l}. \tag{5.9}$$

Among all the possible paths it is useful to identify the skeleton ones. [81] A path $\{R_l\}^n$ of length n is a skeleton path if $R_{l+1} \neq R_{l-1}$ for any $l = 1, ..., n-1$. By definition, for any skeleton path, the hole never retraces its path immediately. It is clear that all the remaining paths can be obtained by dressing each site R_l of the skeleton path by all possible retraceable paths. The retraceable paths can be then summed exactly.

Instead of giving the detailed derivation, we will present the final result and some special cases. The most general Green's function can be written in a formal expansion of skeleton paths of length n:

$$G(R,\omega) = G_{BR}(\omega) \sum_n K(\omega)^{2n} C_n(R) \tag{5.10}$$

where G_{BR} is the Brinkman Rice result (1.8), which includes only retraceable path contribution starting from the origin $R = O$ and coming back to the same site:

$$G_{BR}(\omega) = \frac{1}{\omega\left(1 - \frac{z}{z-1}\Sigma^A(\omega)\right)} = t^{-1}\frac{K(\omega)}{1-K(\omega)^2}, \tag{5.11}$$

the coefficients: $C_n(R) = \sum_{all\ skeleton\ \{R_l\}^{2n}} \Omega(\{R_l\}^{2n})$ and $\Omega(\{R_l\}^n)$ are spin correlation functions, which, generally speaking, depend on the path,

$$\Omega(\{R_l\}^n) = < H|\chi_{R_n,R_{n-1}}\chi_{R_{n-1},R_{n-2}}\cdots\chi_{R_1,R_0}|H > \tag{5.12}$$

In the Ising case $\Omega(\{R_l\}^n)$ vanish for odd n and for even n are simply equal either to zero or one if the corresponding skeleton path change or not the Néel order. They are instead complicated correlation functions in the t-J model for $J \to 0$. In this case expression (5.10) is still valid provided we include the odd n contributions.

The function $K(\omega)$ appearing in (5.10) is the exact contribution of all possible retraceable paths on each site of the skeleton path different from the origin:

$$K(\omega) = \frac{t}{\omega}\frac{1}{1-\Sigma^A(\omega)} = \frac{1}{2(z-1)t}\left[\omega - \mathrm{sgn}(\omega)\sqrt{\omega^2 - 4(z-1)t^2}\right] \tag{5.13}$$

Two possible limits can be exactly solved using the previous expression.

5.2.1 Bethe Lattice Case

The Bethe lattice is defined on a Cailey -tree with coordination z and for $z = 2$ it coincides with the one dimensional chain. In the Bethe lattice each site has $z-1$ sons and one father and there is only one path that connects two arbitrary sites of the lattice because, by definition, there are no closed loops in this lattice. As in one dimension there is only one skeleton path connecting the origin to a given point R and $\Omega(\{R_l\}^n) = \Omega(R_n)$, which is only a function of the final hole position R_n. We can immediately write the exact expression of the Green's function on a Bethe lattice using the previous general expression (5.10):

$$G(R_n, \bar{\omega}) = \Omega(R_n)\ G^{Free}(\bar{\omega}) \tag{5.14}$$

where $G^{Free} = G_{BR}(\bar{\omega})\ K(\bar{\omega})^n$. Note that for $z = 2$ we get the exact expression given in (5.11). It is interesting that the "strong correlation" in the one hole problem in the Bethe lattice is only contained in the static function $\Omega(R_n)$, since $G^{Free}(\omega)$ is exactly the free electron Green's function in the Bethe lattice. This has consequences for the spin charge decoupling. (See next section)

5.2.2 Retraceable Path Approximation

Let us consider the diagonal Green's function $G(R = O, \omega)$ for the t-J_z model. In the general expression (5.10), $\Omega(\{R_l\}^n)$ is either one or zero depending on whether a given permutation preserves the Néel order or destroy it. The shortest skeleton paths with $\Omega(\{R_l\}^n) = 1$ is known to be three times the path around the elementary square plaquette of nearest neighbors. Thus $n = 12$ for such a skeleton path. There are 8 possibilities to build such a path starting from the origin in 2D (4 neighbors times 2 possible opposite directions) and $2d(2d-2)$ in general dimension d. Then the next leading correction to the Brinkman and Rice result is

$$G(R = O, \omega) = G_{BR}(\omega)\left(1 + 2d(2d-2)\ K(\omega)^{12} + ...\right) \tag{5.15}$$

Since $|K(\omega)| \leq \frac{1}{\sqrt{2d-1}}$ for any ω, the correction to the Brinkman and Rice result turns out to be less then 1.1% in $d = 2$ and 0.15% in $d = 3$. This has also been noted in $\frac{1}{d}$ expansion[52] but appears also quite natural in this formalism.

5.3 Spin Charge Decoupling

In 1D, if spin charge decoupling occurs, the one particle Green's function can be written as a simple product of a spinon contribution and a holon contribution:

$$G(R, t) = G^{spinon}(R, t)\ G^{holon}(R, t) \tag{5.16}$$

This property is exact in $d = 1$ for the infinite U Hubbard model and is asymptotically valid for large (R, t) at finite U.[82]

The spin charge decoupling manifests itself in the one particle Green's function and in principle can be detected even at higher dimensionality as speculated by several authors following P.W. Anderson.[3] For $J, J_z \to 0$, or $U \to \infty$ one expects no dynamics for the spinons and that the holon contribution has exactly the free particle behavior, because there is only a unitary charge carried by the single hole.

Thus, as a consequence of spin charge separation, the one hole Green's function should be written in the following way:

$$G(R,t) = \Omega(R)\ G^{Free}(R,t) \tag{5.17}$$

The free electron Green's function is nothing but the free propagator in the Nagaoka limit:

$$G(k,\omega) = \frac{1}{\omega - \epsilon_k + i\delta \mathrm{sgn}\,\omega} \tag{5.18}$$

where $\epsilon_k = 2t(\cos k_x + \cos k_y)$ is the energy of a free hole.

By Fourier transforming in time and by taking the imaginary part of the equation (5.17) we obtain the spectral weight as a function of the final position of the hole and the frequency ω:

$$A(\omega, R) = \Omega(R)\ A^{Free}(\omega, R) \tag{5.19}$$

The previous expression is exact in one dimension even for this simplified t-J_z model where the spinon function is particularly simple $\Omega(R) = \delta_{R,O}$.[82] By Eq. (5.14) spin-charge decoupling is generally valid in the Bethe lattice. Thus we have obtained that the occurrence of spin-charge decoupling is automatically satisfied for lattices that do not allow closed loop paths. In this respect the Bethe lattice is more similar to a 1D lattice rather than to an infinite d one.

Equation (5.19) can be considered as a direct and measurable consequence of spin-charge separation. In fact , by measuring the spectral weight for two different positions of the hole we should get that the ratio:

$$\frac{A(\omega, R')}{A(\omega, R)} = \frac{\Omega(R')}{\Omega(R)} \ = \text{ independent of } \omega \tag{5.20}$$

Since in two spatial dimension we can perform exactly 13 Lanczos steps, it is possible to evaluate with a reasonable accuracy $A(\omega, R)$ for $R = (1,1)$ and $R = (2,2)$. We show in Fig.5.1 the ratio $\frac{A(\omega,R')}{A(\omega,R)}$ that according to expression (5.20) should be independent of ω if spin-charge decoupling is satisfied. This is clearly not true in the present case as the presence of the skeleton paths, strongly renormalizes the spectral weight as a function of the distance of the hole from the origin. The absence of spin-charge decoupling is even more clear for the 2C case (Fig.5.2), where $A(\omega, R)/A(\omega, R = O)$ is ω dependent even for relatively large R and quite low energy.

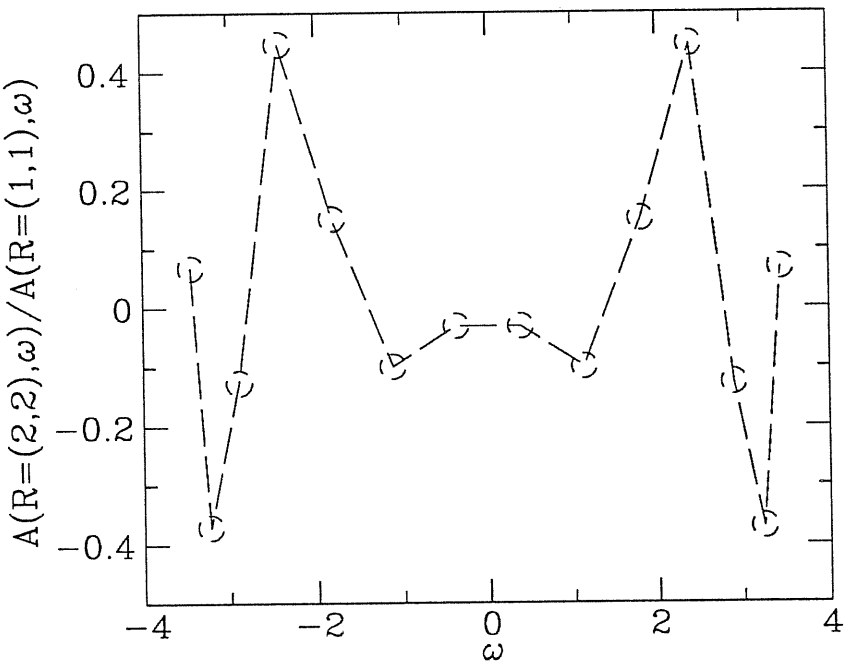

Figure 5.1: The ratio of the spectral weight at different sites for the two dimensional lattice. The method used to calculate $A(R,\omega)$ is described in [83]

Based on the numerical results and the previous analytical ones we conclude that spin-charge decoupling can occur mainly in lattices where closed loop paths are forbidden by the geometry. In these type of lattices the Nagaoka theorem cannot be applied. We have thus found an interesting relation between the Nagaoka theorem, spin charge decoupling and presence or absence of skeleton paths in a given lattice. Of course we cannot rule out more complicated form

of spin-charge decoupling such as the one discussed in [84].

Our results seems to be in disagreement with recent high temperature expansion suggesting spin-charge decoupling in 2D at least at short distance.[60] This work however is done at finite doping for the t-J model. Thus it would be interesting to apply the high temperature expansion directly to the t-J_z model to clarify this issue.

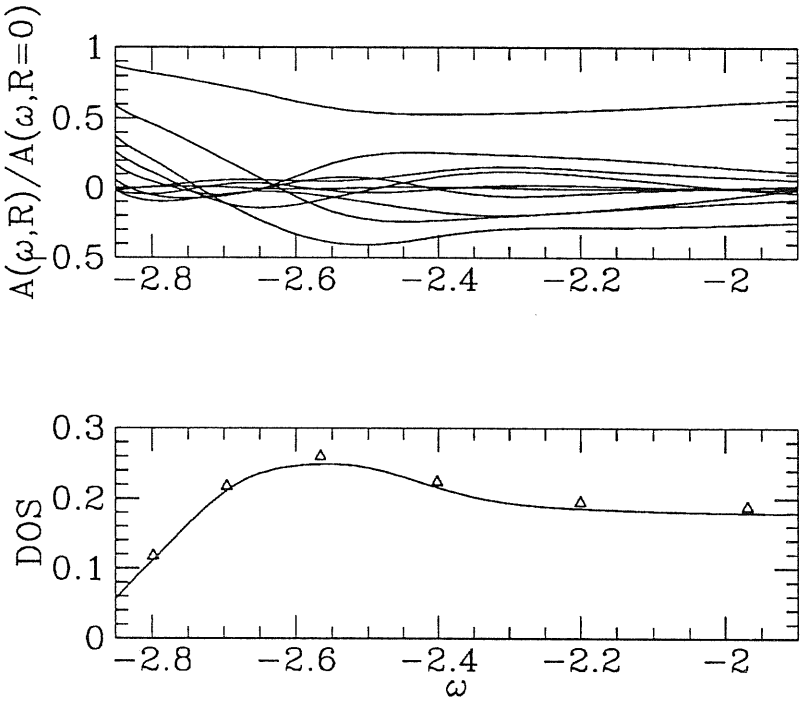

Figure 5.2: (a):The ratio of the spectral weight at different sites for the two chain lattice. The spectral weight as a function of R was obtained by Fourier transforming $A(p,\omega)$ obtained by the standard Lanczos Spectra Decoding. Moreover since at fixed n, $A(R,\omega)$ is exactly zero for R large enough, only a finite number of momenta are necessary to implement *exactly* the mentioned Fourier transform (b):The calculated spectral weight for $R = O$. The solid line is got by summing the spectral weight for all momenta verifying the independent relation $A(R = O,\omega) = \int \frac{dp}{2\pi} A(p,\omega)$. The data points are calculated directly by the Lanczos Spectra Decoding using a trial state with a hole localized at the origin, *i.e.* without using the translation invariance.

Chapter 6

Lanczos Method for Dynamical Correlations

In this chapter, we will first give a short review of the conventional Lanczos method, working in the finite size system. Then, we will explain how to adapt it to the infinite size system. In order to calculate the spectral functions of the single hole in the t-J_z model, we will introduce a novel technique, which we called Lanczos Spectra Decoding.

6.1 Lanczos Scheme in Finite Lattice

The Lanczos technique is widely used in strongly correlated electron systems. Contrary to the quantum Monte Carlo technique, it does not suffer the "fermion sign problem" or any other instabilities at low temperature. Dynamical correlations can be easily obtained using this technique. However, it has been restricted so far to small systems, typically 4×4 (for Hubbard model), or at most 26 sites (for t-J and t-J_z model) and 36 sites (for Heisenberg model).[57] Because of the lack of a systematic way for finite-size scaling analysis in doped system like t-J_z model, some infinite system properties are still unclear or even misleading. In this section, we will develop a scheme, which allows us to analyze the infinite system Lanczos data in a very efficient way, so that we are able to calculate the spectral function of the t-J_z model with good accuracy.

Lanczos method is devised to diagonalize huge Hamiltonian matrix of large dimension N_h. The method starts with a trial wave function ϕ_T. A new basis is generated by Hamiltonian multiplication, $s_i = H^i|\phi_T>$, for i=0,1,...,n. An orthogonal basis $\{ e_i \}$ can be iteratively calculated, after orthogonalization of the vectors s_i. Formally we have

$$b_{i+1}|e_{i+1}> = H|e_i> - a_i|e_i> - b_i|e_{i-1}>$$

$$\begin{aligned} a_i &= < e_i|H|e_i > \\ b_{i+1} &= < e_{i+1}|H|e_i > \end{aligned} \tag{6.1}$$

where $b_0 = 0$, $|e_0 >= |\phi_T >$, a_i are the diagonal elements of the Hamiltonian in the Lanczos basis. for $i = 0, \ldots n$ and b_i the off-diagonal ones for $i = 1, \ldots n$.

Thus in the Lanczos basis the Hamiltonian turns to a tridiagonal form. The spectrum of the tridiagonal matrix will coincide with the one of the original Hamiltonian, when $n = N_h$. Since usually $N_h \sim 10^7$-10^9, it is prohibitive to perform a diagonalization with $n = N_h$ with the available computers. Fortunately the ground state energy and wave function converge for $n \sim 10^2 << N_h$, justifying the success of the method. Anyway, in any diagonalization in a restricted basis with $n << N_h$, the Ritz theorem holds and the variational principle applies for all the eigenvalues and in particular for the ground state.

6.2 Lanczos Scheme in Infinite Lattice

In an infinite system, the Lanczos scheme (6.1) can be applied efficiently, provided it is possible to define a simple *finite* basis that allows to represent the vectors $s_n = H^n|\psi_T >$, generated by the iterative application of H to the trial state. This is in fact the case for our effective t-J_z Hamiltonian (5.7), where it is convenient to work with the basis of spin states with a definite value of $Sz = \pm\frac{1}{2}$ on each site. In fact in such a basis the non-diagonal part of the Hamiltonian is localized around the origin O.

For any fixed momentum p, we start from a Néel state with a hole at origin. Since the J_z term of the Hamiltonian is diagonal, the only part of the effective t-J_z Hamiltonian, relevant to generate new states, is the kinetic term. In each multiplication of the effective Hamiltonian, the hole is translated to its z nearest neighbors by the translation operator T_{τ_μ} (see Fig.6.1). Then the spin exchange operators χ_{O,τ_μ} move the hole back to the origin, leaving an overturned spin background and generating z new states.

The possibility to work with a finite basis even in the infinite system was first noted by Trugman[49]. In fact the overturned spins are located within a region around the hole with radius n. We can thus update only the defects over the Néel state, which are finite at any finite number of multiplications of H. After n steps, the Hilbert space is finite having at most dimension z^n.

This exponential growth of the Hilbert space $\sim z^n$ makes the problem intractable even for relatively small n. Fortunately many of the generated states appear several times during the expansion process of the Hilbert space, due to the presence of the Trugman-like paths,[49] and also due to the translation invariant symmetry implicitly used by means of the effective Hamiltonian (5.7). After all, the dimension of the Hilbert space turns out to be considerably smaller than the previous estimate, and in fact it grows much slower than z^n, e.g. $\sim 1.9^n$ for $z = 3$. In this way we have reached $n = 26$ for the 2C case and $n = 14$ for

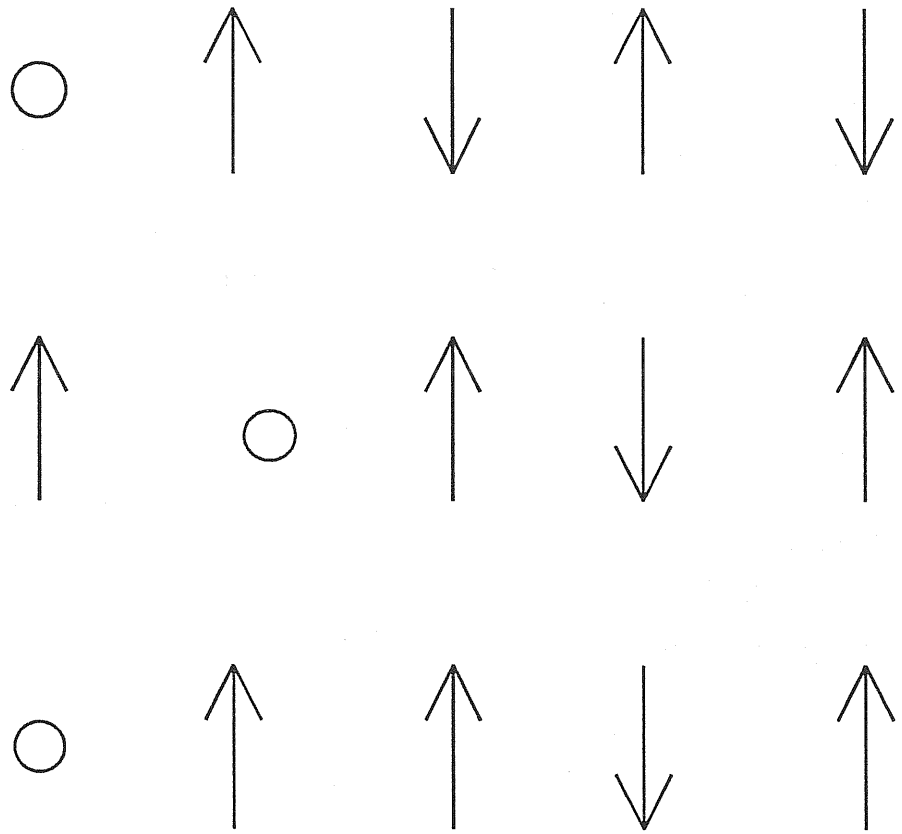

Figure 6.1: The application of the effective t Hamiltonian(5.6) on the trial state. (a):The Néel state with one hole. The hole is located at origin. (b):The state after the action of T_{τ_μ}. T_{τ_μ} translates the Néel state one lattice space along the direction μ. The hole moves to the nearest neighbor. (c):The final state. The spin exchange operator moves the hole back to the origin and leaves an over-turned spin defect in the Néel background.

the 2D case with an Hilbert space dimension at most equal to $\sim 12.2 \times 10^6$.

The *smallest* finite lattice which contains the full information of the first

exact n Lanczos steps has linear dimension $2n+1$. Therefore, our results correspond to a 53×2 lattice in the $2C$ case and to a 27×27 in 2D, which is by far larger than the size of a typical finite size Lanczos calculation[57]. Moreover the possibility to work directly on the infinite system has indeed some advantages. First of all, contrary to any finite size algorithm, in our scheme the ground state energy is a variational estimate for the infinite system at any *finite* n. Secondly in any finite size algorithm the Néel state contains the ferromagnetic state with probability of order 2^{-N}, while our trial wave function is always free of the ferromagnetic component for $N \to \infty$. Thus, in the infinite system we can avoid a fictitious transition to the fully polarized state for small but finite J_z, which is clearly only a finite size effect as we will show in the next section.

However the finiteness of n often leads to appreciable systematic errors. In these cases we overcome this difficulty by carrying out a systematic extrapolation in $1/n \to 0$, following a scheme which is analogous to the finite size scaling analysis for finite lattice calculations.

We conclude this section with some technical comments about the algorithm. The basis generated by the iterative application of H_p^{eff} does not depend on the momentum p of the hole. Hence we only need to generate it once, which takes less than two hundred seconds of CPU time on a Cray-C90. After that, we can do the usual Lanczos iterations for fixed parameters p and J_z, which typically takes 10^2-10^3 seconds of computer time.

6.3 Lanczos Spectra Decoding: a Novel Technique

With the $n+1$ eigenvalues E_i and eigenfunction $|\Psi_i>$ of the Lanczos matrix truncated after n step, the spectral weight can be formally calculated as

$$\begin{aligned} A(k,\omega) &= \mathrm{Im}\tfrac{1}{\pi}\langle\Psi_T|\tfrac{1}{\omega-H-i\delta}|\Psi_T\rangle \\ &= \sum_{i=0}^{n}|\langle\Psi_i|\Psi_T\rangle|^2\delta(\omega-E_i) \end{aligned} \tag{6.2}$$

In the following we assume that the energies E_i are set in ascending order : $E_{i+1} > E_i$.

As a result of the finiteness of our restricted Hilbert space, we get a sum of δ-functions in the spectral weight at any fixed n. This feature appears in the exact spectral function in all Lanczos calculations on any finite lattice. An estimate of the thermodynamic limit is obtained by smoothing the δ-functions in Eq. (6.2) with Lorenzians of a given small width δ,[57, 58]

$$\delta(\omega-E_i) \to \mathrm{Im}\frac{\pi^{-1}}{\omega-E_i-i\delta} \tag{6.3}$$

For small δ, reasonable results can be obtained, provided that the resolution of the energy levels becomes much smaller than δ when n is sufficiently large but still much less than N_h. [57]

Of course, $n = 26$ and $n = 14$ for 2C and 2D respectively are by far smaller than the conventional number of Lanczos iterations in a finite system calculation. Even though the ground state energy is already convergent up to 10^{-3} or even more for $J_z > 0.2$, such a small number of Lanczos steps is usually far from enough for the spectral weight. In fact by the conventional method of smoothing the δ-functions described in (6.3), either one miss the details of the spectral weight for δ large or in the opposite case one gets too rapid oscillations which are obviously unphysical.[78]

A more efficient method for evaluating the spectral weight was recently introduced by us.[78] In the following, for reason of completeness we will give a brief review of this new method named Lanczos Spectra Decoding. In this simple method, we introduced an interpretation of the Lanczos scheme. With this interpretation, the spectral function can be calculated accurately, efficiently and easily even with a small number of iterations n. Of course our method is particularly important whenever the limitation of working with a small n is really prohibitive. As we have seen in fact the Lanczos scheme in the infinite system has a computational cost growing exponentially with n, whereas in any finite size calculation the algorithm is only linear in n. We expect therefore that our method is essential in the first case but maybe helpful only for a small computer-time factor in a finite size calculation.

As well known the spectral weight $A(\omega)$ is a distribution that may be divided into two parts $A(\omega) = A_{coh}(\omega) + A(_{incoh}(\omega)$, a coherent one $A_{coh}(\omega)$ which contains only $\delta-$function contributions and an incoherent one $A_{incoh}(\omega)$ which is a continuous and usually smooth function of ω. The Lanczos Spectra Decoding has been introduced to make use of the smoothness properties of $A_{incoh}(\omega)$ in a simple and efficient way . In the following we therefore assume that the spectral weight is incoherent. This is not a limitation since coherent peaks can be easily separated out from the incoherent part by identifying all the quasiparticle weights $Z_i = |\langle\Psi_i|\Psi_T\rangle|^2$ that remain finite for $n \rightarrow \infty$.

If the spectral weight is incoherent , since by completeness $\sum_{i=0}^{n} Z_i = 1$, one expects that $Z_i \propto \frac{1}{n}$. Thus

$$Z(\omega) = (n+1)Z_i \tag{6.4}$$

may define a smooth function of ω at the discrete Lanczos energies $\omega = E_i$. The full spectral weight is then closely related to the previous function:

$$A(\omega) = Z(\omega)\rho_L(\omega) \tag{6.5}$$

where ρ_L represents the Lanczos density of states (LDOS) in the restricted

Hilbert space generated by the Lanczos algorithm:

$$\rho_L(\omega) = \frac{1}{n+1}\sum_{i=0}^{n}\delta(\omega - E_i) \tag{6.6}$$

where the factor $\frac{1}{n+1}$ is determined by the normalization condition $\int_{-\infty}^{\infty} d\epsilon \rho_L(\epsilon) = 1$. For $n = N_h$ in a finite system, ρ_L coincides with the actual density of states of the many body system, but, in an infinite lattice ($N_h = \infty$), $\rho_L(\omega)$ does not generally converge to the many-body density of states for $n \to \infty$. This will be shown exactly in the Bethe lattice case.

By definition, the number of states dN between energies ϵ and $\epsilon + d\epsilon$ are given by

$$dN = (n+1)\rho_L(\epsilon)d\epsilon. \tag{6.7}$$

So the Lanczos density of states can be calculated as

$$\rho_L(\epsilon) = \frac{1}{n+1}\frac{dN}{d\epsilon} \tag{6.8}$$

Finally , using finite difference instead of differential, the coarse grained Lanczos density of states can be estimated up to order $O(\frac{1}{n^2})$ by

$$\rho_L(\bar{\epsilon}_i) = \frac{1}{(n+1)(E_{i+1} - E_i)}, \tag{6.9}$$

where the energies

$$\bar{\epsilon}_i = \frac{E_i + E_{i+1}}{2} \tag{6.10}$$

lie at the middle of two consecutive eigenvalues.

The function $Z(\omega)$ which is known at energies E_i can be easily interpolated at the energies $\bar{\epsilon}_i$ where also ρ_L is known:

$$Z(\bar{\epsilon}_i) = (Z_{i+1} + Z_i)/2. \tag{6.11}$$

If $Z(\omega)$ is a twice-differentiable function, eq. (6.11) is accurate up to $O(\frac{1}{n^2})$ as well. Thus within the same accuracy $A(\omega) = Z(\omega)\rho_L(\omega)$ easily follows at the discrete energies $\omega = \bar{\epsilon}_i$:

$$A(\bar{\epsilon}_i) = \frac{1}{2}\left(\frac{Z_{i+1} + Z_i}{E_{i+1} - E_i}\right). \tag{6.12}$$

The knowledge of $A(\omega)$ close to the previous "special" points $\bar{\epsilon}_i$ can be easily achieved by standard piecewise interpolations or extrapolations. At the end, we can verify the sum rule $\int A(\omega)d\omega = 1$, as a check for the accuracy of the calculation.

Chapter 7

Low Energy Physics of t-J_z Model

In this chapter, we will first show the efficiency and the validity of Lanczos Spectra Decoding in the Bethe lattice, where the t-J_z model is exactly soluable at $J_z = 0$ limit. Then, we will discuss the low energy physics of the t-J_z model at finite J_z in the Bethe lattice and at any J_z in the two chain and two dimensional lattice.

7.1 A Single Hole in the t-J_z Model for the Bethe Lattice

In this section we will show that $Z(\omega)$ and $\rho_L(\omega)$ are well defined functions and can be calculated exactly in the Bethe lattice.

On the Bethe lattice, the problem is exactly solvable because the skeleton paths are absent and the retraceable paths can be summed analytically. This exact solution has two meaning for us: (1) as a test for our scheme and assumptions, (2) as an hint to interpret the Lanczos scheme for the physical 2C and 2D lattice.

The spectral function in the Bethe lattice is dispersionless and completely incoherent (see Eq.1.9).

Using the Lanczos algorithm eq.(6.1), the Hamiltonian on the restricted basis has vanishing diagonal part ($a_n = 0$) and

$$\begin{aligned} b_1 &= \sqrt{z} \\ b_n &= \sqrt{z-1} \qquad \text{for} \quad n > 1 \end{aligned} \tag{7.1}$$

This can be easily understood. On the Bethe lattice, each multiplication of the Hamiltonian generates $z - 1$ new states, except for the first iteration, which

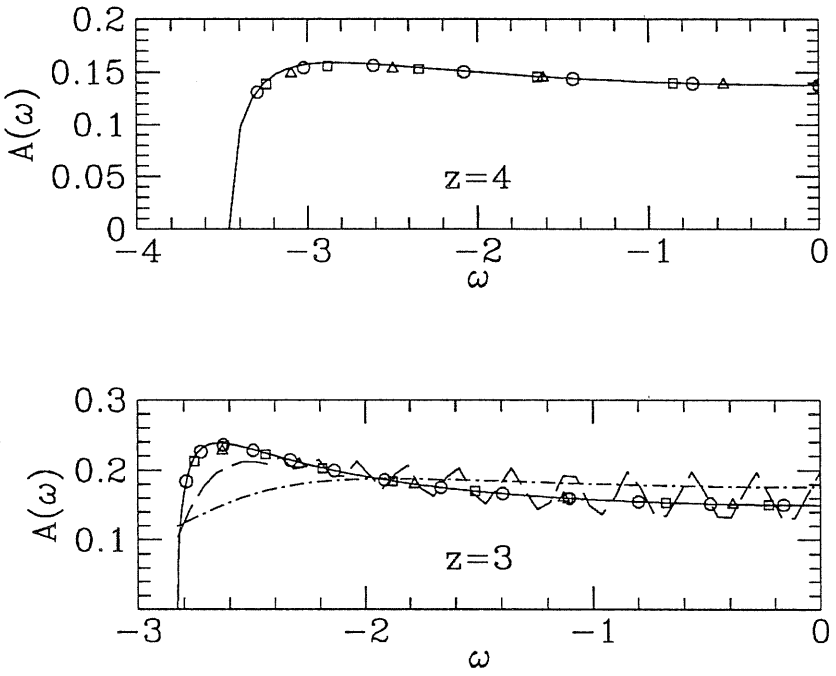

Figure 7.1: Comparison of the spectral weight obtained by the Lanczos Spectra Decoding (6.12) for 10, 18 and 26 (8,11 and 13) Lanczos iterations with the corresponding analytical results (solid lines) for the Bethe lattice with coordination number $z = 3$ ($z = 4$). Triangles, squares and circles correspond to the small, medium and large n calculation respectively. The long dashed lines and dashed-dot lines are fit of $A(\omega)$ obtained by the standard method (see Eq.6.3) with $\delta = 0.05$ and $\delta = 0.1$ respectively.

generates z states. The problem maps onto a one dimensional problem. Then

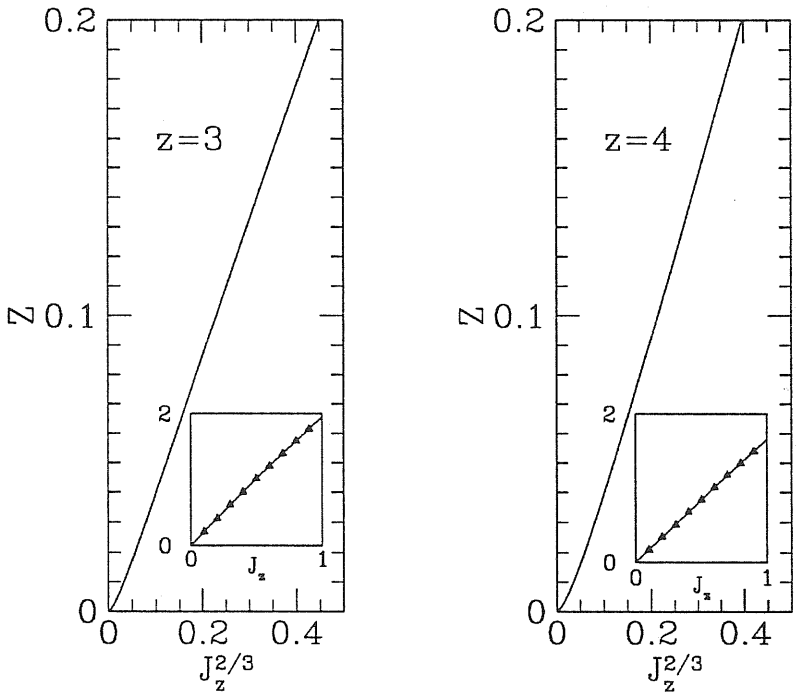

Figure 7.2: The single hole quasiparticle weight of the t-J_z model on the Bethe lattice with $z = 3$ and $z = 4$ respectively. The inset is an expansion of the small J_z region and the axes have been scaled by a factor 1000. The Lanczos matrix was truncated after $n = 40000$ Lanczos steps, by far enough to obtain convergent $n = \infty$ results even for very small J_z.

it is possible to compute analytically Z and ρ_L in Eqs.(6.4,6.6), because of the simple structure of the Lanczos matrix in the Bethe lattice. In fact the wavefunction components ψ_i, $i = 0, 1, , \cdots n$ of an eigenstate with energy ω

satisfy the iterative relation in the Lanczos basis:

$$\begin{aligned} \sqrt{z}\psi_1 &= \omega\psi_0 \qquad i=0 \\ \sqrt{z}\psi_0 + \sqrt{z-1}\psi_2 &= \omega\psi_1 \qquad i=1 \\ (\psi_{i+1}+\psi_{i-1})\sqrt{z-1} &= \omega\psi_i \qquad i\geq 2 \end{aligned}$$

Thus from the third equation solutions are possible for $\omega^2 < \epsilon_{BR}^2$ where $\epsilon_{BR} = -2t\sqrt{z-1}$ is the Brinkman-Rice approximation for the single hole ground state. Then the components of the eigenstates on the Lanczos basis are given by: $\psi_i = \mathrm{Re}A\lambda^{i-1}$, where $\lambda = \dfrac{\sqrt{\omega^2-\epsilon_{BR}^2}-\omega}{\epsilon_{BR}}$ and the complex number A is determined by the first two equations, yielding $\psi_1 = \frac{\omega}{\sqrt{z}}\psi_0$ and $\psi_2 = \dfrac{\omega^2-z}{\sqrt{z(z-1)}}\psi_0$. Finally ψ_0 is determined by the normalization condition $\sum_i \psi_i^2 = 1$, and the function $Z(\omega) = \lim_{n\to\infty} \psi_0^2(n+1)$ reads:

$$\begin{aligned} Z(\omega) &= \frac{z^2t^2[\epsilon_{BR}^2-\omega^2]}{2[z^4t^4-(2z+1)t^2\omega^2]} \qquad \text{for} \qquad \omega^2 < \epsilon_{BR}^2 \\ \rho_L(\omega) &= A(\omega)/Z(\omega) \end{aligned}$$

Here $A(\omega)$ is the Bethe lattice density of states in Eq.(1.9). In this case, $\rho_L(\omega)$ has singular inverse square root behavior near the band tail.

By use of the Lanczos Spectra Decoding introduced in the previous section we have obtained good approximation to the exact solution with $n \sim 10$, much less than in the conventional calculation (see Fig7.1).

At finite J_z, the only change is with the diagonal part of the Lanczos matrix

$$a_0 = \frac{J_z}{4}z \tag{7.2}$$

$$a_i = \frac{J_z}{4}(3z-1+2(z-2)(i-1)) \quad \text{for } i\neq 0 \tag{7.3}$$

This result can be easily obtained by counting the number of broken bonds in the states generated at different Lanczos iterations. In this formalism we obtain therefore that the motion of a hole in a Bethe lattice is exactly equivalent to a one dimensional motion of a particle in a linear potential, provided we identify the distance of the particle from the origin with the label i of the Lanczos basis.

By diagonalizing numerically the Lanczos matrix for large n we can easily confirm the prediction of the long wavelength Hamiltonian (1.10), namely that the spectral function is k-independent, i.e. it is dispersionless, and that $A(\omega)$ contains only δ-function peaks, i.e. there is no incoherent part. In fact due the linear potential *all* the one- hole states are localized bound states. It is important to remark that the corrections to the asymptotic $J_z \to 0$ behavior is

quite important for the quasiparticle weight Z even for very small J_z. For Z the correct linear behavior $\propto J_z$ is found only for $J_z \sim 10^{-3}$ (see Fig.7.2), whereas the behavior of the ground state energy and the gap is more reasonable.

7.2 A Single Hole in the t-J_z Model for the Two Chains and Two Dimensional Lattice

7.2.1 Spectral Weight for $J_z = 0$ Case

For $J_z = 0$ the spectral weight $A(\omega)$ is an even function of ω and in the following we will concentrate on its negative frequency region. In this model we found [78] a sharp peak in the spectral weight $A(\omega)$ located at an energy close to the retraceable path prediction, $\epsilon_{BR} = -2t\sqrt{z-1}$, and, a second peak at energy $\sim -t$. In the 2D case, the spectral weight looks similar, although the first peak is rather small. In 1D, the exact BR solution leads only to one peak but with a divergent spectral weight $\sim \frac{1}{\sqrt{\omega-\epsilon_B}}$ at the bottom ϵ_B of the band. Already in the 2C case such a divergence disappears within the retraceable path approximation, as well as in our numerical scheme, which includes all closed-loop paths. In fact the peak in Fig.7.3,7.4 does not depend much on the number n of Lanczos steps.

We also found that the first peak in the spectral function has a remarkable dispersive feature although the bottom of the spectrum appears k-independent. The dispersion of the first peak is not present neither in 1D or in infinite dimension[52] and the importance to go beyond the retraceable path approximation is already clear even in 2D.

For the density of states $D(\omega) = \int \frac{dp^d}{(2\pi)^d} A(\omega, p) = A(R = O, \omega)$, our results (Fig.7.4) present some small oscillation around the retraceable path analytic solution (1.8). In 2D however the retraceable path expression for $z = 4$ seems already quite accurate, at least away from the band tails.[78] All the above results have been recently confirmed.[81]

As discussed in the introduction a key question is the determination of the band edge energy ϵ_B, i.e. the threshold energy where the spectral weight begin to vanish. As a first step we identify the Lanczos ground state energy for $n \to \infty$, E_∞, which may or may not converge to the Nagaoka energy. For instance, by neglecting closed loop paths, i.e. in a smaller Hilbert space, one obtains the Brinkman-Rice energy ϵ_{BR} as a variational estimate of E_∞. In the retraceable path approximation ϵ_B coincides with E_∞, as it is reasonable to expect in general.

In order to have an accurate estimate of E_∞, it is useful to have a guess about the asymptotic behavior of the quantity $\Delta_n = E_n - E_\infty$ for $n \to \infty$. The way Δ_n vanishes for $n \to \infty$ is related to the form of the Lanczos density of states at low energy. In the Brinkman-Rice case the exact solution in (1.9) gives $\rho_L(\epsilon) \sim (\omega - \epsilon_B)^{-1/2}$. Thus, using Eqs. (6.9), $\Delta_n^{-1/2} \sim \frac{1}{n\Delta_n}$, yielding $\Delta_n \sim \frac{1}{n^2}$.

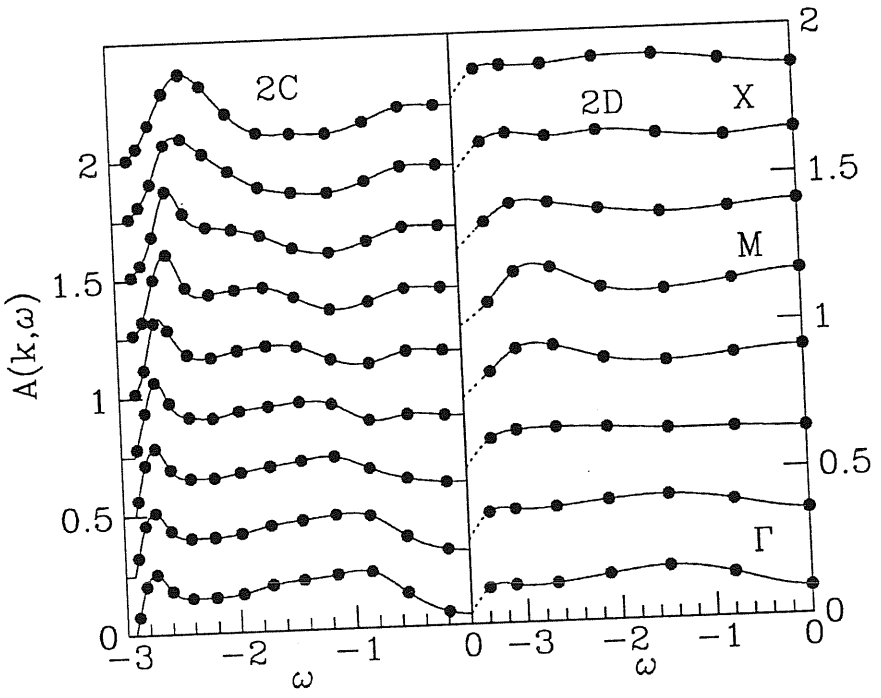

Figure 7.3: Calculated momentum dependent spectral function for different k in the magnetic Brillouin zone. For the 2C $A(k,\omega)$, the wavevector k ranges from from $(0,0)$ (bottom) to $(\pi,0)$ (top) with nine equally spaced values. For each k, we have shifted the spectral function by 0.25 successively. For the 2D $A(k,\omega)$ the k-path in the magnetic Brillouin zone is $\Gamma \rightarrow M \rightarrow X \rightarrow \Gamma$, where $\Gamma = (0,0)$, $M = (\pi,0)$ and $X = (\pi/2,\pi/2)$.

For $J_z = 0$ the inclusion of the skeleton paths seems to support a finite Lanczos density of states (see Fig.7.5), yielding, by the same argument $\Delta_n \sim \frac{1}{n}$. We have

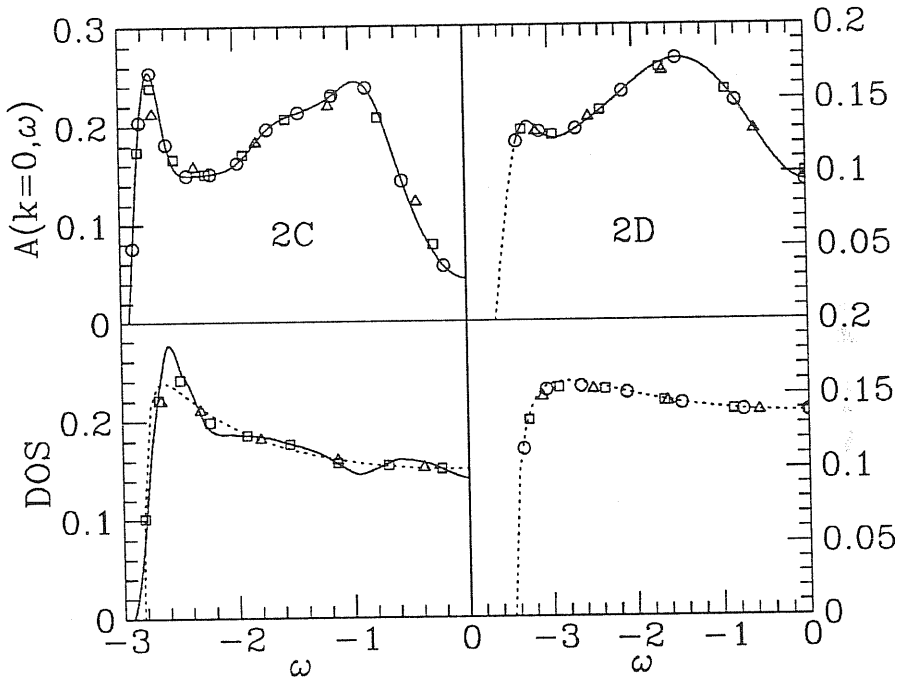

Figure 7.4: Calculated $k = 0$ spectral weight and one particle density of states for $n = 10, 18, 26$ $(8, 11, 13)$ for the 2C (2D) model. Solid lines are cubic interpolations of the largest n, and the dashed lines are the Brinkman-Rice densities of states (Eq. 1.9) and guides to the eye for the 2D $A(k,\omega)$. The lines and the points for the DOS are calculated as described in Fig.5.2. The symbols for the points are as in Fig.7.1.

plotted in Fig.(7.6) the estimated ground state energies as a function of $1/n$ for several momenta for the 2C case. Many of the estimated Lanczos energies –

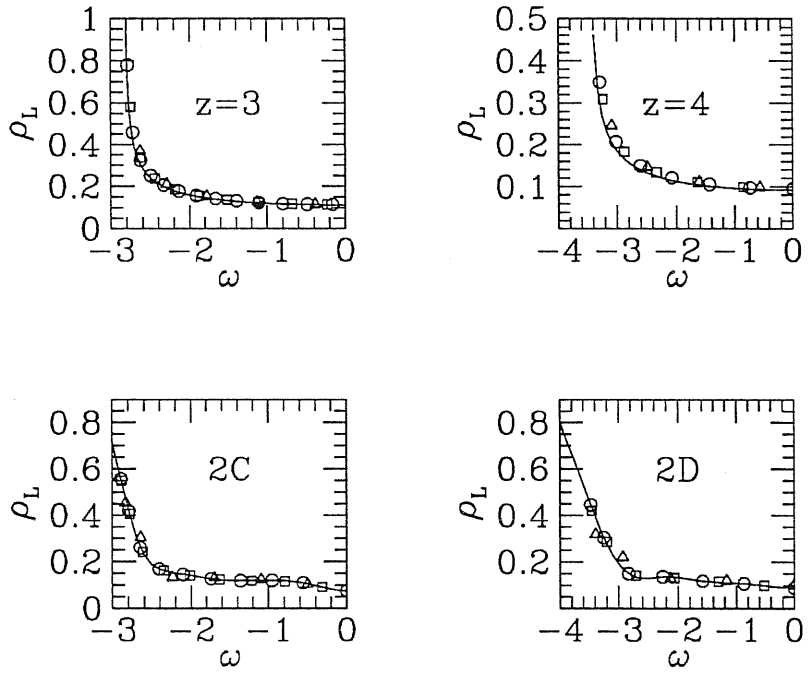

Figure 7.5: The Lanczos density of states on the Bethe lattice (for $z = 3$ and $z = 4$), the 2C and 2D lattice respectively. The symbols for the points are as in Fig.7.1. The continuous lines are the exact results for the Bethe lattice and guides to the eye for the 2C and 2D lattices

exact upper bound of the true ground state energy – are clearly below ϵ_{BR} (even for the 2D case also shown in the picture). Thus, a previous suggestion that the one hole energy in a quantum antiferromagnet should be close to ϵ_{BR} [85, 86] *is not confirmed* by our numerical results. In Fig.(7.6) it is a remarkable

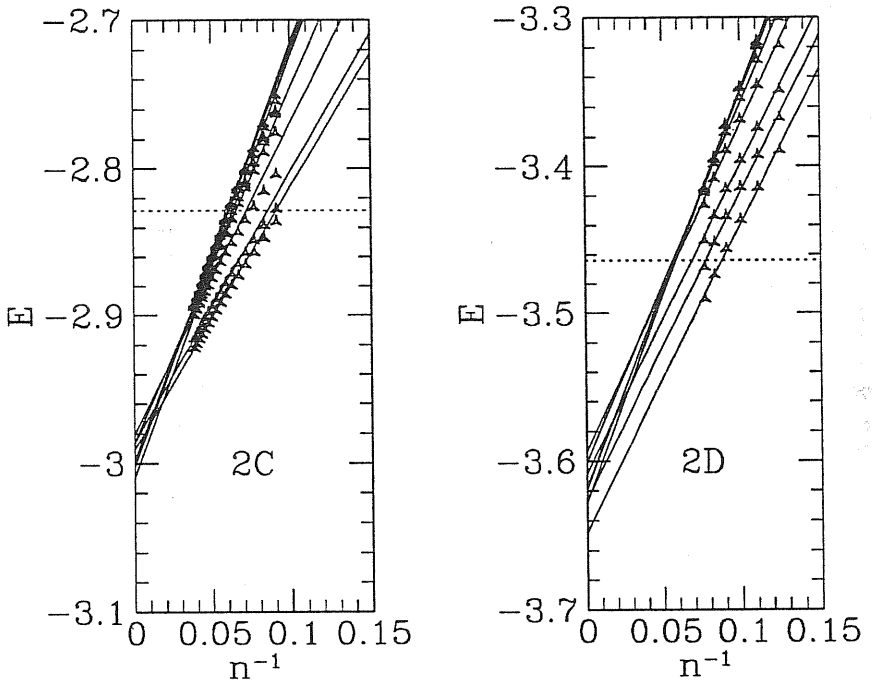

Figure 7.6: Plot of the lowest eigenvalues of the $2C$ and 2D model as a function of $1/n$, the inverse of the Lanczos-iteration number, for the same momenta shown in Fig.7.3. The horizontal dashed lines denote the Brinkman-Rice ground state energies.

property that all the extrapolated energies are very close to the Nagaoka energy, independent of the momentum of the hole, $E_\infty = -3 \pm 0.02$.

The above results give a robust evidence that ρ_{LDOS} is finite up to the Nagaoka energy. Even in this case the spectral weight $A(\omega) = Z(\omega)\rho_{LDOS}(\omega)$

can in principle vanish for $\omega > \epsilon_N$ due to the vanishing of the factor $Z(\omega)$. This is the scenario suggested in [81] using the expansion for the Green's function in terms of $K(\omega)$ (5.10). In the interval $K(\omega)\alpha < 1$ (for $|\omega|/t > \frac{(z-1)}{\alpha} + \alpha$) when the expansion (5.10) converges the Green's function is surely real, thus determining a lower bound for ϵ_B. After some extrapolation it was found in [81] that $\alpha < z - 1$, *i.e.* ϵ_B should be higher than ϵ_N for the 2C or the 2D case using the first 18 or 12 coefficients $C_n(R)$ of the Green's function expansion, respectively. Although the above analysis is surely correct, the basic conclusion is affected by systematic errors due to the knowledge of too few coefficients in the expansion.

As it is shown in Fig.7.7, this scenario looks already unlikely within the Lanczos Spectra Decoding method because $Z(\omega)$ seems to be smoothly connected to the Nagaoka energy. It is clear however that this is not enough for a definite conclusion.

In order to solve the latter controversy without relying on the Lanczos Spectra Decoding, we have reproduced the Müller-Hartmann–Ventura expansion (Tab. 7.2.1) and extended it up to the first 26 coefficients for the 2C case. This information was already contained in the first 26 Lanczos steps in an infinite lattice since the iterations defined in (6.1) can be formally obtained by the knowledge of the first $2n+1$ momenta of the Hamiltonian on the trial state. As it is shown in Tab. 7.2.1 the Müller-Hartmann–Ventura extrapolation:

$$C_n(R) = C(R)\frac{\alpha^{2n}}{(2n)^{\beta(R)}} \tag{7.4}$$

used to determine the radius of convergence α is not stable when large skeleton paths are included. For large n, we find that α, $\beta(R=O)$ and $C(R=O)$ are always going up. At $n = 26$, $C(R=O)$ becomes 5 times larger than their value obtained for $n = 18$, while α changes from 1.88 to 1.92. (Tab. 7.2.1)

Instead of using the fit (7.4) with the calculated momenta $C_n(R)$, we apply the well established ratio method, well known for the study of critical phenomena. Using this method we evaluate the radius of convergence α, analogous to the critical temperature in the language of critical phenomena, and the power law exponent θ describing the vanishing of the Green's function at the band tails, analogous to a conventional critical exponent in the same language.[87] We define

$$\mu(n) = \sqrt{\frac{C_n}{C_{n-1}}} \tag{7.5}$$

and the linear intercept at $\frac{1}{n} \to 0$ with two next consecutive points

$$\mu(n, n-2) = \frac{1}{2}[n\mu(n) - (n-2)\mu(n-2)]. \tag{7.6}$$

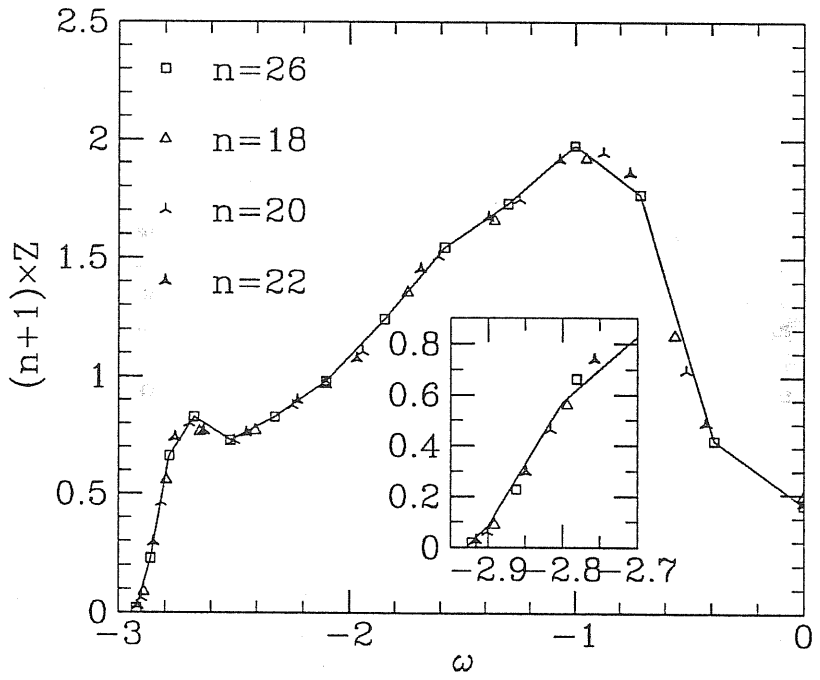

Figure 7.7: The expected smooth quantity $Z(\omega) = (n+1) \times Z$ at $J_z = 0$ plotted as a function of the energy for different Lanczos iterations. The continuous line connects the $n = 26$ data. By comparing the data at different Lanczos iterations, $Z(\omega)$ seems to be non vanishing just above ϵ_N.

In fact μ is expected to behave as

$$\mu(n) = \alpha[1 + \frac{g}{n} + O(\frac{1}{n^2})] \tag{7.7}$$

where α gives the position of the singularity and $\theta = -(1+g)$ gives the exponent of the Green's function at the band tail $G(\omega) \propto (\omega - \epsilon_B)^\theta$. This kind of analysis is much more stable than the extrapolation used in [81]. In Fig.7.8 the data for the linear intercept $\mu(n, n-2)$ suggests that the $\frac{1}{n}$ corrections are well behaved, and approximately linear for $n > 20$. By accident this number is very close to the maximum n reached in the previous analysis [81], giving further evidence that for this problem a very large number of coefficients C_n are necessary to obtain reasonably converged results.

Then, by estimating α , by a linear fit in the region $n > 20$, we obtain $\alpha = 2.00 \pm 0.02 \simeq z - 1$ both for $R = 0$ and for $p = 0$, as an independent check that α should not depend on R ($C_n(p=0) = \sum_R C_n(R)$). Thus we have a clear evidence that the band edge energy coincides with the Nagaoka energy since $G(\omega)$ appears to be real only for $\omega < \epsilon_N$ in the 2C case.

For the critical exponent θ we have a much less accurate result probably because the vanishing of the spectral weight close to ϵ_N is characterized by overall essential singularities of the type $e^{-\frac{1}{\omega - \epsilon_N}}$, as we have suggested in our previous paper.[78]

Here we can give a very simple argument supporting this singular behavior for $Z(\omega)$. For the spectral weight the behavior close to ϵ_N should be the same, because, as we have previously shown, the Lanczos density of states is approximately constant in this region. After n Lanczos steps the hole forms a polaron state $|P>$ with maximum spin but total $S_z = 0$ in a region of linear size $\xi \sim n$, as it is also confirmed by direct calculation of the spin arrangement around the hole (see next section). The overlap of the ground state of the Hamiltonian matrix truncated after n Lanczos steps is then approximately given by [1]

$$Z_0 \sim \frac{1}{\binom{V}{V/2}} \to \sqrt{\frac{\pi V}{2}} 2^{-V} \tag{7.8}$$

where V is the volume of the polaron equal to 2ξ for the 2C case and $\propto \xi^d$ for general spatial dimension $d > 1$. The quantity $Z_0 \times n$ according to the Lanczos Spectra Decoding method characterizes the behavior of the smooth function $Z(\omega)$ at an energy $\omega = \epsilon_N + \text{const.}/n$. Solving for n from the latter equation and assuming , as we have already mentioned, that $\xi \propto n$ we can substitute $V \propto (\omega - \epsilon_B)^{-d}$ in (7.8) and obtain:

$$A(\omega) \propto Z(\omega) \quad \propto \quad (\omega - \epsilon_N)^{-3/2} e^{-\frac{\Delta}{(\omega - \epsilon_N)}} \quad \text{for 2C} \tag{7.9}$$

$$A(\omega) \propto Z(\omega) \quad \propto \quad (\omega - \epsilon_N)^{-d/2-1} e^{-\frac{\Delta}{(\omega - \epsilon_N)^d}} \tag{7.10}$$

[1] The state $< P|$ with maximum spin and $S_z = 0$ has the same overlap with all the possible states of the Hilbert space with $S_z = 0$, thus in particular $< P|N >^2 = \frac{1}{\binom{V}{V/2}}$, where $V = \xi^d$ is the volume occupied by the polaron, and the binomial coefficient $\binom{V}{V/2}$ is the number of ways to put $V/2$ spin up and $V/2$ spin down in a region of V spins.

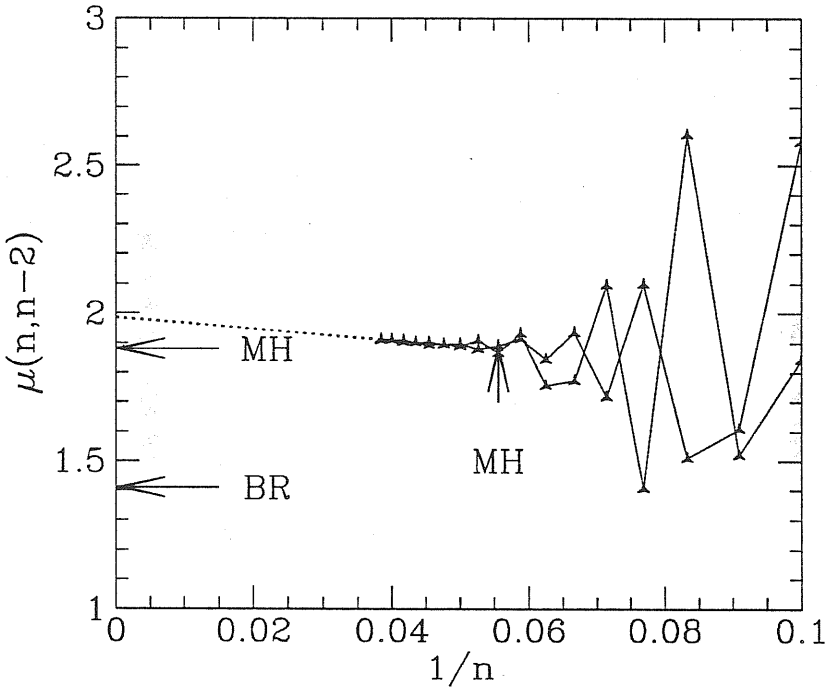

Figure 7.8: The linear intercept $\mu(n, n-2)$ defined in the text (7.6) as a function of $\frac{1}{n}$ for $p = (0,0)$ and $R = (0,0)$. The dashed lines are linear extrapolations of the last six points. The two horizontal arrows indicate the Brinkman-Rice and Müller-Hartman estimates. The vertical arrow indicates the largest n analyzed in [81].

where Δ is an overall constant depending on the dimensionality. Using the above formulas we have obtained good agreement with numerical results over a range for Z covering up to two decades (see Fig.7.9).

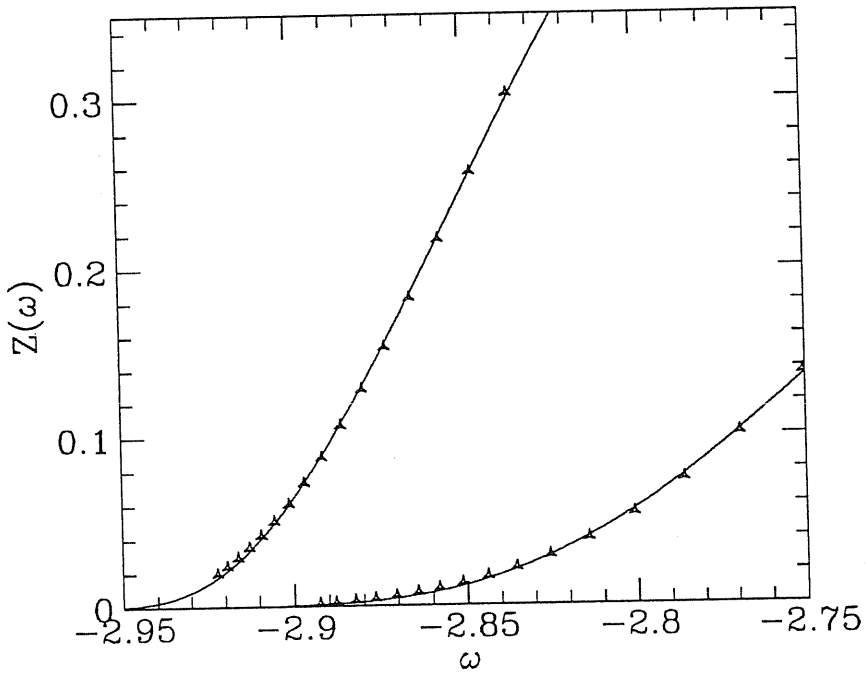

Figure 7.9: The behavior of $Z(\omega)$ at band tail for $p = (0, 0)$ and $p = (\pi, 0)$. The solid lines are the least square fit by expression (7.10).

7.2.2 Spectral Weight for Finite J_z

For finite J_z a coherent part shows up in the spectral weight although, contrary to the string picture, at most only the first few energy levels contribute to the spectral weight with true δ-functions. (See Fig.7.10) In order to characterize these δ-function contributions we can check whether the quasiparticle weight Z_i

converge to some *finite* value for $n \rightarrow \infty$, whereas if the energy level E_i belongs to the incoherent part only $Z(\omega) = (n+1)Z_i$ remains finite for $n \rightarrow \infty$. Another method to distinguish the coherent part from the incoherent one is to analyze directly the wavefunction components of the eigenstate Ψ_i on the Lanczos basis $\{e_j\}$. As we have seen in the previous section the label j measures the length of overturned spins in the state i. The quasiparticle weights $Z_i > 0$ only if the Néel state $e_{j=0}$ will have a non vanishing component with the state Ψ_i. This obviously occurs if the eigenstate Ψ_i is "localized" in the Lanczos basis even for $n \rightarrow \infty$, otherwise only a probability $\sim \frac{1}{n}$ to be in the Néel state is expected to survive.

Using the above criteria, shown in Fig.7.11 and Fig.7.12, we have a clear evidence of a single quasiparticle weight for J_z not too large, and an incoherent part which is rather similar to the $J_z = 0$ one. For larger J_z the incoherent part moves quite fast at higher energy, leaving probably more than one δ-function contributions to the spectral weight. Thus it is possible to conclude that the inclusion of closed loop paths does not suppress the first quasiparticle weight, but completely washes out all the quasiparticle excitations at higher energies. Even the few peaks that appears in the incoherent part cannot be associated to "string state" resonances – as suggested by [58, 88] – because are rather similar to the $J_z = 0$ ones, where localized string states cannot exist. We thus confirm the conclusions of [57] for physical values of J_z.

As far as the energy spectrum $E(p)$ is concerned we obviously found that the lowest energy state has a finite quasiparticle weight and has momentum $p = (0,0)$, instead of $(\frac{\pi}{2}, \frac{\pi}{2})$ as commonly accepted for the t-J model. [89, 50] This is because in the t-J_z model the spin fluctuations are neglected, while they play an important role for the energy dispersion $E(p)$ (See Fig.7.13).

Finally for the quasiparticle weight as a function of J_z we can apply the same argument at the end of the previous section by assuming that Z is basically the overlap of an $S_z = 0$ polaron state of size ξ, where ξ may be roughly identified with the correlation length within the string picture $\xi \propto J_z^{-1/3}$. We should get essential singularities like

$$\begin{aligned} Z &\propto J_z^{-1/6} e^{-\Delta J_z^{-1/3}} \quad \text{for 2C} \\ Z &\propto J_z^{-d/6} e^{\frac{-\Delta}{J_z^{d/3}}} \quad \text{for } d > 1. \end{aligned} \tag{7.11}$$

As in the string picture where we could not detect the correct $Z \propto J_z$ behavior for reasonable values of J_z (see Fig.7.2), we expect that these kind of singularities are important only at a value of $J_z \sim 10^{-3}$. For larger values of J_z one obtains a crossover to a $J_z^{2/3}$ behavior surprisingly valid for a quite large range of J_z both in the string picture or in the realistic cases shown in Fig.7.2 and 7.14. In the latter picture it is also evident that at some small value of J_z the Z factor should vanish much faster than $J_z^{2/3}$, otherwise we should get an unplausible critical value of J_z, where the quasiparticle weight vanishes. This

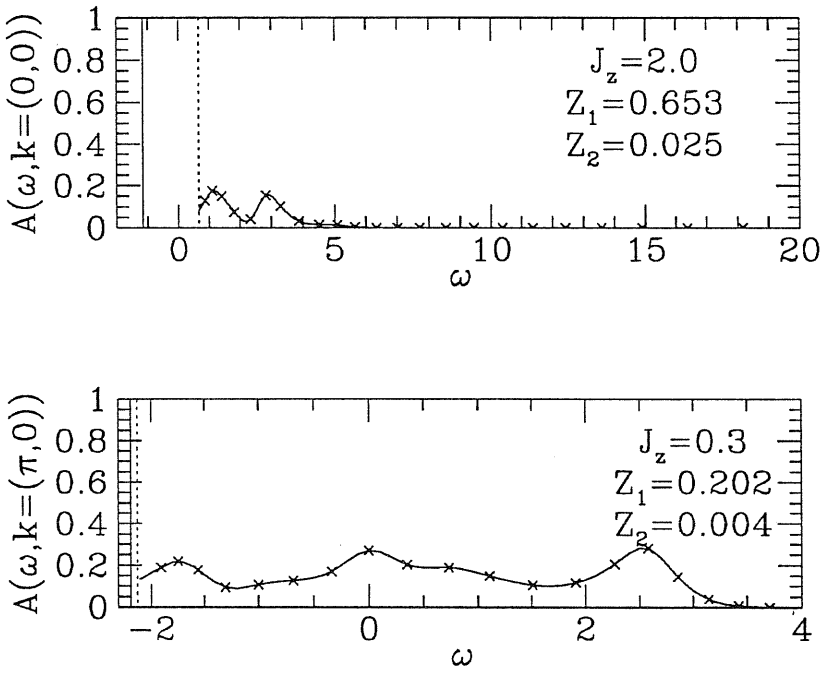

Figure 7.10: The spectral function at $J_z = 0.30$ and $k = (\pi, 0)$ and $J_z = 2.00$ and $k = (0, 0)$.

at least supports the existence of essential singularities in the $J_z \to 0$ limit for the quasiparticle weight as in Eq.(7.11).

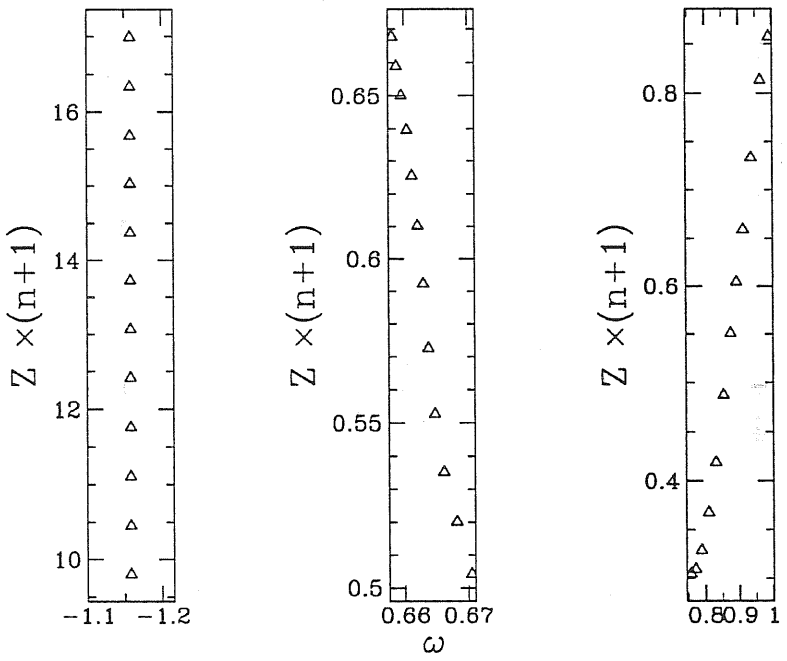

Figure 7.11: The dependence of $Z \times (n+1)$ on the Lanczos iteration number n for $J_z = 2.00$. From left to right, the ground state, the first excited state and the second excited state are plotted. The ground state quasiparticle weight is convergent up to 10^{-10} and $Z \times (n+1)$ is proportional to n as expected. The first excited quasiparticle weight is poorly convergent instead. However, the $Z \times (n+1)$ still show an approximate linear behavior. Finally for the second excited state, $Z \times (n+1)$ is decreasing with increasing n, clearly indicating the incoherent nature.

7.2.3 Ground State Properties for Small J_z

The accurate determination of the ground state energy in the small J_z region is important to detect a possible transition between an essentially antiferromag-

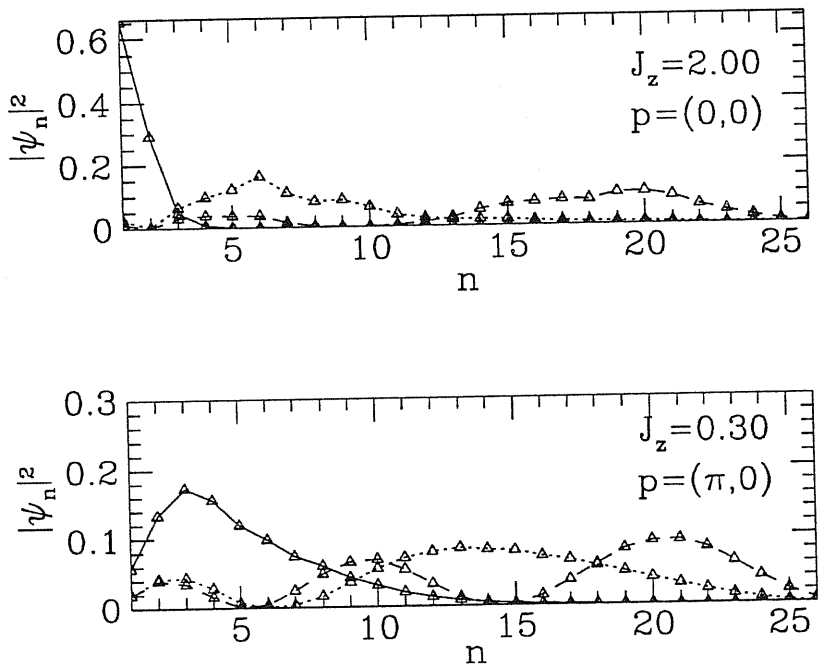

Figure 7.12: The 2C wavefunction of the single hole in the Lanczos basis for $J_z = 2$, $p = (0,0)$ and $J_z = 0.3$, $p = (\pi, 0)$. The solid line denotes the ground state, the dotted one the first excited state and the dashed one the second excited state.

netic state and a state where the hole fully polarize the spins in a finite region of space with size ξ^d, that remains somehow phase-separated from the remaining antiferromagnetic region. In fact the latter variational state has an energy that approaches the Nagaoka energy for $\xi \to \infty$. At finite J_z, by optimizing the

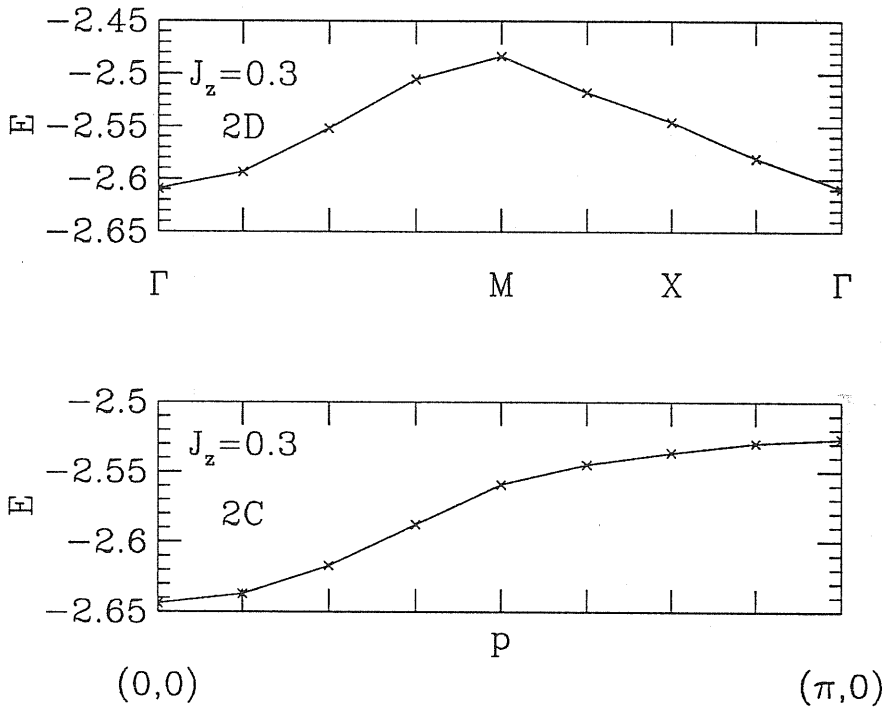

Figure 7.13: The energy dispersion of the lowest quasi particle state for $J_z = 0.3$. The path in the magnetic Brillouin zone is the same as in Fig.7.3.

size ξ of the ferromagnetic region, one gets[86] corrections to the asymptotic Nagaoka energy proportional to $J_z^{\frac{2}{d+2}}$.

Supports to a possible transition come from the infinite dimension limit predicting that the antiferromagnetic state defined at large J_z is analytically con-

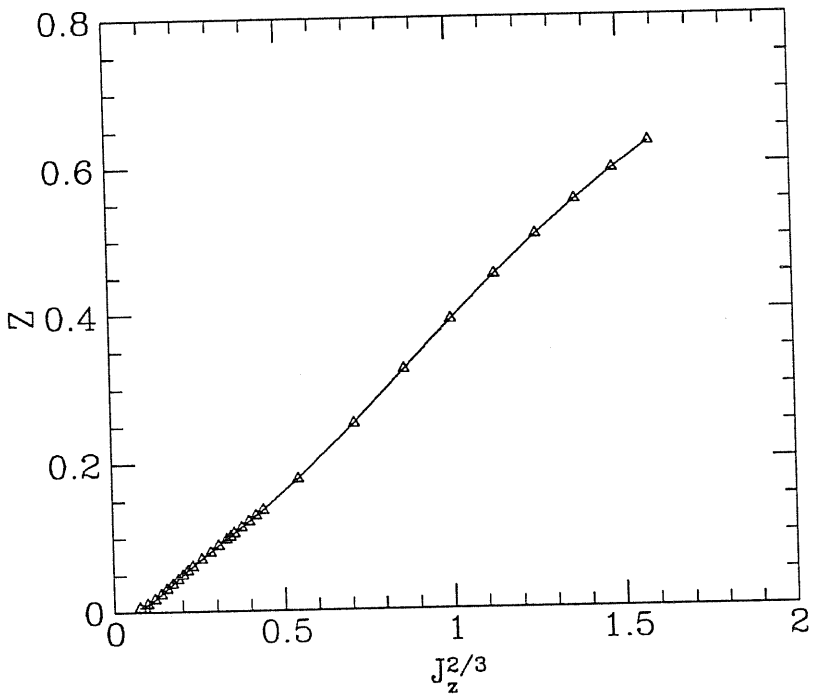

Figure 7.14: Calculated quasiparticle weight Z as a function of $J_z^{2/3}$.

nected at small J_z not to the Nagaoka energy but to the much higher Brinkman-Rice energy. Thus there should be a critical value J_c where the 'phase separated' state becomes lower in energy as we decrease J_z.[86, 58] This is somehow the scenario proposed by Emery *et al* for the doped t-J model. We will show in the following a clear numerical evidence that the above scenario *is not confirmed* in the t-J_z model for a single hole.

Contrary to the string picture or the infinite dimension limit we see in

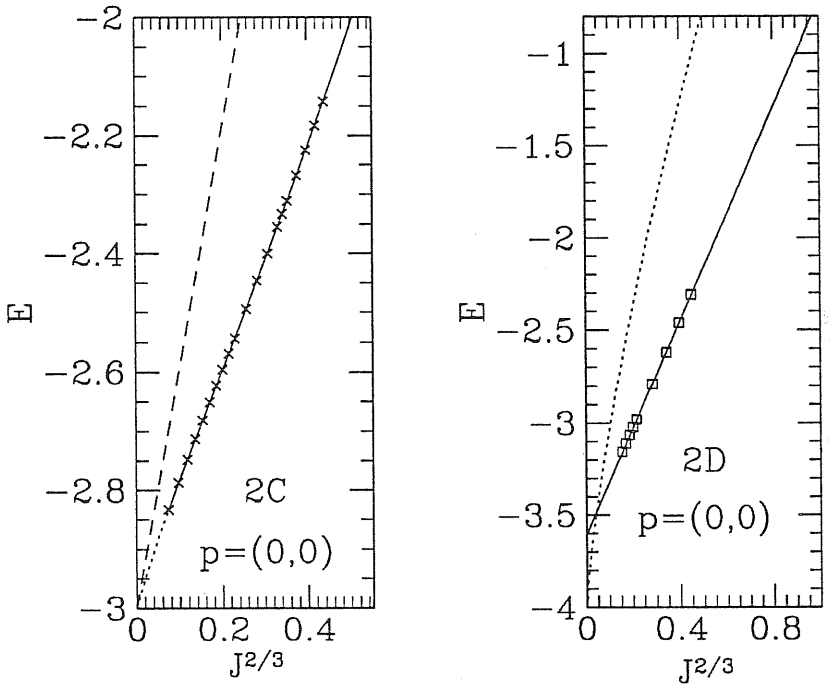

Figure 7.15: The ground state energy as a function of $J_z^{2/3}$. The data points refers to $n = 26$ (2C) and $n = 14$ (2D). The continuous lines are a fit $E = a+bJ_z^{2/3}+cJ_z$ of the data. The dotted line is the energy of the "phase separated polaron" described in the text.

Fig.7.15 that the asymptotic value for the energy is clearly given by the Nagaoka energy, although the leading corrections to the energy seem quite well fitted by the string picture exponent $J_z^{2/3}$. In fact the diagonal elements of

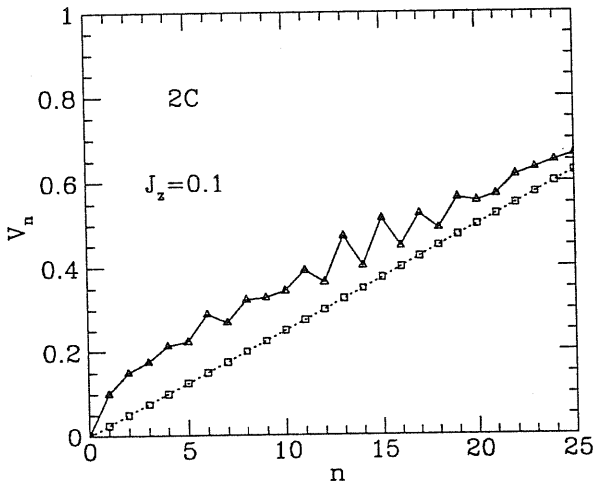

Figure 7.16: The diagonal matrix elements of the Hamiltonian in the Lanczos basis. The solid line refers to the two-chain lattice and the dashed line to the Bethe lattice with $z = 3$.

the Hamiltonian in the Lanczos basis describe approximately a linear potential (Fig.7.16) as in the string picture. This is obviously important for the small J_z correction to the energy. Moreover in Fig.7.15 it is shown that the 'phase separated' state is well above the estimated energies even for very small J_z, leaving open a possible transition at an unphysically small value of $J_z \sim 10^{-4}$ for 2C. However, for 2D, we do not have the enough accuracy as show in Fig.7.17.

7.2.4 Spin Arrangement in the Ground State

Although we have shown that the Nagaoka energy is the ground state energy of the t-J_z model for $J_z \to 0$ it is not clear what spin background is favoured, in this limit. For instance we could have that the Nagaoka state is degenerate in the thermodynamic limit with an antiferromagnetic state.

In order to solve this issue, we have calculated the hole-spin-spin correlation

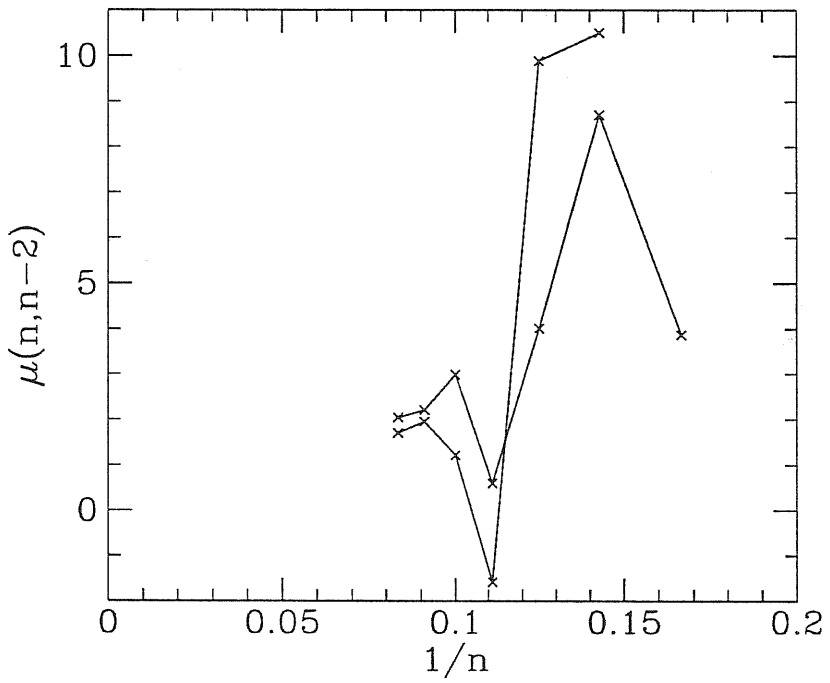

Figure 7.17: Same as in Fig.7.8 for the 2D case, the data are taken from [81].

function, by measuring the one involving the spins in the z-direction of the staggered magnetization

$$\begin{aligned} C_z^{\mu}(R_i) &= N < \psi_p | h_o^{\dagger} S_{R_i}^z S_{R_i+\tau_\mu}^z | \psi_p > \\ &= < S_O | S_{R_i}^z S_{R_i+\tau_\mu}^z | S_O > \end{aligned} \tag{7.12}$$

and its spin rotation invariant version

$$\begin{aligned} C^{\mu}(R_i) &= N < \psi_p | h_o^{\dagger} \mathbf{S}_{R_i} \mathbf{S}_{R_i+\tau_\mu} | \psi_p > \\ &= < S_O | \mathbf{S}_{R_i} \mathbf{S}_{R_i+\tau_\mu} | S_O > \end{aligned} \tag{7.13}$$

where $h_o^{\dagger}$ is the hole creation operator at origin. These correlation functions measure how the spin background is perturbed by the hole.

For small J_z, as expected the finite n corrections are important and tends erroneously to enhance the antiferromagnetism (see Fig.7.19). Instead by studying the behavior of $C(R)$ as a function of $1/n$ it is quite clear that the spins are strongly correlated in the x-y plane and for $n \rightarrow \infty$ the isotropic correlation seem to approach the fully polarized value 1/4 for $J_z = 0$, presumably at any finite distance from the hole.

The symmetrized correlation function $C^{\mu}(R_i)$ has been introduced since, for $J_z \rightarrow 0$, the total spin is a well defined quantum number and the isotropic hole spin-spin correlation does not depend on the polarization of the total spin. Thus even in the $S_z = 0$ sector a polaron solution with maximum spin leads to a maximum $C(R_i) = \frac{1}{4}$, whereas $C_z^{\mu}(R) = 0$ for this polarized state since the contribution of the parallel spins are exactly cancelled by the one of antiparallel spins (all these contributions have the same weight in the polaron solution). In this way, we can unambiguously distinguish the ferromagnetic region with $C^{\mu}(R_i) > 0$ from the antiferromagnetic one with $C^{\mu}(R_i) < 0$. As shown in Fig.7.18, we have found that for large J_z all the spins are correlated in the z direction since the two previous correlation functions are almost identical. There is a clear evidence of an antiferromagnetic correlation which approaches the asymptotic value $C(R) \rightarrow -1/4$ with a correlation length similar to what appears in the wavefunction components in the Lanczos basis (see Fig.7.12).

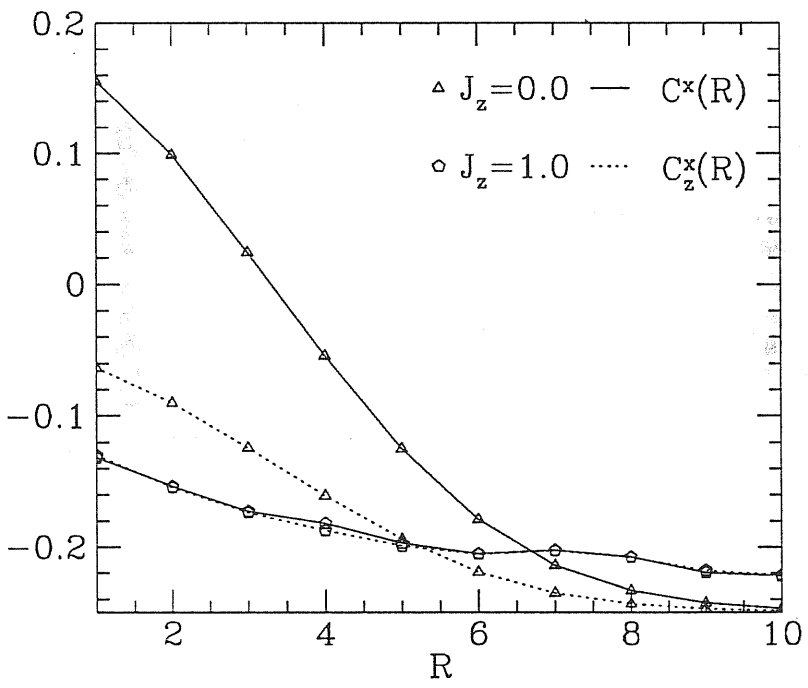

Figure 7.18: The hole spin-spin correlation function $C^{\mu}(R)$ and $C_z^{\mu}(R)$ with $\tau_{\mu} = (1,0)$. For large J_z $C(R)$ is purely antiferromagnetic. However for vanishing (or small) J_z, the ferromagnetic component in the S_x-S_y plane are important.

$2n$	$C_n(0)$	$C_n(2)$	$C_n(4)$	$C_n(10)$
6	0	2	0	0
10	0	2	8	0
12	4	2	3	0
14	18	4	6	10
16	36	28	15	14
18	120	66	33	28
20	270	244	151	96
22	846	668	404	182
24	2400	1868	1305	734
26	7052	5590	3906	2238
28	21432	16250	11503	7378
30	63538	49950	35581	22844

$2n$	$C_n(16)$	$C_n(26)$	$C_n(36)$	$C_n(50)$	$C_n(p=0)$
6	0	0	0	0	0
10	0	0	0	0	4
12	0	0	0	0	12
14	0	0	0	0	14
16	0	0	0	0	58
18	21	0	0	0	150
20	50	0	0	0	416
22	127	48	0	0	1352
24	440	150	0	0	3704
26	1118	440	107	0	11394
28	3792	1688	422	0	33850
30	11949	5050	1418	238	103498

$2n$	$C_n(0)$	$C_n(2)$	$C_n(4)$	$C_n(10)$
32	193448	152314	108676	70960
34	590154	472488	340675	223698
36	1824844	1471492	1068182	708496
38	5677040	4609274	3385018	2264848
40	17818480	14539266	10760828	7287326
42	56220728	46154304	34459409	23573566
44	178693158	147425926	110826815	76581474
46	570790364	473551402	358473393	249911680
48	1834737522	1529492974	1164976270	819090516
50	5926011194	4963905566	3804186739	2695446152
52	19240493885	16187397249	12476330859	8905934658

$2n$	$C_n(16)$	$C_n(26)$	$C_n(36)$	$C_n(50)$	$C_n(64)$
32	39081	17614	5714	1140	0
34	128823	58446	19510	4294	534
36	414196	196574	70917	18258	2981
38	1348874	670086	251056	67790	12460
40	4397638	2245908	883914	258922	55639
42	14437674	7572526	3126095	968326	222326
44	47561630	25474418	10934279	3569044	886787
46	157303528	85932926	38263835	13147300	3468307
48	521903825	290492088	133406362	47855170	13327978
50	1737377480	983973358	464563759	173622392	50912034
52	5800668507	3338934862	1616935261	626834742	192138728

$2n$	$C_n(82)$	$C_n(100)$	$C_n(122)$	$C_n(144)$	$C(p=0)$
32	0	0	0	0	984446
34	0	0	0	0	3087090
36	0	0	0	0	9727036
38	1190	0	0	0	30898232
40	7634	0	0	0	98692630
42	35058	2661	0	0	317324618
44	164380	19237	0	0	1025581138
46	697614	96205	5944	0	3332494632
48	2901958	472897	47830	0	10882673258
50	11813430	2117499	258896	13277	35702392358
52	47077158	9171222	1332690	117733	117646241223

Table 7.1: The non vanishing coefficients $C_n(R)$ of the t-J_z Hamiltonian on the 2C lattice. Only those coefficients which are not included in the Müller-Hartmann's table are shown. The notation is similar to the one in ref. [81], i.e. $d^2 = |R|^2$ and n_{d^2} is the number of skeleton paths at a given distance and for a given direction (note that there is an extra factor two for $R \neq O$ if we do not distinguish the two possible directions as in ref. [81]). The data for $n = 26$ are accurate up to ± 5.

α	$\beta_{R=O}$	$C_{R=O}$	$2n$
1.88136	2.39084	1.26191	22-36
1.88356	2.42844	1.38458	22-38
1.89515	2.63760	2.34793	22-40
1.89049	2.54888	1.86730	22-42
1.89824	2.70449	2.81409	22-44
1.89667	2.67137	2.57441	22-46
1.90428	2.83985	4.08250	22-48
1.90575	2.87370	4.48588	22-50
1.91050	2.98860	6.20875	22-52

α	$\beta_{R=O}$	$C_{R=O}$	$2n$
1.88136	2.39084	1.26191	22-36
1.88399	2.43662	1.41397	24-38
1.89752	2.68445	2.65495	26-40
1.89228	2.58627	2.06374	28-42
1.89925	2.72657	2.98843	30-44
1.89721	2.68362	2.66328	32-46
1.90523	2.86235	4.34957	34-48
1.90657	2.89433	4.75851	36-50
1.91148	3.01404	6.68424	38-52

Table 7.2: Fit of the coefficients $C_n(R)$ for $R = O$ using the ansatz (7.4), in the given intervals of n given in the rightmost column.

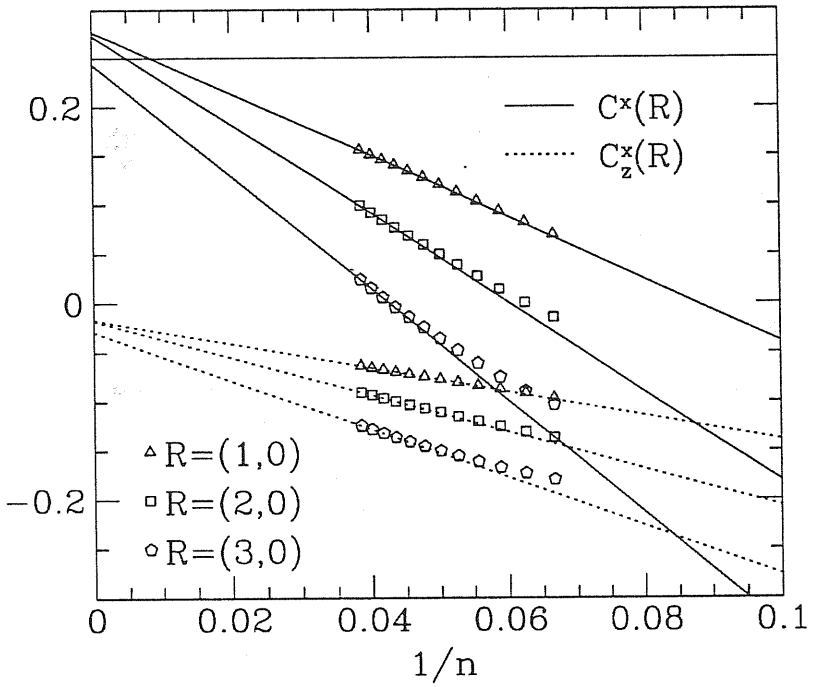

Figure 7.19: The extrapolation $n \to \infty$ of $C^{\mu}(R)$ and $C_z^{\mu}(R)$ for the three lattice sites closest to the hole at $J_z = 0$. The horizontal line is the value of $C^{\mu}(R)$ for the fully polarized Nagaoka state.

Chapter 8

Conclusion

In this thesis, we have developed a scheme to generalize the spin wave theory to a finite size lattice, and we have applied it to the frustrated 2D Heisenberg model, the anisotropic Heisenberg model and the Heisenberg model on the triangular lattice. The same technique is applicable to more general Hamiltonians with or without frustration, including triangular and Kagome' lattice, anisotropic models, *etc. etc.* where it can yield accurate results with a minor computational effort. It has the advantage that one can directly check the accuracy of the results on the small size system, while yielding reliable prediction on the infinite system. In the J_1-J_2 Heisenberg model we have found that SWT works very well for small frustration ($J_2 < 0.2$) and an accurate estimate of spin-rotation invariant quantities can be obtained with only a few term of the expansion in $\frac{1}{S}$. We finally confirm the existence of a non classical spin liquid state for large J_2. Contrary to the previous results, the finite size spin wave successfully shows that the Heisenberg model on the triangular lattice has indeed a long range ordered ground state.

Our numerical and analytical results strongly support a spin liquid state existing in the J_x-J_y model. The spin liquid state is shown to have gapless low energy excitation. A phase diagram of this model is presented by the numerical results, showing that this spin liquid state behaves as a set of the decoupled one dimensional chains. This is an example of how the one dimensional behavior might extend even in two spatial dimensions.

Let us conclude by mentioning our results on the single hole problem for the t-J_z model, which has taken most of the time during my Ph.D studies. After all, the picture of the one hole ground state in the t-J_z model seems clear. In fact, as we decrease J_z, we approach the Nagaoka state with maximum spin and with total $S_z = 0$ (which is by the way a conserved quantity) due to the proliferation of closed loop paths that strongly enhance the ferromagnetic correlations around the hole in the x-y plane. Thus there exist a ferromagnetic polaron with a length which diverges for $J_z \rightarrow 0$, but that is continuously

connected to the antiferromagnetic length obtained at finite large J_z. In this way this polaron state is somehow similar to the phase separated variational state[86], but we have to emphasize that in our approach the localized polaron conserves the translational symmetry because it is defined after the Galileo transformation (5.1) and consequently it is not "phase separated". Moreover the total spin projection on the z-axis vanishes, as it is conserved locally by the effective Hamiltonian (5.6). The energy of this state is much smaller than the "phase separated" variational state and represents the real picture of the single hole ground state in the t-J_z model.

We have presented here a successful attempt to go beyond the retraceable path approximation and the string picture for the hole dynamics in an antiferromagnetic spin background. A new Lanczos-type of analysis of the Hamiltonian enabled us to get very accurate results for the 2C problem and qualitatively similar ones for the 2D case. At $J_z = 0$, a clear dispersion of the main incoherent peak of $A(k,\omega)$ both for the 2C and the 2D case was found. Contrary to the prediction of the large spatial dimension, we found, at least for the 2C model, that the bottom of the incoherent band is dispersionless and coincides with the Nagaoka energy ϵ_N, *i.e.* the minimum possible energy by the Nagaoka theorem. This resolve a controversy recently proposed by Müller-Hartmann. In fact, based on the Lanczos Spectra Decoding method, we have given an argument implying that $A(\omega) \propto (\omega - \epsilon_N)^{-d/2-1} e^{\frac{-\Delta}{(\omega-\epsilon_N)^d}}$ and if for instance $\Delta \propto (\epsilon_{BR} - \epsilon_N)^d$, we can easily understand why the infinite dimension limit get erroneously no weight for $\omega < \epsilon_{BR}$.

For finite J_z, contrary to the string picture, we found only one coherent quasi-particle weight and an incoherent broad spectrum at higher energy. A second quasiparticle peak may appear in the spectral function but has always a very small weight. The possibility of a phase transition as a function of J_z is not compatible with our numerical results for the ground state energy, unless for an unrealistically small value of the coupling, and, in consequence, the Emery's argument about the phase separation for small J is found unlikely in the t-J_z model.

The spin charge decoupling is surely not evident at small distance R. However, it still remains open whether the spin charge decoupling happens asymptotically at large distance, although for the 2C case we have ruled out this possibility up to a distance of about 10 lattice spacings.

Appendix A

Quasiparticle Weight, Green's Function and Current Operators

An important quantity to characterize the dynamics of the single hole is the so called quasi-particle weight appearing as the residue of a simple pole in the one-hole dynamical Green's function. This residue can be alternatively calculated [90] by means of the overlap of the ground state $|\psi_p>$ of one hole with momentum p and the state $c_{p,\sigma}|H>$, where $|H>$ is the translation invariant ground state without holes:

$$Z_p = |<H|c^{\dagger}_{p,\sigma_O}|\psi_p>|^2 = |<H|S_O>|^2 \tag{A.1}$$

where we have explicitly used that $n_{\sigma,O}|S_O>=|S_O>$. For $t>0$, *i.e.* positive time, the Green's function is defined as

$$G(p,t) = -2i<H|c^{\dagger}_{p,\sigma}e^{-i(H-i\delta-E_0)t}c_{p,\sigma}|H> \tag{A.2}$$

where E_0 is the corresponding energy of the state $|H>$. Here the factor two comes from the requirement that $G(p,t\rightarrow 0^+)=-2<H|n_{p,\sigma}|H>=-i$. The normalized state $|\psi_p>=\sqrt{2}c_{p,\sigma}|H>$ is of the form (5.1), if we choose

$$S^H_O = \sqrt{2}n_{\sigma,O}|H>. \tag{A.3}$$

Due to the correspondence of eigenstates between H^{eff}_p and H, we can expand $|S_O>$ in terms of eigenstates of H^{eff}_p and easily check that the propagation of $|S_O>$ with the effective Hamiltonian, $|S_O>_t=e^{iH^{eff}_p t}|S_O>e^{-iH^{eff}_p t}$, corresponds exactly to the propagation of ψ_p with the exact t-J_z Hamiltonian and

$$G(p,t) = -i<S^H_O|e^{-i(H^{eff}_p-i\delta)t}|S^H_O> \tag{A.4}$$

Using that $|S_O^H >= \sqrt{2} n_{i,\sigma} |H >$, that the commutator $\left[H_p^{eff}, n_{\sigma,O}\right]$ vanishes and that G does not depend on σ, we get, after Fourier transform $G(p,\omega) = \int_0^\infty dt\ G(p,t)\ e^{i\omega t}$,

$$G(p,\omega) =< H|\frac{1}{\omega + i\delta - H_p^{eff}}|H > . \tag{A.5}$$

Another important quantity is the current operator, which is useful when we calculate the transport properties. On a discrete lattice, it is defined as[7]:

$$j = \left[ie_0 t \sum_{R\sigma} c^\dagger_{R\sigma} c_{R+\tau_\mu \sigma} + h.c.\right] \tag{A.6}$$

The matrix elements of the current operator between two one-hole states with given momentum p define an effective current operator j^{eff} acting on spin states only:

$$< \psi_p^{S'}|j|\psi_p^S >=< S'|j^{eff}|S > \tag{A.7}$$

Analogously to calculation shown in Section II, the effective current operator can be written as

$$j^{eff} = [-ie_0 t e^{ip\tau_\mu} \chi_{O\tau_\mu} T_{\tau_\mu} + h.c.] \tag{A.8}$$

Bibliography

[1] D.F. Wang, Q.F. Zhong and P. Coleman Phys. Rev. B 48 8476 (1993)

[2] J.G. Bednorz and K.A. Muller, Z. Phys. **B64**, 189 (1986)

[3] P.W. Anderson, Science 235, 1196 (1987).

[4] M.C. Gutzwiller, Phys. Rev. Lett. **10**, 159 (1963).

[5] J. Hubbard, Proc. Roy. Soc. **A276**, 238 (1963).

[6] J. Kanamori, Progr. Theor. Phys. **30**, 275 (1963).

[7] F.C. Zhang and T.M. Rice, Phys. Rev. B **37**, 3759 (1988).

[8] F.D.M. Haldane, J. Phys. C **14**, 2585 (1981); Phys. Lett. **93A**, 464 (1983); Phys. Rev. Lett. 61, 1029 (1988).

[9] F. Dyson, E.H. Lieb, and B. Simon, J. Stat. Phys. 18, 335 (1978)

[10] N.D. Mermin, and H. Wagner, Phys. Rev. Lett. 22, 1133 (1966)

[11] E.J. Neves, and J.F. Perez, Phys. Lett. A 114A, 331 (1986)

[12] I. Affleck, Phys. Rev. B37 5186 (1988)

[13] P. Fazekas, P.W. Anderson, Philos. Mag. **30**, 423 (1974).

[14] H. Nishimori and S.J. Miyake, Prog. Theor. Phys. **73**, 18 (1985).

[15] T. Jolicoeur and J.C. Le Guillou, Phys. Rev. B 40, 2727 (1989).

[16] S.J. Miyake, J. Phys. Soc. Jpn. **61**, 983 (1992).

[17] T. Oguchi, H. Kitatani, and H. Nishimori, J. Phys. Soc. Jpn. **56**, 3858 (1987).

[18] R.R.P. Singh and D.A. Huse, Phys. Rev. Lett. **68**, 1766 (1992).

[19] N. Eltsner, R.R.P. Singh, and A.P. Young, Phys. Rev. Lett. **71**, 1629 (1993).

[20] D.A. Huse and V. Elser, Phys. Rev. Lett. 60, 2531 (1988).

[21] P. Sindzingre, P. Lecheminant, and C. Lhuillier, preprint (unpublished).

[22] T. Oguchi, H. Nishimori, and Y. Taguchi, J. Phys. Soc. Jpn. 55, 323 (1986).

[23] V. Kalmeyer and R.B. Laughlin, Phys. Rev. Lett. 59, 2095 (1987).

[24] K. Yang, L.K. Warman, and S.M. Girvin, Phys. Rev. Lett. 70, 2641 (1993).

[25] J.D. Reger and A.P. Young, Phys. Rev. B 37, 5978 (1988).

[26] M. Gross, E. Sanchez-Velasco, and E. Siggia, Phys. Rev. B 39, 2484 (1989).

[27] N. Trivedi and D. Ceperley, Phys. Rev. B 41, 4552 (1990).

[28] S. Liang, Phys. Rev. B 42, 6555 (1990).

[29] J. Carlson, Phys. Rev. B 40, 846 (1989).

[30] L.G. Marland and D.D. Betts, Phys. Rev. Lett. 43, 1618 (1979).

[31] S. Fujiki, Can. J. Phys. 65, 489 (1987).

[32] H. Nishimori and H. Nakanishi, J. Phys. Soc. Jpn. 57, 626 (1988).

[33] M. Imada, J. Phys. Soc. Jpn. 56, 311 (1987).

[34] M. Imada, J. Phys. Soc. Jpn. 58, 2650 (1989).

[35] T. Jolicoeur, E. Dagotto, E. Gagliano, and S. Bacci, Phys. Rev. B 42, 4800 (1990).

[36] R. Deutscher, H.V. Everts, S. Miyashita, and M. Wintel, J. Phys. A. Math. Gen. 23, L1043 (1990).

[37] P.W. Leung and K. Runge, Phys. Rev. B 47, 5861 (1993).

[38] E.Dagotto and A. Moreo, Phys. Rev. Lett. 63, 2148 (1989)

[39] H.J. Schulz and T.A.L. Ziman, Europhys. Lett. 18, 355 (1992)

[40] P.Chandra and B.Doucot, Phys. Rev. B38, 9335 (1988)

[41] J. Oitmaa, D.D. Betts, Can. J. Phys. 56, 897 (1978).

[42] K.J. Runge, Phys. Rev. B 45, 7229 (1992); *ibid*,12292.

[43] T. Oguchi, Phys. Rev. 117, 117 (1960).

[44] See for instance C. Bourbonnais, L.G. Caron, Int. J. Mod. Phys. 5, 1033 (1991).

[45] A. Parola, Phys. Rev. B, 40, 7109 (1989).

[46] M. Azzouz, B. Doucot Phys. Rev. B, 47, 8660 (1992).

[47] S. Chakravarty *et al.* Phys. Rev. Lett. 60, 1057 (1988).

[48] Y. Lu, Z.B. Su and Y.M. Li Chinese Journal of Physics **31**, 579 (1993) and reference therein.

[49] S.A. Trugman, Phys. Rev. B **37**, 1597 (1988).

[50] C.L. Kane, P.A. Lee and N. Read, Phys. Rev. B **39**, 6880 (1989), S. Schmitt-Rink, C. M. Varma, and A. E. Ruckenstein, Phys. Rev. Lett. **60**, 2793 (1988).

[51] P. Prelovšek and I. Sega, Phys. Rev. **B 49** 15241 (1994)

[52] W. Metzner, P. Schmit and D. Vollhardt Phys. Rev. B **45**, 2237 (1992), R. Strack and D. Vollhardt Phys. Rev. B **46**, 13852 (1992).

[53] Y. Nagaoka, Phys. Rev. **147**, 392 (1966)

[54] W.F. Brinkman and T.M. Rice, Phys. Rev. B **2**, 1324 (1970).

[55] L.N. Buleavskii, E.L. Nagaev and D.I. Khomskii, Sov. Phys. JETP **27**, 638 (1968).

[56] B.I. Shraiman and E.D. Siggia, Phys. Rev. Lett. **60**, 740 (1988).

[57] D.Poilblanc H. J. Schulz and T. Ziman, Phys. Rev. B **47**, 3268 (1993), *ibidem* Phys. Rev. B **46** 6435 (1992).

[58] E. Dagotto, R. Joynt, A. Moreo, S. Bacci and E. Gagliano Phys. Rev. B **41**, 9049 (1990).

[59] P. Prelovšek, I. Sega and J. Bonca Phys. Rev. B **42** 10706 (1990) *ibidem* Phys. Rev. B **39**, 7074 (1989).

[60] W. O. Putikka, R. I. Glenister , R. R. Singh and H. Tsumetsugu, preprint NHMFL-93-988 , ETH-TH/93-33 , available on cond-mat@babbage.sissa.it by e-mail.

[61] M. Ogata , M. Luchini, S. Sorella and F. Assaad , Phys. Rev. Lett. **66**, 2388 (1991).

[62] Q.F. Zhong, S. Sorella, Europys. Lett. **21**, 629 (1993).

[63] P.W. Anderson, Phys. Rev. 86, 694 (1952)

[64] T. Holstein, and H. Primakoff, Phys. Rev. 58, 1098 (1940)

[65] R. Kubo, Phys. Rev. 87 568 (1952)

[66] K. Kubo and T. Kishi, Phys. Rev. Lett. 61, 2585 (1988)

[67] J.E. Hirsch and S. Tang, Phys. Rev. B40, 4769 (1989)

[68] M. Takahashi, Phys. Rev. B40, 2494 (1989)

[69] E. Lieb and D. Mattis, J. Math. Phys. 3, 749 (1962)

[70] A. Parola, S. Sorella and Q.F. Zhong, Phys. Rev. Lett. 71 4393 1993

[71] Q.F. Zhong and S. Sorella, to be published

[72] D.S. Fisher, Phys. Rev. B 39 11783 (1989).

[73] H. Neuberger, T. Ziman, Phys. Rev. B 39, 2608 (1989).

[74] B. Bernu, P. Lecheminant, C. Lhuillier and L. Pierre, preprint

[75] B. Bernu *et al.* Phys. Rev. Lett. 69, 2590 (1992).

[76] S.P. Strong, A.J. Millis, Phys. Rev. Lett. 69, 2419 (1992).

[77] T. Barnes *et al.* Phys. Rev. Lett. Phys. Rev. B 47 3196 (1993).

[78] Q.F. Zhong, S. Sorella and A. Parola, Phys. Rev. B 49, 6408 (1994)

[79] Q.F. Zhong and S. Sorella, to be published

[80] A. Parola unpublished, T. Xiang Phys. Rev. B 44, 2276 (1992).

[81] E. Müller-Hartmann and C.I. Ventura, preprint, (1994).

[82] A. Parola and S. Sorella, *Phys. Rev. B* 45, 13156 (1992); S. Sorella and A. Parola, *J. Phys. Cond. Mat.* 4 3589 (1992).

[83] S. Sorella and Q.F. Zhong in "Correlation Effects in Low -Dimensional Electron System" edited by A. Okiji and N. Kawakami, p.185, Springer-Verlag (1994).

[84] M. Fabrizio and A. Parola Phys. Rev. Lett. 70, 226 (1993).

[85] Y. Hasegawa and D. Poilblanc, Phys. Rev. B 40, 9035 (1989).

[86] V.J. Emery, S.A. Kivelson and H.Q. Lin Phys. Rev. Lett. 64, 475 (1990).

[87] D.S. Gaunt and A.J. Guttmann in *Phase Transition and Critical Phenomena* Vol. 3, Academic Press Inc. (London) Ltd. (1974).

[88] Z. Lin and E. Manusakis Phys. Rev. B 44, 2414 (1991).

[89] M.D. Johnson, C. Gros and K.J. von Szczepanski, Phys. Rev. B **43**, 11207 (1991).

[90] P. W. Anderson, Phys. Rev. Lett. **64**, 1839 (1990); **65**, 2306.